

**DISCOVERY AND CHARACTERIZATION OF G PROTEIN-GATED,  
INWARDLY-RECTIFYING, POTASSIUM CHANNEL MODULATORS**

By

**Krystian Andrzej Kozek**

Dissertation

Submitted to the Faculty of the  
Graduate School of Vanderbilt University

in partial fulfillment of the requirements

for the degree of

**DOCTOR OF PHILOSOPHY**

in

Pharmacology

October 31, 2018

Nashville, Tennessee

**Approved:**

**C. David Weaver Ph.D. (Mentor)**

**Jerod S. Denton Ph.D. (Committee Chair)**

**Corey R. Hopkins Ph.D.**

**Danny G. Winder Ph.D.**

**Charles C. Hong M.D., Ph.D.**

This work is dedicated to my loving wife Lindsay and my adorable son. Their love, unconditional support, and endless encouragement make my life an absolute joy.

## ACKNOWLEDGMENTS

I would like to thank the Vanderbilt Medical School for the fantastic education during the preclinical years leading up to my graduate studies. It was during this time that I became acutely aware of just how phenomenal the concept of ions moving between cellular structures to generate electrical activity truly is. I am extraordinarily grateful to Dr. David Weaver for providing me the opportunity to study this phenomenon in his laboratory and alongside him at the bench. I am thankful for all the time he has taken to share his mind and for all his efforts to bring drug screening to Vanderbilt University, making it a world-class academic neuroscience drug screening campus. Dr. Weaver is the greatest example of an expert scientist among many diverse, challenging, and interesting fields. He wears multiple metaphorical hats each day as he pushes the boundaries of ion channel mechanisms, fluorescent probe development, optical imaging technology, and small-molecule development for targeted modulation of ion channels. Nevertheless, he always keeps his door open for questions from his students, and his patient words demonstrate a deep understanding of the mentorship he provides.

The Weaver Laboratory is home to an incredible group of scientists with whom I am forever grateful to have studied. They have supported me throughout many of the most important events in my life and have been incredible lab mates, friends, critics, and professional colleagues. They all contributed to making the high-throughput screen I describe a reality and supported my scientific efforts often. They are all incredible and driven scientists. Thank you to Francis J. Prael III for your discussions about science and for bringing new techniques to the lab. Thank you to Dr. Brittany Spitznagel for lending a hand anytime times get tough in the lab. Thank you to Dr. Brendan Dutter, Dr. Susan Ramos-Hunter, and Dr. Kristopher Abney for their support throughout the many facets of research. Finally, thank you to Dr. Yu (Sunny) Du, who is always smiling and

makes every day extra exciting through sharing of results, discussing philosophy, helping design experiments, and being an inspirational parent and role model. I have learned a lot from the people in the Weaver Laboratory, and I will never forget my time with you.

I would like to thank Dr. Paige Vinson for her work in making the Vanderbilt High-Throughput Screening Core Facility an indispensable resource at Vanderbilt. Thank you to Corbin Whitwell, Emily Days, and all the High-throughput Screening Core Facility colleagues that have made an immense number of compounds available to researchers like myself. I would like to thank the Laboratory of Dr. Jerod Denton for developing and sharing the many ion channel-expressing cell lines, especially Dr. Sujay Kharade for his work and collaboration. I would like to thank the Laboratory of Dr. Corey Hopkins for the synthesis of analogs of the molecules described within. Thank you to the Vanderbilt Department of Pharmacology for creating one of the best places to study pharmacology, with a rich curriculum and cutting-edge roster of speakers, teachers, and students. Thank you also to the Vanderbilt Medical Scientist Training Program and its leadership team, past and present, for creating one of the best places in the world to train as a physician scientist. Special thanks to Dr. Chris Williams, Melissa Krasnove, Dr. Megan Williams, Dr. Terry Dermody, Dr. Michelle Grundy, Dr. Jim Bills, Dr. Larry Swift, and Dr. Lourdes Estrada. You have all helped shape the person I am today, and I am grateful.

I would also like to thank my committee members, Drs. Jerod Denton, Danny Winder, Corey Hopkins, and Charles Hong for their support, guidance, and collaboration, all of which was essential to the completion of this body of work and my graduate studies. Thank you to Dr. Denton for serving as my committee chair and for his expertise in inwardly-rectifying potassium channels and his work developing models to study these channels. Thank you to Dr. Hopkins for his expert insight and guidance surrounding the development of analogs of compounds discovered through

screening. Thank you to Dr. Winder for his support throughout my scientific efforts and for creating a vibrant community of addiction researchers at Vanderbilt University. And thank you to Dr. Hong, for his career discussions and for being an aspirational example of a physician scientist.

I would like to acknowledge my support for this work from the National Institute of Mental Health (5R21MH099363) and the National Institute of General Medical Sciences (T32GM007347) of the National Institutes of Health. This research was supported by funds from the Vanderbilt University Pharmacology Department and Vanderbilt Institute of Chemical Biology. Research funding was also provided through the PhRMA Foundation's Paul Calabresi Medical Student Research Fellowship.

I would like to thank D. Joseph Tracy, currently at North Carolina State University, for believing that college freshmen ought to pursue an independent research project. In his laboratory, I first learned how to think critically, problem solve, conduct experiments, present data, and write scientifically. Thank you also to his wife Dr. Lisa Tracy, who, together with Joe, helped me choose my career path as a physician scientist.

I wholeheartedly thank all those who have taught and inspired me along my journey towards a greater understanding of our beautiful world.

# TABLE OF CONTENTS

	Page
DEDICATION .....	ii
ACKNOWLEDGMENTS .....	iii
LIST OF TABLES .....	ix
LIST OF FIGURES .....	x
ABBREVIATIONS .....	xii
Chapter 1: INTRODUCTION.....	1
Overview .....	1
A Historical Perspective .....	2
Ionic Gradients of Living Cells.....	3
Ion Channels Diversity .....	7
Ion Channel Gating .....	8
Physiological Relevance of Ion Channels.....	10
The Membrane Potential.....	10
The Action Potential .....	14
An Introduction to G Protein-gated, Inwardly-rectifying, Potassium Ion Channels .....	15
GIRK Channel Composition and Expression .....	18
G Protein-Coupled Receptors and Phosphatidylinositol 4,5-bisphosphate Regulate GIRK Channels .....	21
Additional Regulators of GIRK Channel Function .....	22
Natural and Synthetic Modulators of GIRK Channel Trafficking.....	23
Information Gleaned from the Crystal Structure of GIRK2 Channels .....	24
GIRK Channels in Normal and Pathological Physiology.....	25
A Brief Overview of Opioid and Alcohol Drug Abuse in the United States of America...28	
Non-GIRK1-containing GIRK Channel Involvement in Processes Underlying Addiction and Drug Abuse .....	31
The Utility of Selective GIRK Channel Modulators .....	32
Previous Discoveries and Reports of GIRK Channel Activators .....	33
Previous Discoveries and Reports of GIRK Channel Inhibitors .....	36
Previous Efforts Identifying Non-GIRK1-containing GIRK Channel Activators.....	37
Chapter 2: DISCOVERY OF NOVEL NON-GIRK1-CONTAINING GIRK CHANNEL MODULATORS USING HIGH-THROUGHPUT THALLIUM FLUX ASSAYS .....	42
Abstract .....	42
Introduction.....	43
Methods.....	50
General Equipment Utilized Throughout this Research .....	50
Cell Line Generation.....	52
Cell Culture.....	52
Generation of Monoclonal Cell Lines.....	53
Cell Plate Preparation for Thallium Flux Experiments.....	53

Pertussis Toxin Treatment of Cells for Thallium Flux Experiments .....	54
Compound Plate Preparation for High-throughput Experiments.....	54
Conducting a Thallium Flux Experiment .....	55
Data Analysis for Thallium Flux Experiments .....	57
High-throughput Screen using the Thallium Flux Assay .....	58
Screened Compound Library .....	61
Western Blot .....	62
Results.....	64
Validating the Expression of GIRK2 and NPY4R in HEK293 Cells.....	64
Selection and Counter Screening of Hits from the GIRK2 Channel High-throughput Screen.....	64
Discussion .....	67
 Chapter 3: CHARACTERIZATION OF VU0529331 ACTIVITY ON GIRK CHANNELS..	71
Abstract .....	71
Introduction .....	72
Methods.....	75
Cell Line Generation.....	75
Cell Culture Conditions .....	76
Generation of Monoclonal Cell Lines.....	77
384-well Cell Plate Preparation for Fluorescence-based Experiments.....	77
Pertussis Toxin Treatment of Cells for Thallium Flux Experiments.....	78
Compound Dissolution and Maintenance .....	78
Compound Plate Preparation for High-throughput Experiments.....	78
Execution and Analysis of Thallium Flux Experiments .....	79
SuperClomeleon Chloride (Cl <sup>-</sup> ) Influx Assay of Cys-Loop Receptor Activity .....	80
Whole-cell Voltage-clamp Electrophysiology .....	82
Results.....	84
Dependence of VU0529331 Activity on GIRK2 Expression and G <sub>i/o</sub> -coupled G Protein-coupled Receptor Activity .....	84
Characterization of VU0529331 Selectivity Among GIRK Channels .....	88
Characterization of VU0529331 Selectivity Among a Broad Variety of Channels .....	88
Characterization of VU0529331 Influence on the GIRK Channel Current-Voltage Relationship Using Whole-cell Voltage-clamp Electrophysiology .....	94
Characterization of VU0529331 Analog Activity on GIRK Channels .....	101
Discussion .....	101
 Chapter 4: CONCLUSION AND FUTURE DIRECTIONS .....	117
Conclusion .....	117
Future Directions .....	119
Understanding the Mechanism of Action of VU0529331 .....	119
Characterizing the Activity of VU0529331 on the K <sub>ir</sub> 6 Channel Family.....	124
Identifying Non-GIRK1-Containing GIRK Channels in Isolated Dopaminergic Neurons .....	125
Discovery of GIRK Channel Inhibitors from the GIRK2 High-throughput Screen.....	128
Interpretation and Impact.....	131

REFERENCES .....133



## LIST OF TABLES

<b>Table 1.</b> Nine compounds that resulted from the GIRK2 high-throughput screen .....	67
<b>Table 2.</b> VU0529331 activity on a variety of engineered HEK293 cell lines.....	89
<b>Table 3.</b> VU0455661, VU0592331, and ivermectin activity on wildtype and mutant GIRK channels.....	109

## LIST OF FIGURES

<b>Figure 1.</b> Models of cell membranes and membrane transporters .....	4
<b>Figure 2.</b> Models of K <sup>+</sup> ion channels and the K <sup>+</sup> channel family tree .....	6
<b>Figure 3.</b> Models of K <sub>ir</sub> channel structure, an excitatory neuron, and an action potential.....	11
<b>Figure 4.</b> Models of a current-voltage relationship, the Nernst equation, and the K <sub>ir</sub> family tree .....	13
<b>Figure 5.</b> Models of GIRK channel properties and modulation.....	17
<b>Figure 6.</b> Models of GIRK channel structure and localization .....	19
<b>Figure 7.</b> U.S. drug deaths and the drugs involved in overdose deaths .....	30
<b>Figure 8.</b> The activity of VU0466551 and ML297 on GIRK channels .....	34
<b>Figure 9.</b> The activity of ivermectin and its analogs on GIRK2 channels .....	38
<b>Figure 10.</b> Models of the thallium flux assay.....	44
<b>Figure 11.</b> The Thallos dye structure and activation and monovalent cation properties .....	45
<b>Figure 12.</b> Model of the protocol utilized during high-throughput screening .....	48
<b>Figure 13.</b> The compound screening and counter screening pathway .....	51
<b>Figure 14.</b> An example of the high-throughput screening process .....	56
<b>Figure 15.</b> GIRK1 and GIRK2 protein expression in engineered HEK293 cells .....	65
<b>Figure 16.</b> The activity of VU0529331 on GIRK channels .....	85
<b>Figure 17.</b> Raw thallium flux traces of VU0529331 and VU0466551 activity .....	86
<b>Figure 18.</b> VU0529331 activity in cells treated with pertussis toxin.....	87
<b>Figure 19.</b> The activity of VU0529331 in the presence of VU0466551 .....	90
<b>Figure 20.</b> A dendrogram illustrating the similarity of channels tested with VU0529331 .....	91

<b>Figure 21.</b> The activity of VU0529331 and ivermectin in Cl <sup>-</sup> influx assays .....	93
<b>Figure 22.</b> Representative electrophysiology data .....	95
<b>Figure 23.</b> The effects of VU0529331 on the GIRK channel current-voltage relationship.....	96
<b>Figure 24.</b> The effect of VU0529331 on GIRK channel rectification ratio .....	98
<b>Figure 25.</b> Recordings of inward GIRK channel currents in the presence of VU0529331 .....	99
<b>Figure 26.</b> Inhibition of inward GIRK channel currents in the presence of VU0529331 .....	100
<b>Figure 27.</b> Inactive purchased VU0529331 analogs .....	102
<b>Figure 28.</b> Inactive synthesized VU0529331 analogs.....	103
<b>Figure 29.</b> The activity of VU0529331 on K <sub>ir</sub> 6.1/SUR2a and K <sub>ir</sub> 6.1/SUR2b channels .....	115

## ABBREVIATIONS

Ba <sup>2+</sup>	barium ion
CFP	cyan fluorescent protein
Cl <sup>-</sup>	chloride ion
CNS	central nervous system
DA	dopaminergic
DMSO	dimethyl sulfoxide
EC <sub>50</sub>	potency
eGFP	enhanced green fluorescent protein
EP	electrophysiology
FRET	fluorescence resonance energy transfer
G2Y4	GIRK2 and NPY4R-expressing HEK293 cells
G <sub>i/o</sub>	inhibitory G protein
GIRK	G protein-gated, inwardly-rectifying, potassium channel
GIRK1/X	GIRK1-subunit-containing GIRK channel
GPCR	G protein-coupled receptor
hPP	human pancreatic polypeptide
HTS	high-throughput screen
IV	current-voltage
K <sup>+</sup>	potassium ion
KCC2	potassium-chloride transporter member 5
kDa	kilodalton

KES	20 mM potassium ion extracellular solution
K <sub>ir</sub>	inwardly-rectifying potassium channel family
Na <sup>+</sup>	sodium ion
NPY4R	neuropeptide Y4 receptor
PBS	phosphate-buffered saline
pF	picoFarads
PIP <sub>2</sub>	phosphatidylinositol 4,5-bisphosphate
PKA	protein kinase A
PKC	protein kinase C
PLC	phospholipase C
P <sub>o</sub>	open probability
RT	room temperature
Tl <sup>+</sup>	thallium ion
VTA	ventral tegmental area
VU331	VU0529331
YFP	yellow fluorescent protein

# CHAPTER 1

## INTRODUCTION

### Overview

Ion channel proteins in the cellular and intracellular membranes of cells are regulated pores that are permeable to the various water-soluble ions involved in sustaining life.<sup>1</sup> These channels facilitate the diffusion of sodium ( $\text{Na}^+$ ), potassium ( $\text{K}^+$ ), chloride ( $\text{Cl}^-$ ), and calcium ( $\text{Ca}^{2+}$ ) and other ionic species between the intracellular and extracellular spaces.<sup>2</sup> In doing so, ion channels exploit ion concentration gradients and generate changes in the membrane potentials of excitable cells. In cells such as neurons, these electrical changes can propagate along a cell and facilitate electrochemical signaling. One protein family that is capable of modifying the ability of an electrical signal to form is the G protein-gated, inwardly rectifying  $\text{K}^+$  (GIRK) channel family.<sup>3</sup> GIRK channels are widely expressed throughout excitable cells of the body, such as the neurons of the central nervous system (CNS) and the pace-setting cardiomyocytes of the cardiac sinus node. These channels regulate excitable cells by increasing the amount of stimulation a neuron requires to generate an action potential. The GIRK channel family is comprised of four unique subunits that assemble into channels as either heterotetramers or homotetramers, which depends on the specific GIRK subunits expressed within a cell. Differential GIRK subunit expression throughout various organs leads to specific channel combinations in certain tissues and organs. The discrete populations of cells that express specific GIRK channels are, in some tissues, involved in unique functions. For instance, in the ventral tegmental area (VTA) of the brain, a region implicated in addiction and reward signaling, dopaminergic (DA) neurons do not express the GIRK1 subunit.<sup>4</sup>

These neurons likely express a population of GIRK2 homotetrameric and GIRK2/3 heterotetrameric channels on their cellular membranes, and they are critically implicated in the circuitry underlying addiction, a sometimes-deadly illness with great social costs.<sup>5</sup> Because of the relevance of the GIRK2 subunit, and potentially GIRK2 homomeric channels, to addiction circuitry, targeting these DA neurons with modulators of GIRK2 channel activity may help unveil a novel pharmacological target for the treatment or prevention of addiction.<sup>6,7</sup> However, researchers lacked efficacious, potent, and selective pharmacological probes with which to study GIRK2 channels.<sup>5,7</sup> Herein, we describe our efforts to discover efficacious, potent, and selective modulators of GIRK2 homotetrameric channels.

### **A Historical Perspective**

Scientists have been developing their knowledge of electrochemical communication within the excitable cells of animals for hundreds of years. While difficult to acknowledge all the individuals and hypotheses involved in bringing our knowledge to the point it is at today, the story begins around 1780, when Luigi Galvani recognized that electricity was able to stimulate the movement of frog legs.<sup>8</sup> Later, around 1840, Carlo Matteucci demonstrated the existence of measurable currents in damaged muscles.<sup>8</sup> Near the same time, Emil du Boise-Regmond, at the Johannes Mueller laboratory in 1841, demonstrated that the stimulation of nerves modulated electrical currents.<sup>8</sup> In 1865, du Boise-Regmond made the first measurement of the time course of the action potential. Discovering the underlying biology of these electrical signals took many more decades of investigations.<sup>8</sup>

In the 1880s, Sidney Ringer recognized that soluble ions at precise concentrations were necessary for the function of organs, such as the heart.<sup>1</sup> In the early 1900s, Julius Bernstein

proposed that the various ions were separated by a selectively-permeable membrane between the inside and outside of a cell.<sup>1</sup> However, the ionic theory of membrane excitation was not accepted until the 1930s, when Alan Hodgkin and Andrew Huxley, 1963 Nobel Prize winners in Physiology or Medicine, uncovered the ionic mechanism of action potentials. From this discovery, the field of electrophysiology arose, encompassing the study of electrical properties of biological cells and tissues.

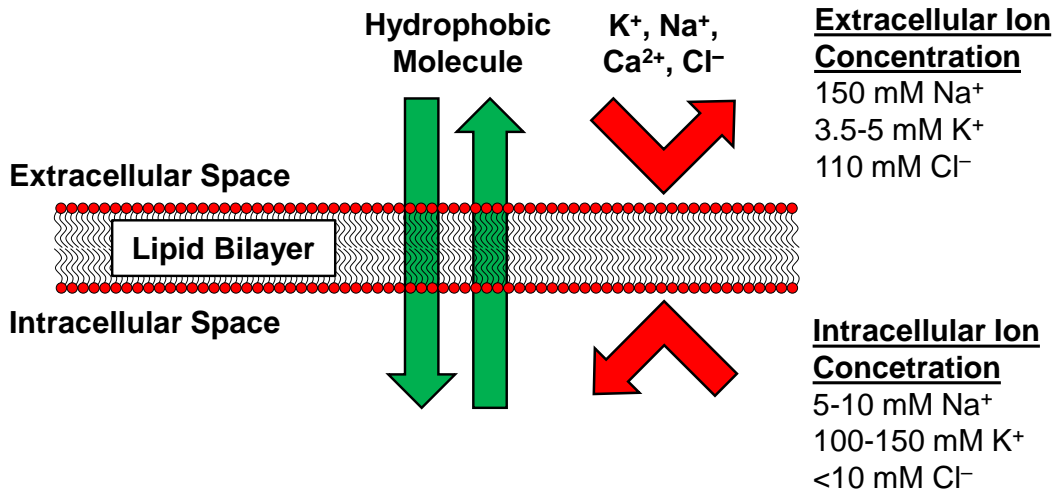
The immense quantity of ions separated across the cell membrane causes measurable electrochemical voltage on the cellular membrane. With the development of electrical current amplifiers and computers, scientists could record and manipulate the currents and membrane potentials of individual cells.<sup>1,8</sup> Bernard Katz and Erwin Neher won the 1991 Nobel Prize in Medicine for their work measuring current through ion channels using electrophysiological recording machines in the 1970s. Katz and Neher measured the change in voltage potential due to a single ion channel, an observation nearly 200 years in the making.<sup>9</sup> They demonstrated that ion channels were essential for electrical activity within biological organisms. The work of these scientists and many others underly all of the knowledge that has enabled the descriptions of nature and the newest research conducted within this work.

### **Ionic Gradients of Living Cells**

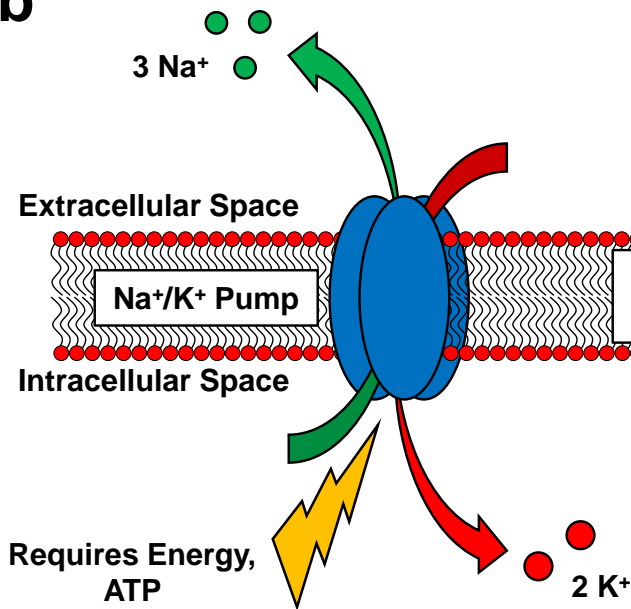
Living cells maintain a highly sophisticated and active surface membrane in order to maintain the processes critical to life.<sup>1</sup> At the simplest level, cells are microscopic bubbles enveloped by a lipid bilayer. This lipid bilayer is the foundation of the cellular membrane, which separates the intracellular from the extracellular space (*Figure 1a*). A pure lipid bilayer membrane is selective with regard to the chemical species that may pass through. For example, it allows



**a**



**b**



**c**

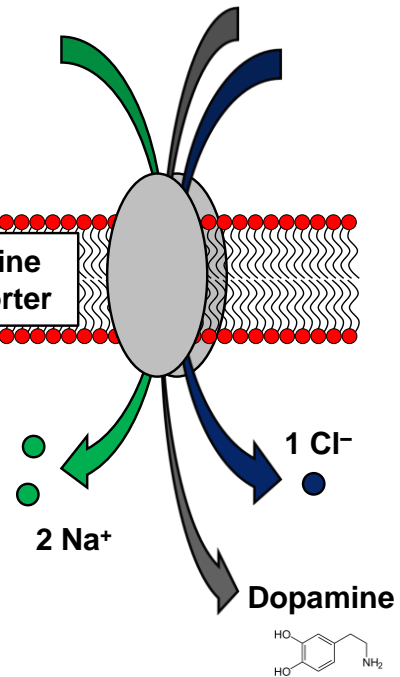


**Figure 1.** (a) The lipid bilayer separates the intracellular and extracellular spaces. It enables the passage of certain chemicals, such as hydrophobic molecules, but inhibits the passage of other chemicals, such as water-soluble ions. (b) An active transporter, the sodium-potassium ( $Na^+/K^+$ ) pump requires energy to move ions against their concentration gradients. (c) A passive transporter, the dopamine transporter utilizes the  $Na^+$  gradient set by the  $Na^+/K^+$  pump and the  $Cl^-$  gradient to move dopamine intracellularly.

hydrophobic molecules across, but it is impermeable to ions.<sup>1</sup> However, cells have evolved a staggering diversity of proteins that they use to mediate the movement of chemical species across their membranes. Cells can therefore establish a precise equilibrium between the intracellular and extracellular spaces, generating concentration gradients for chemicals across the cellular membrane.<sup>1</sup>

Water-soluble ions are one of the most dynamically regulated species of substrates across the cell surface. Among these ions are  $\text{Na}^+$ ,  $\text{K}^+$ ,  $\text{Cl}^-$ , and  $\text{Ca}^{2+}$ , each existing at different intracellular and extracellular concentrations.<sup>1</sup> For example,  $\text{Na}^+$  concentrations are greater extracellularly (~150 mM vs 5-10 mM), while  $\text{K}^+$  concentrations are greater intracellularly (100-150 mM vs 3.5-5 mM) (*Figure 1a*).<sup>10</sup> Further, each ionic concentration gradient is maintained by the concerted activity of membrane-localized primary and secondary transporters.<sup>1</sup> Primary transporters, such as the  $\text{Na}^+/\text{K}^+$  pump, require chemical energy, primarily in the form of ATP hydrolysis, to move ions against the concentration gradient. Secondary transporters utilize the stored energy of a concentration gradient of an ion to move another chemical species, such as an ion, against its concentration gradient (*Figure 1b*). For instance, transporters may utilize ion gradients to transport small molecules, such as the dopamine neurotransmitter, across the cell membrane (*Figure 1c*).<sup>1</sup>

The equilibrium created by a cell is often disrupted, however. Ions are able to passively diffuse down their concentration gradients when the cell membrane is no longer impermeable, which happens when ion channels are opened (*Figure 2a*). Upon opening, ion channels selectively mediate the passage of ions across the cellular membrane in accordance with the specific ion's concentration gradient.<sup>1</sup> When an ion-specific channel opens, ions diffuse through a water-molecule-filled pore, that can be <5 ångströms in width, at rates of >1,000,000 ions per second

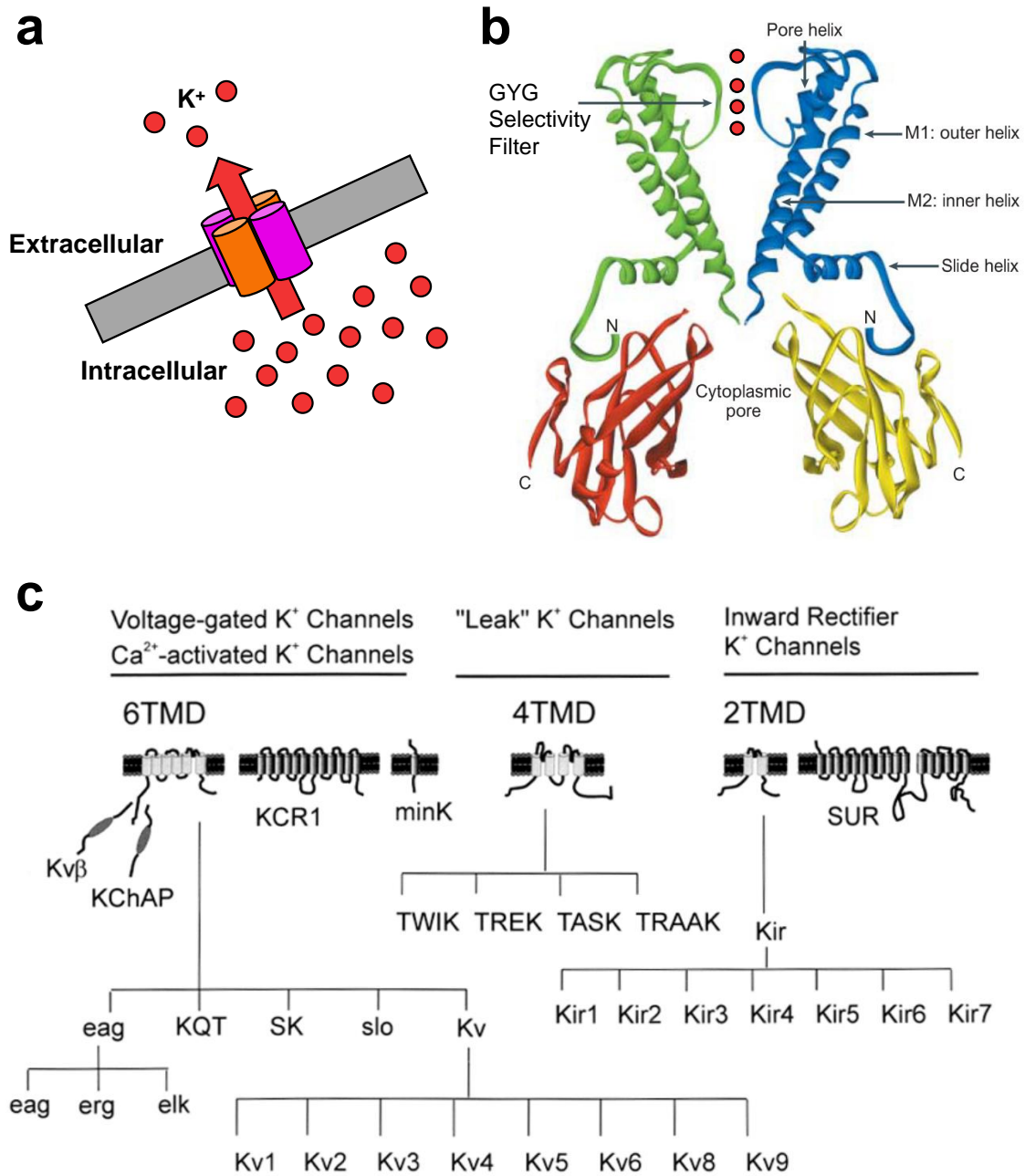


**Figure 2.** (a) A  $K^+$  channel passes  $K^+$  down the concentration gradient, extracellularly. (b) The cutaway ribbon structure of the pore-forming,  $\alpha$ , subunits of an inwardly-rectifying  $K^+$  channel illustrating the GYG selectivity filter. Figure adapted from Bichet, D. *et al.*, *Nat. Rev. Neurosci.* **2003**. (c) The diversity of channels within the  $K^+$  channel family tree. Figure adapted from Coetzee, W. A. *et al.*, *Ann. N. Y. Acad. Sci.* **1999**.

through a single channel.<sup>1,2</sup> Understandably, this disrupts the ion concentrations near the membrane of a cell and causes pumps and transporters to work to equilibrate the ions once again, so that this cycle can begin anew.

## **Ion Channel Diversity**

A wide variety of ion channels with a broad spectrum of characteristics have been described.<sup>1</sup> Ion channels are classified based on a variety of different properties, such as ion selectivity and gating mechanism. Broadly, ion channels can be selective for individual ions, i.e. Na<sup>+</sup>, K<sup>+</sup>, Cl<sup>-</sup>, and Ca<sup>2+</sup> channels, or for groups of ions, i.e. anion and cation channels. Selectivity for these various ions is determined by the structure of the individual protein sequence that comprises the pore of a channel.<sup>1</sup> For example, K<sup>+</sup> channels have a specific amino acid sequence, namely the GYG sequence (**Figure 2b**), within the pore, which is key for K<sup>+</sup> selectivity.<sup>11</sup> The individual proteins that combine to form ion channels are diverse and underlie many different functions in addition to ion selectivity.

When ion channel families are broken down into their most structurally-similar units, they are subdivided based on the subunits that are required to generate the pore of the ion channel, or the pore-forming subunits also known as the alpha ( $\alpha$ ) subunits (**Figure 2b**).<sup>1</sup> Variations in channel structure can be significant, such as requiring different numbers of subunits to generate a pore. For example, the inwardly-rectifying K<sup>+</sup> (K<sub>ir</sub>) channels require 4 subunits while the Cys-loop receptor ion channels (e.g. ionotropic glycine receptor) require 5 subunits to form channels. Differences can also be smaller, in which the pore-forming  $\alpha$  subunits generally maintain their structural similarity and vary only by the identity of amino acids throughout certain portions of the protein. **Figure 2c** demonstrates the variations within the K<sup>+</sup> channel family, which is broken into channels

that have either 2, 4, and 6 transmembrane domains.<sup>12</sup> Within each of these families, the channels are further subdivided by structural differences that underlie functional differences. Additional classification is shown later in *Figure 4d*, which demonstrates the individual subunits within the branches of the K<sub>ir</sub> family.<sup>12</sup>

In addition to  $\alpha$  subunits that create the pore, beta ( $\beta$ ) subunits that interact with the  $\alpha$  subunits are for certain channels required to enable proper channel function. *Figure 2c* illustrates a subset of the  $\beta$  subunits involved in K<sup>+</sup> channel formation. For example, the K<sub>ir</sub>6 channel family requires expression of the sulfonyl-urea receptor (SUR)  $\beta$  subunit for functional channel formation.<sup>13</sup> The full extent to which different  $\alpha$  and  $\beta$  subunits within and between multiple families interact and, in many cases, the exact stoichiometries of these interactions remains unknown. Different splice variants within a single  $\alpha$  subunit or  $\beta$  subunit also exist, further increasing diversity. Additionally, some subunits within a channel family may not be able to interact, while the subunits that can interact mix in an unknown ratio. Such diversity has the potential of generating multiple channels with variable stoichiometry using just 2 subunits. Attempting to identify the specific ratio of the subunits that generate a channel is still technically heroic. Altogether, the sheer number and variety of  $\alpha$  and  $\beta$  subunits within just the K<sup>+</sup> channel family, and the many combinations these subunits might form on the surface of a cell, has the potential to generate a tremendously vibrant diversity of ion channels.<sup>1</sup>

## **Ion Channel Gating**

Ion channels exist in a variety of conformations within a cell at any given time. The summation of all the channels existing in the various conformations provides us with a snapshot of the behavior of the population of channels. The probability of finding a specific channel in an

open conformation, which allows for ions to diffuse through, at any point in time is known as the open probability ( $P_o$ ) of that channel.<sup>1</sup> When observing the activity of a population of channels, the individual  $P_o$  of each channel combines to generate a flow of ions through the open channels and through the cellular membrane. Each ion channel family has a characteristic  $P_o$  that is dependent on a variety of physiological conditions. With variations in these regulating factors, the channels open, or close, and modulate the  $P_o$  of that channel.<sup>1</sup> In turn, this modifies the overall flow of ions passing through these channels as a group. A flow of ions through a channel, whether as individual ions or a group of ions, produces an electrical current, which can change depending on the forces and factors interacting with a channel. Activating channels causes them to open either for longer or more often, or both, which increases the  $P_o$  and generates an increase in current through the cell membrane.<sup>1</sup>

The mechanisms that modulate channels and change the  $P_o$  are varied. Each of them, however, modify the preferred structural conformation of the channel at a given point in time. These factors are said to “gate” channel activity. For example, the  $P_o$  of voltage-gated ion channels is dependent on the particular membrane potential at a given point in time. These channels have a differential ability to achieve an open conformation over the various membrane potentials; therefore, they will be more likely to be open at one membrane potential versus another. The  $P_o$  of a ligand-gated ion channel increases upon the binding of a specific molecule, or molecules. For example, channels may remain mostly inactive until a particular molecule binds to the channel and facilitates an open conformation. Other channels, such as the two-pore-domain background, or leak,  $K^+$  channels (K2P) have a constant efflux of  $K^+$  ions, and their  $P_o$  can be modified by physical or chemical stimuli, such as ligands, membrane stretching, acidosis, and heat. Further, other channels have been shown to be gated by mechanical forces, called mechanosensory gating, and

light, called optical gating. In order to generate such a variety of function and sensitivity to different forces and molecules, each individual channel is composed of highly-evolved proteins that have a staggering structural diversity.<sup>1</sup>

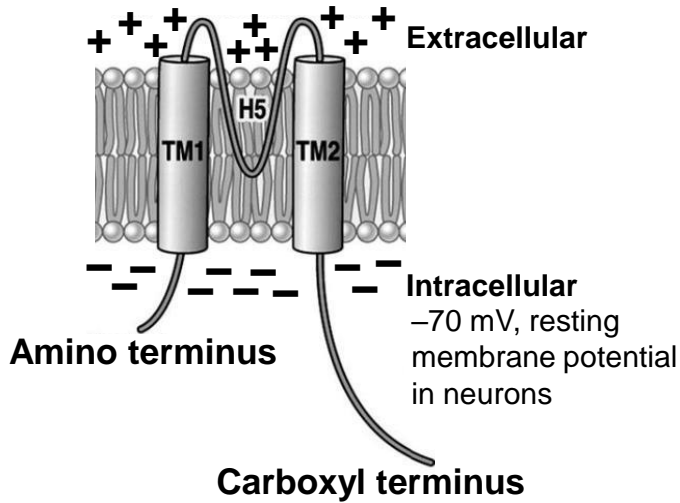
### **Physiological Relevance of Ion Channels**

The structural and combinatorial diversity of ion channels is the cornerstone of their tissue specificity and functional diversity. Ion selectivity, membrane expression, and responsiveness to biological or electrical stimuli are some of the features of channels that influence their role in cellular, tissue, organ, and even whole-organism physiology.<sup>1</sup> In the kidney, ion channels regulate ion balance between the blood and the urine. In the pancreas, ion channels are responsible for the appropriate release of insulin when blood glucose concentration increases after a meal. Most important to our work, they maintain the electrical signaling of excitable cells, notably the neurons of the brain.<sup>6</sup> Because of the scope of this work, we will focus our discussion to the importance of a specific family of K<sup>+</sup> channels in regulating neuronal action potential generation and intercellular signaling.

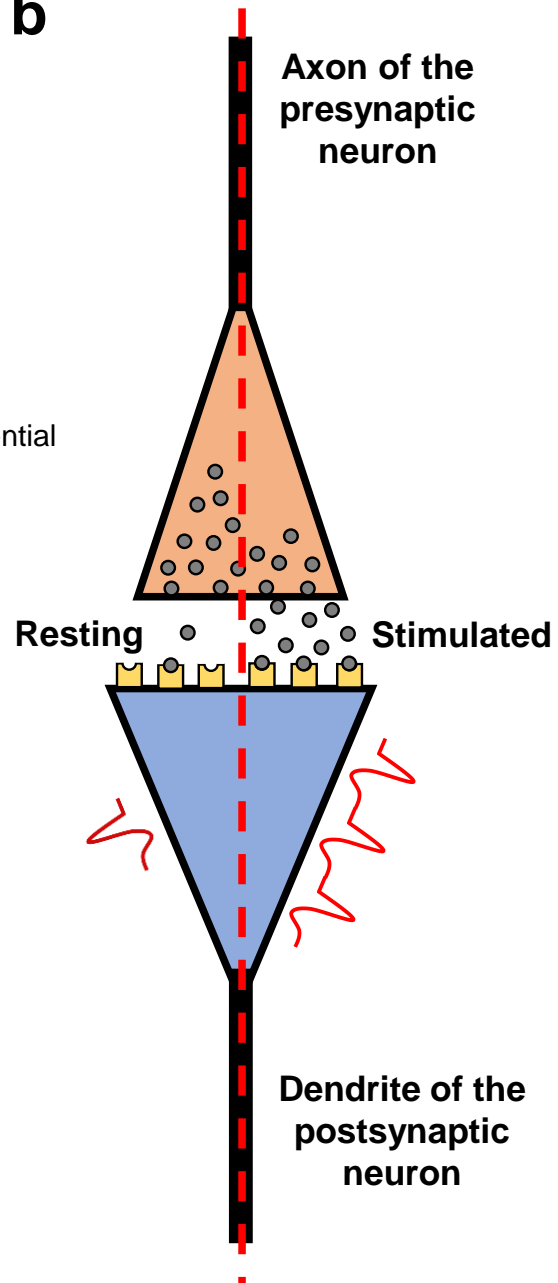
### **The Membrane Potential**

Excitable cells, such as neurons and cardiomyocytes, exploit the concentration gradients of water-soluble ions to create a small, but measurable, electrical voltage across their cellular membranes.<sup>1</sup> This is known as the membrane potential, which builds up due to the separation of ions across the selectively permeable cell membrane. The potential across the membrane at equilibrium, in neurons, is approximately  $-70$  mV (**Figure 3a**). By convention, a negative value indicates that the negative charge is on the intracellular surface of the cell membrane.

**a**  $K_{ir}$  channel subunit



**b**



**c**

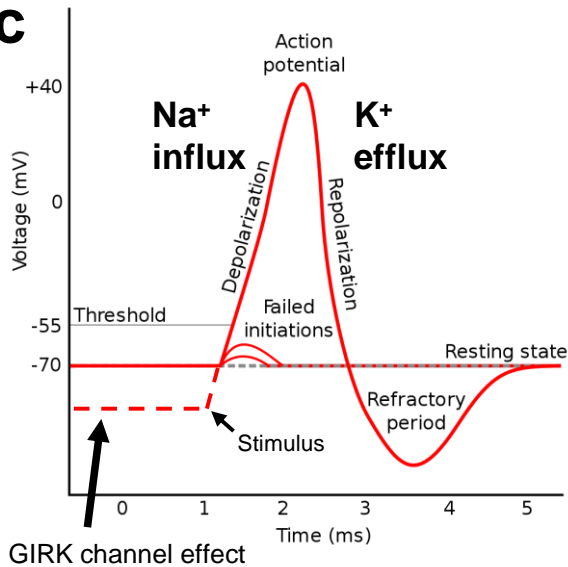


**Figure 3.** (a) The GIRK channel subunit structure and the separation of ions across cellular membranes. Figure adapted from Hibino, H., et al. *Physiol. Rev.* **2010**. (b) An excitatory neurotransmitter release from a presynaptic neuron onto a postsynaptic neurons generates an increased frequency of action potential firing. (c) The neuronal action potential and the interplay of channels function and ion movement involved. GIRK channel activation increases the stimulus required for the generation of an action potential. Adapted image originally created by Chris 73 for Wikipedia.org and is utilized under the Creative Commons License.



Before the value of the membrane potential could be measured experimentally, mathematical equations were developed to calculate the contribution of different ion gradients to the voltage potential. The Nernst equation, developed by Walther Nernst in 1887 (*Figure 3b*), enables calculation of the voltage generated by different concentrations of an ion across a non-permeable membrane.<sup>1</sup> This is also the membrane potential at which the flow of a specific ion across the membrane would be at equilibrium, called the reversal potential ( $E_{ion}$ ). For  $K^+$ , the reversal potential at equilibrium ( $E_K$ ) is approximately  $-85$  mV (*Figure 4a*). Later, scientists described the Goldman-Hodgkin-Katz voltage equation, which accounts for contribution of the various ion gradients to the voltage potential and enables the calculation of the resting membrane potential for an entire cell.<sup>1</sup> Eventually, researchers developed instrumentation that allowed the potentials given by these equations to be measured.

When ion channels open, the cellular membrane is no longer ion impermeable, and the flow of ions across the membrane affects the potential. The change in potential depends on the charge of the ions that cross and the direction in which these ions travel. Cations leaving the cell cause the potential to become more negative, while cations entering the cell cause the potential to become more positive. The shift of voltage potential away from the resting membrane potential towards, and beyond,  $0$  mV is known as depolarization. The shift of membrane potential more negative than the cellular equilibrium potential is known as hyperpolarization. By these standards, movement of  $Na^+$  into the cell causes cells to depolarize. For instance, this happens in a dramatic fashion upon the opening of voltage-gated  $Na^+$  ( $Na_v$ ) channels. When  $Na_v$  channels open, the influx of  $Na^+$  leads to the depolarization of the membrane, creating a very fast series of events on the neuronal cellular membrane, culminating in the perpetuation of signaling between neurons.<sup>1</sup>

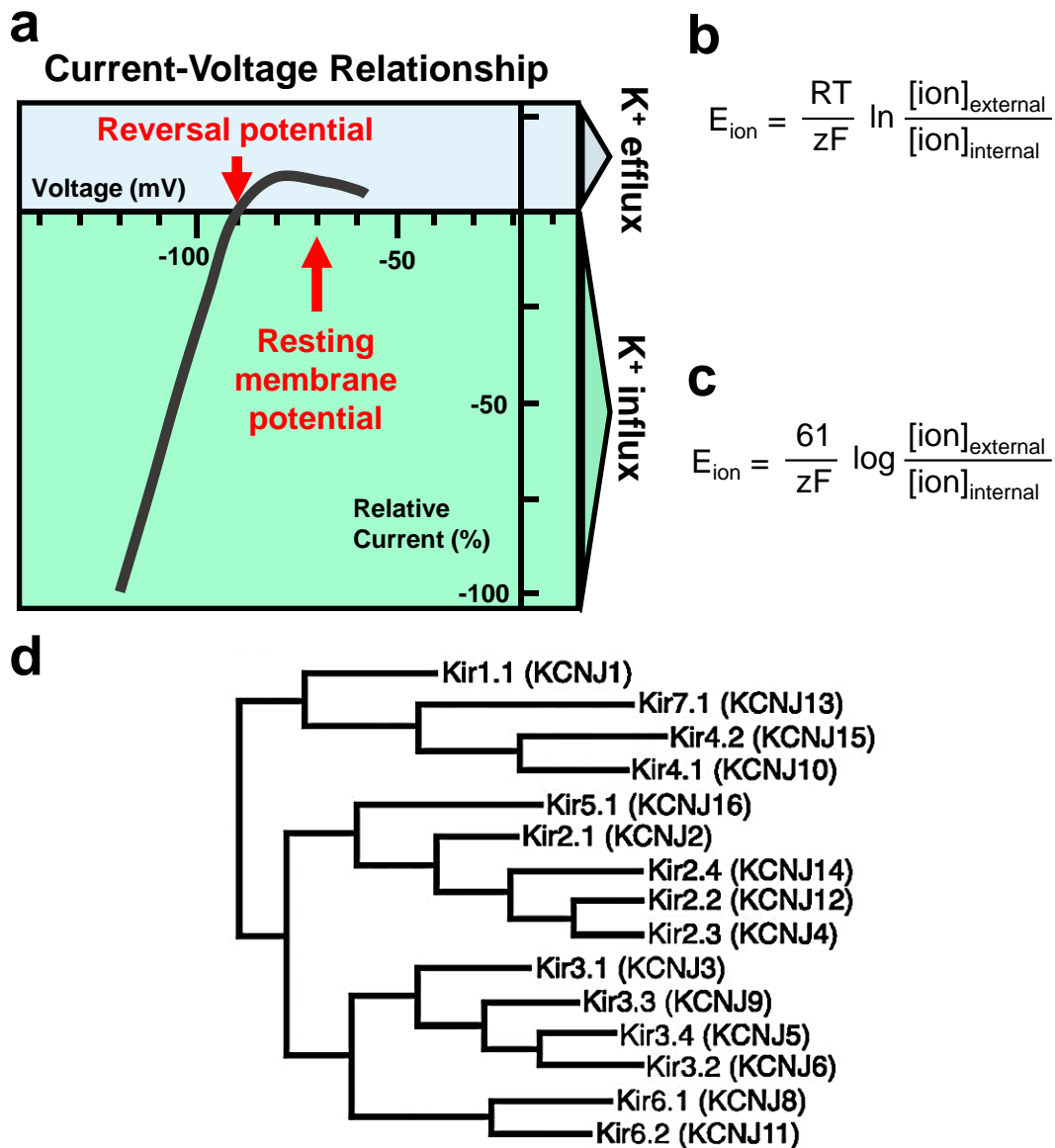


**Figure 4.** (a) The current-voltage relationship for GIRK channels, with a reversal potential of -85 mV. The neuronal resting membrane voltage potential of -70 mV is identified as well. Image adapted from Luscher *et al.*, *Nature Reviews*, **2010**. (b) The Nernst equation for calculating the reversal potential ( $E_{\text{ion}}$ ) of a specific ion across a cellular membrane. (c) The Nernst equation simplified for mammalian cells at 37 °C. (d) A family tree of the inwardly-rectifying potassium channels ( $K_{\text{ir}}$ ) family. Figure adapted from Hibino, H., *et al.* *Physiol. Rev.* **2010**.

## The Action Potential

The membrane potential is critical for the existence and manipulation of electrochemical communication between two neurons. The physical space where two neurons meet and interact is called a synapse (*Figure 3c*). At a synapse of an excitatory neuron, the presynaptic neuron, or the one generating a stimulus, attempts to create a response on the postsynaptic neuron, or the receiving neuron. The stimulus is neurotransmitter release from the presynaptic nerve terminal to the postsynaptic neuron. Although the actions of an individual neurotransmitter binding on the postsynaptic neuron may be small, the cumulative membrane potential change due to the activity of a large population of receptors may eventually depolarize the postsynaptic neuron and generate a measurable excitatory postsynaptic potential (EPSP). When multiple interactions between neurons generate enough EPSP to reach a threshold, at approximately  $-50$  mV for neurons, a bioelectrical phenomenon called the action potential has a drastically higher likelihood of occurring (*Figure 3b,c*).<sup>5</sup>

Action potentials are incredibly brisk ion density changes between the intracellular and extracellular spaces of a neuron. An action potential begins when  $\text{Na}_v$  channels open to allow for the immediate influx of  $\text{Na}^+$ . As this  $\text{Na}^+$  influx depolarizes the cellular membrane, it generates a cascade of events. First, voltage-gated  $\text{K}^+$  ( $\text{K}_v$ ) channels open and enable the efflux of  $\text{K}^+$ , which limits the extent of depolarization caused by the influx of  $\text{Na}^+$ . All the while, a consortium of transporters works to reestablish the membrane potential and concentration gradients, returning the neuron to equilibrium to prepare for the next action potential. The interplay of different ions and the effect on the membrane potential during an action potential is shown in *Figure 3c*.<sup>1</sup>

These changes propagate as a wave across the membrane of the neuron, from one part of a neuron to the next. The end goal of each of these action potentials is to integrate the activity of one

or more neurons onto a single neuron and to relay this activity down the axon to the synapse to mediate the release of neurotransmitters, which in turn modulates the activity of the next neuron it synapses with. In turn, such events mediate the generation of new action potentials on the adjoining neurons. Any biological process that alters the ease or difficulty of a neuron to generate an action potential modulates how neurons communicate. Ultimately, modifying the movement of a single ion species across the cellular membrane with a single ion channel population can alter the generation of actions potentials. Further, this can alter the behavior of excitable cells and the living organism they exist in. In this work, we describe the role of GIRK channels in modifying neuronal activity.<sup>1</sup>

### **An Introduction to G Protein-gated, Inwardly-rectifying, K<sup>+</sup> Channels**

Nearly 100 years ago, the first observation linking a physiological response modulated by GIRK channels was published.<sup>14</sup> In 1921, Dr. Loewi reported that he could move a solution from a stimulated heart to a non-stimulated heart and change the heart rate of the non-stimulated heart. He postulated that a chemical in his solutions was responsible for this activity. Little did he know that he was using secreted acetylcholine to stimulate muscarinic receptors, which then activated GIRK channels to hyperpolarize the cellular membrane and decrease heart rate. It took scientists until the 1990s to identify the genes encoding GIRK1/4 channels,<sup>15</sup> and to this day, scientists are working hard to more deeply understand the relationship between muscarinic receptors and GIRK channels.<sup>16</sup> Below, we curated what we do know, 100 years later, about GIRK channels and their physiological importance to the function of excitable cells.

GIRK channels, as their name describes, are gated by G proteins, display inward rectification, and are K<sup>+</sup> selective, all properties we will discuss below. Like most K<sup>+</sup> channels,

GIRK channels contain a  $K^+$  selectivity filter within their pore, which results in a significant preference for conducting  $K^+$ . GIRK channels are part the larger family of inwardly-rectifying  $K^+$  ( $K_{ir}$ ) channels, depicted in *Figure 4d*.<sup>3</sup> All of the  $K_{ir}$  channels exhibit channel rectification, which is a non-uniform inward and outward current through the channel. These channels have an inhibited, therefore limited, outward current, which means that  $K^+$  efflux is hindered (*Figure 5a*) and the outward currents through the channels are much smaller as compared to the inward current (*Figure 4a*). This is mechanistically achieved through block of the pore by intracellular magnesium ions ( $Mg^{2+}$ ) and polyamines (*Figure 5b*).<sup>17</sup> The outward current generated by a GIRK channel over the entirety of a cell is still significant even in light of inward rectification. When comparing the current through a GIRK channel over the various membrane potentials, under normal physiological neuronal conditions, which is  $-70$  mV for neurons, open GIRK channels mediate efflux of  $K^+$  (*Figure 4a*) across the cellular membrane. This leads to a stabilization of the membrane potential at the reversal potential of  $K^+$  ( $E_K$ ), making depolarization more difficult to accomplish, and, therefore, making action potentials more difficult to generate. In this way GIRK channels can mediate an inhibitory postsynaptic potential (IPSP) in neurons.<sup>18</sup> Because of an IPSP, action potentials are more difficult for a cell to generate, and cellular communication is modified. Hence, activating GIRK channels affects neuronal communication and, therefore, animal physiology. The endogenous control over the IPSPs through GIRK channels is heavily regulated by a varied array of cellular factors, which we will discuss in detail. But first, we will describe the GIRK channel expression throughout the body and the various insights gained through studying the structure of GIRKs before delving into GIRK channel regulation.

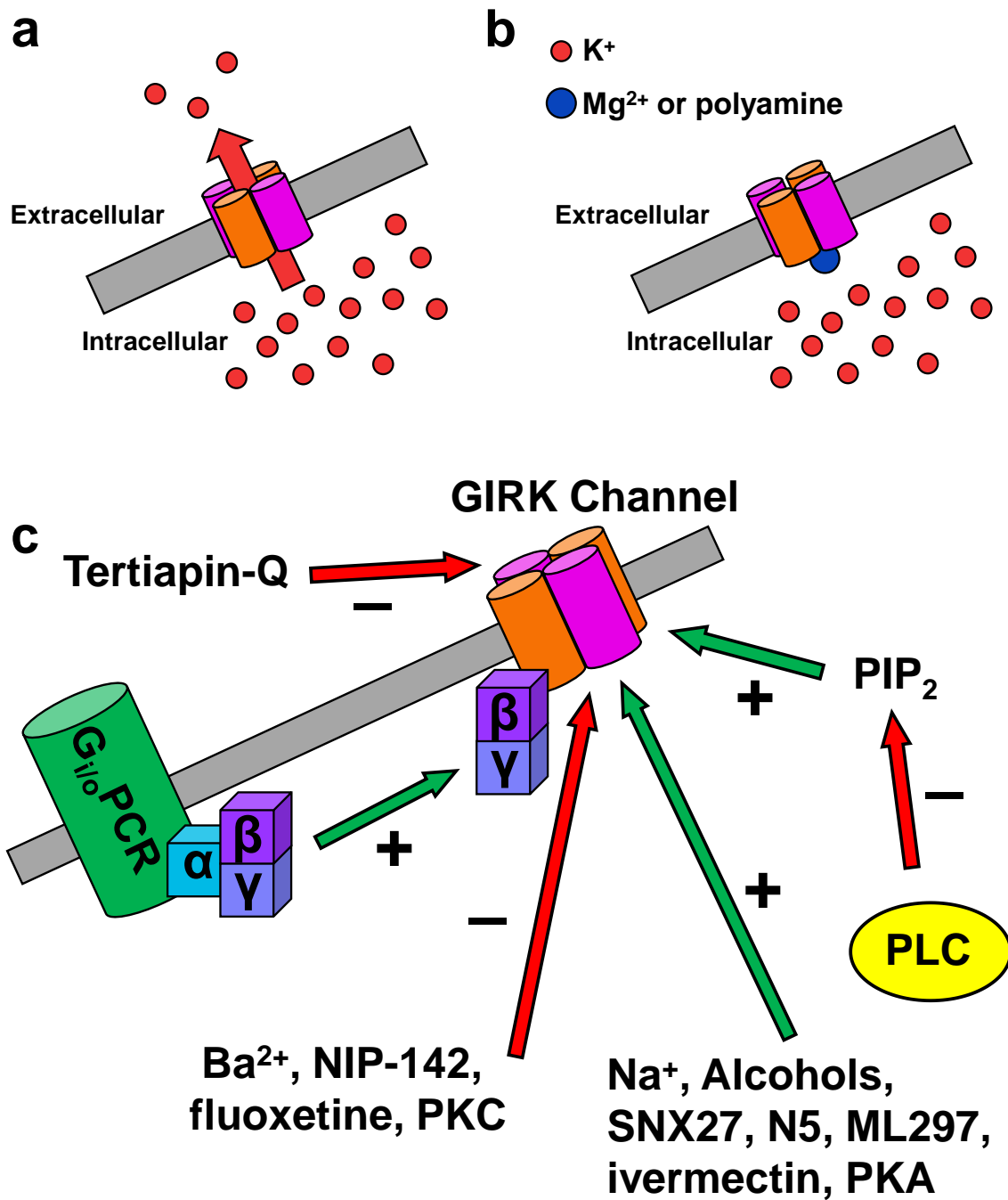


**Figure 5.** (a) GIRK channels efflux K<sup>+</sup> under normal physiological conditions. (b) Blockade of GIRK channels internally inhibits K<sup>+</sup> efflux and causes inward rectification. (c) GIRK channels activity and surface expression are regulated in a complex fashion by a variety of factors to change GIRK currents on cells.

## GIRK Channel Composition and Expression

The GIRK channel family, also known as the  $K_{ir}3$  family, is part of the larger inwardly-rectifying  $K^+$  ion channel family (**Figure 4d**). Specifically, the GIRK channel family is comprised of GIRK1, 2, 3, and 4 ( $K_{ir}3.1$ , 3.2, 3.3, and 3.4) subunits that are encoded by the KCNJ3, 6, 9, and 5 genes, respectively. These subunits contain both their amino and carboxyl termini intracellularly, with 2 transmembrane components to the channel (**Figure 3a**). Further, the GIRK2 subunit has 4 different isoforms, namely GIRK2a-d. Alone, a GIRK subunit does not form a channel; instead, these individual subunits form homotetrameric and heterotetrameric channels from combinations of the GIRK1-4 subunits (**Figure 6a**). However, the stoichiometry of GIRK channel assembly has not yet been proven. In reality, GIRK channels may assemble from 3 or 4 different subunits in all the possible stoichiometries. However, for simplicity in our discussions, we assume a 1:1 ratio of up to 2 different GIRK subunits in GIRK channels capable of forming heterotetramers.

Understanding the different channels that GIRK subunits can form is important in the scheme of tissue-specific GIRK channel expression. Throughout the body, differential GIRK channel expression between various human organs and cell types has been identified.<sup>7</sup> Briefly, GIRK1, GIRK2a-c, and GIRK3 subunits are widely expressed throughout the CNS<sup>4,19,20</sup> while GIRK1 and GIRK4 subunits are expressed predominantly throughout peripheral organs, i.e. in the heart<sup>21,22</sup> and pancreas.<sup>23</sup> **Figure 6b,c** illustrates an example of the channels we expect to find in brain and the heart. Due to the nearly ubiquitous expression of GIRK1 and the propensity of GIRK1 subunits to form heterotetrameric channels, homotetrameric GIRK channels, such as GIRK2 and GIRK4, are difficult to study. Wherever the GIRK1 subunit is expressed, GIRK1-containing GIRK (GIRK1/X) channels are therefore expressed. However, GIRK1 or GIRK3 homotetrameric channels are not believed to be expressed *in vivo*.<sup>6,20,21</sup> Therefore, while GIRK1/X

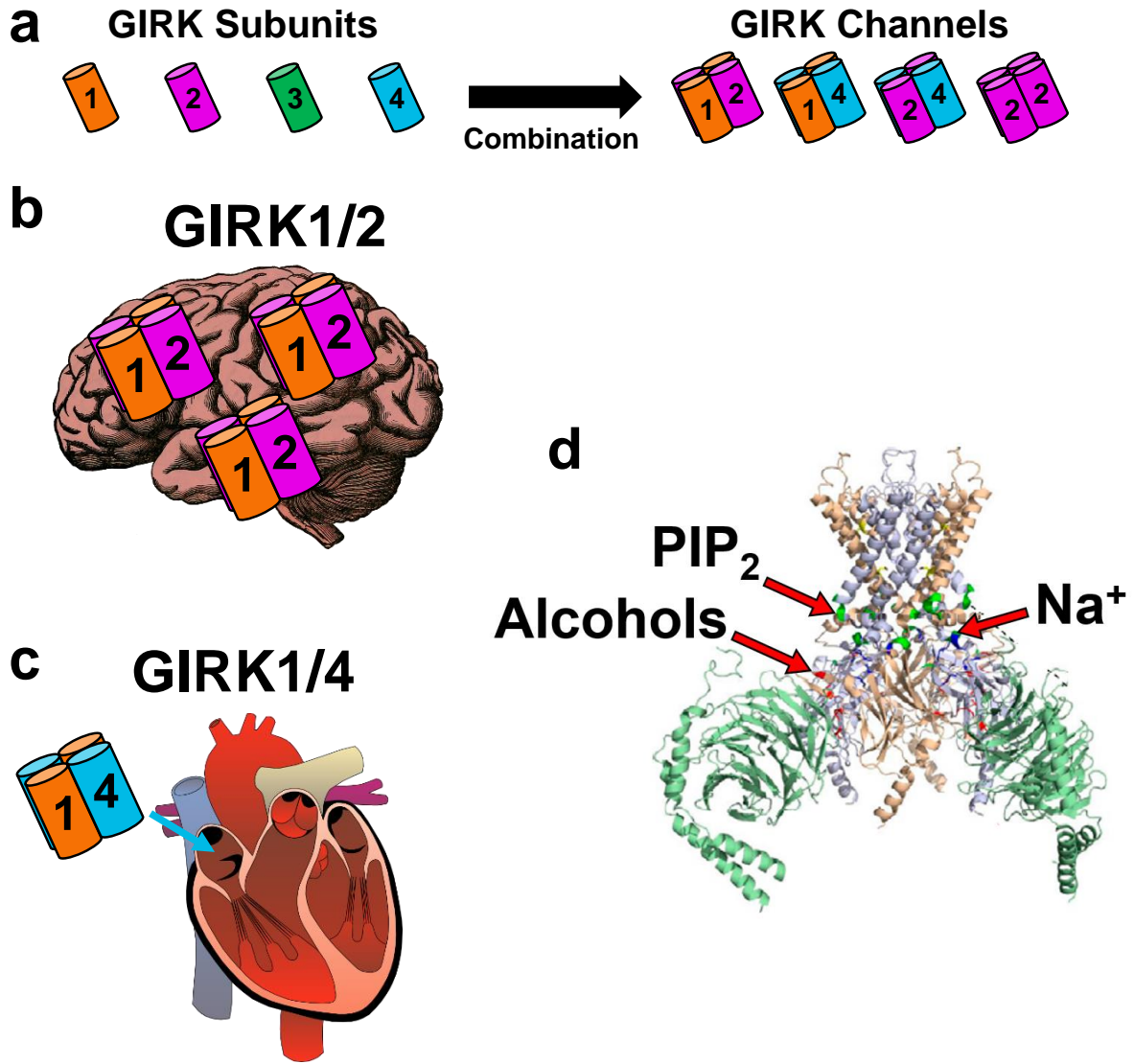


**Figure 6.** (a) GIRK channels are composed of four different subunits, namely GIRK1, GIRK2, GIRK3, and GIRK4. These subunits combine into homotetrameric and heterotetrameric channels throughout different organs in the body. (b) The prototypical GIRK channel expressed throughout the brain is GIRK1/2. (c) The sinoatrial node of the heart expresses GIRK1/2 channels. (d) The crystal structure was solved by the laboratory of Dr. MacKinnon. Figure adapted from Wydeven *et al.*, *PNAS*, 2014.



heterotetrameric channels are believed to be the most commonly found GIRK channels throughout the body, GIRK1 homotetramers are one less confounding factor to consider in our studies. However, non-GIRK1-containing GIRK (non-GIRK1/X) channels have been reported, using *in situ* hybridization, in discrete brain regions.<sup>4</sup> Due to their rarity, they are specific to certain cell types within tissue. For example, GIRK1 does not express in DA neurons of the VTA, while GIRK2 and GIRK3 subunits do.<sup>4,24</sup> Here, these subunits generate GIRK channels<sup>25</sup> that regulate the heavily-studied activity of circuitry underpinning reward and addiction.<sup>26-32</sup>

While the channels formed by the expression of GIRK1, GIRK2, and GIRK4 subunits in various combinations have been studied using fluorescence assays and decades of electrophysiology, the role of the GIRK3 subunit on GIRK channel function has only grown more puzzling. The case for GIRK3-containing GIRK channels on the cell membrane surface is difficult to make. Previous studies have demonstrated that the expression of GIRK1/3, and potentially GIRK2/3 and GIRK3/4, channels on the surface of cells may be limited by presence of GIRK3 due to a lysosomal targeting sequence near the C terminus on GIRK3.<sup>25,33</sup> Previous work by D. Ma, *et al.*<sup>25</sup> utilized engineered immortalized *Cercopithecus aethiops* kidney (COS-7) cells to express various GIRK subunits and to investigate the surface expression of GIRK1 subunits. They found that GIRK1 alone does not form channels and that GIRK1/3 channels do not appear on the cell surface membrane. Further, they found that expression of GIRK3 subunits decreased the surface localization of GIRK1 in cells already expressing GIRK1/2 and GIRK1/4 channels. While they did not study the currents in this last case, the general idea put forward is that GIRK3 subunits suppress plasma membrane GIRK channel expression by overriding GIRK2 and GIRK4 subunit forward trafficking signals. Kofuji *et al.* showed further, in *Xenopus* oocytes, that GIRK3 inhibits currents generated by GIRK2 channels.<sup>33</sup> On the other hand, newer studies claim that

GIRK2c/GIRK3 channels can be observed in murine neurons, but that these channels require the presence of a GIRK channel trafficking regulator (described below).

All in all, it is interesting to consider that GIRK3 is as widely expressed as GIRK1 throughout the body, but its ability to form channels is still uncertain. While the field is still resolving the role of GIRK3 subunits, the true function of GIRK3 subunits is not of immediate concern throughout the studies described within because we utilized engineered cell lines that have not been shown to express GIRK3 subunits. Therefore, when we express GIRK1, GIRK2, and GIRK4 subunits within cells, we expect and, in fact, observe channels formed by these subunits to the cell surface.

## **G Protein-Coupled Receptors and Phosphatidylinositol 4,5-bisphosphate Regulate GIRK Channels**

Modulation of GIRK channel activity by a variety of intracellular proteins and ligands has been studied since the channels' discovery.<sup>34</sup> True to their name, GIRK channel activity is regulated by G protein-coupled receptors (GPCRs), which are a major class of cell surface receptors fundamental to cellular signaling. G proteins are a key regulator of GIRK channel activity. G proteins are heterotrimeric proteins comprise of an  $\alpha$  subunit and a  $\beta\gamma$  subunit that comprise 3 major intracellular signaling pathways, namely the  $G_s$ ,  $G_{i/o}$ , and  $G_q$  protein signaling pathways. Certain GPCRs are preferentially bound to specific G proteins; one such group are the  $G_{i/o}$  protein-coupled GPCRs. This  $G_{i/o}$  protein pathway is the major regulator of GIRK channel activity. GIRK activity is increased when a ligand binds to a  $G_{i/o}$  protein-coupled GPCR and signals through the  $G_{i/o}\beta\gamma$  subunit, which is released when the trimeric  $G_{i/o}$  proteins undergo a conformational change.<sup>35</sup> Both the separated  $G_{i/o}\beta\gamma$  and  $G_{i/o}\alpha$  subunits generate intracellular

responses. A released  $G_{i/o}\beta\gamma$  subunit activates GIRK channels.<sup>36,37</sup> This originally controversial pathway is now generally accepted as the mechanism of the GPCR to GIRK signaling pathway. Early on, investigators were unsure whether the  $G\alpha$  or the  $G\beta\gamma$  subunits activated GIRK channels after receptor activation. Even now, researchers continue to investigate the regulation of GIRK channel activity by  $G_{i/o}\alpha$  subunits.<sup>38</sup>

Phosphatidylinositol 4,5-bisphosphate ( $PIP_2$ ) binding to GIRK channels is essential for the channel to open, while the  $G_{i/o}\beta\gamma$  subunit is thought to facilitate the binding of  $PIP_2$ .<sup>15</sup> Together,  $G_{i/o}$  proteins and  $PIP_2$  are the major endogenous intracellular GIRK channel regulators. Intracellular modulation of  $PIP_2$  in turn affects GIRK channel activity.<sup>39</sup> This leads to a dynamic environment in which  $G_q$  protein signaling modulates  $PIP_2$ , since  $PIP_2$  is a substrate for phospholipase C (PLC). PLC is a downstream effector of  $G_q$  protein-coupled GPCR activation,<sup>40</sup> and PLC degrades intracellular  $PIP_2$ . Degradation of  $PIP_2$  causes the loss of  $PIP_2$  from GIRK channels, inhibiting GIRK channel activity. This mechanism underlies the cardiac pacing equilibrium that is in part controlled through GIRK1/4 channels. In hearts, acetylcholine regulation of heart rate is balanced between the  $G_{i/o}$  and  $G_q$  signaling through different types of the muscarinic acetylcholine receptors.  $G_{i/o}$  signaling slows heart rate by increasing GIRK1/4 currents while  $G_q$  signaling inhibits the extent to which GIRK1/4 channels are activated.

### **Additional Regulators of GIRK Channel Function**

GIRK channels are regulated by multiple intracellular mechanisms aside from GPCR signaling (*Figure 5c*). Increased intracellular  $Na^+$  concentrations increase  $Na^+$  binding to GIRK channels and enhance their activity.<sup>41</sup> Cholesterol interacts with GIRK channels at the cell membrane, but the exact function has not been resolved. In some studies, cholesterol has been

shown to downregulate GIRK channels, while other works have demonstrated it to upregulate GIRK channels.<sup>42-44</sup> GIRK can be phosphorylated by protein kinase A (PKA),<sup>45,46</sup> which has been shown to increase GIRK channel activity. On the other hand, GIRK has been demonstrated to be phosphorylated by protein kinase C (PKC),<sup>47</sup> which has been shown to decrease GIRK channel activity. Early on, GIRK channels were also identified as potentially one of the many physiologically-important targets of alcohol action,<sup>48</sup> and, eventually, a discrete alcohol binding pocket on GIRK channels was discovered and characterized.<sup>49-51</sup> Binding of alcohols to GIRK channels increases channel activity, and a variety of alcohols have been shown to be active, from ethanol to larger species, such as 2-methyl-2,4-pentanediol.

While GIRK channel modulation by a broad array of factors and proteins has been thoroughly studied, none of these entities can serve as tool compounds to selectively modulate and study the activity of GIRK channels in *ex vivo* or *in vivo* systems. Hence, our laboratory and others have aimed to discover synthetic GIRK channel modulators to serve as probes, efforts we describe in further detail later on.

### **Natural and Synthetic Modulators of GIRK Channel Trafficking**

Endosomal sorting nexin 27 (SNX27), an intracellular protein containing a PDZ domain, has been demonstrated to be important to the trafficking and surface expression of certain GIRK channels.<sup>52,53</sup> PDZ domains are common structural domains on proteins that modulate anchoring of membrane proteins to cytoskeletal structures. GIRK2c (the longer isoform of the GIRK2 subunit that we have herein referred to as simply GIRK2) and GIRK3 both have a PDZ binding motif, namely “E(N/S)ESKV,” on their C terminus. SNX27 reportedly regulates GIRK2c and GIRK3 subunit surface trafficking, potentially being a critical element in the surface trafficking of GIRK2c

homotetrameric channels and GIRK2c/3 heterotetrameric channels.<sup>29</sup> If this mechanism can be utilized to generate the surface expression of GIRK2/GIRK3 channels in engineered cell lines, then it will enable the exploration of GIRK modulator activity on GIRK2/3 channels, which has yet to be accomplished through our work and the work of others.

### **Information Gleaned from the Crystal Structure of GIRK2 Channels**

When GIRK channel modulation by ligands was initially studied, site-directed mutagenesis was used to pinpoint the amino acids involved in binding. However, with the advancement of protein X-ray crystallography at the McKinnon laboratory, many K<sup>+</sup> channel crystal structures have been quickly solved. One of the channels solved, described by Wharton *et al.*,<sup>54</sup> was the GIRK2 homotetramer. This structure provided the field with considerable insight into GIRK channel structure and function. One of the most impressive feats was discovering the binding sites for several GIRK ligands and partner, including PIP<sub>2</sub>, Na<sup>+</sup>, and the G<sub>i/o</sub>βγ subunit (**Figure 6d**).<sup>11</sup> This work informed further mutations that studied the binding of these ligands and other, such as the alcohols. Although many GIRK channel binding site mutants were known before the crystal structure, this work enabled the generation of additional mutants, which confirmed the binding sites identified from the crystal structure. A variety of mutants around the PIP<sub>2</sub> pocket revealed how important PIP<sub>2</sub> is to GIRK channel activity.<sup>15</sup> Being able to observe the GIRK2 channel structure also informed the gating order of the channels, in which binding of the G<sub>i/o</sub>βγ subunit stabilizes the binding pocket for PIP<sub>2</sub>, which facilitates channel opening when bound, further described below. Further, this structure also enabled the localization of the alcohol binding pocket on GIRK channels.<sup>49-51</sup> The relationships between these ligands and GIRK channel activity are described in further detail in the following sections.

## **GIRK Channels in Normal and Pathological Physiology**

Researchers have utilized a multitude of methods to elucidate the functioning of GIRK channels. Some of the physiological processes regulated by GIRK channels have been identified from the investigation of GIRK channel knock-out animal models, while other have utilized GIRK channel knock-in animal models. Further, these animal models could be whole-body manipulations or targeted to a specific subset of cells. Also, modulation of GIRK channels with small molecules has already identified a variety of important functions of GIRK channels. Finally, the investigations into mutations and alterations of GIRK channel expression and function in human beings through reports of pathological physiology by medical professionals has also shed light on GIRK channel importance in physiology.

Overarchingly, GIRK channels modulate the excitability of excitable cells, such as neurons and cardiomyocytes, by limiting membrane depolarization. However, the signaling which enables GIRK channel function stems from the  $G_{i/o}$  protein-coupled GPCRs, as described above. One way to consider the importance of GIRK channels throughout physiology is to consider the function and tissue specificity of the  $G_{i/o}$  protein-coupled GPCRs that signal to GIRK channels. For example, GIRK channels in the heart couple with subtypes of muscarinic acetylcholine receptors, while GIRK channels in the CNS couple with subtypes of opioid, dopamine,  $GABA_B$ R, and serotonin receptors. By understanding the physiological effects induced by the receptors that signal through GIRK channels, we glimpse the potential disease mechanisms that may be regulated through direct GIRK channel activation or inhibition. Many studies investigating the function of GIRK channels from various research angles have demonstrated that GIRK channels are important in the function of neural processes<sup>6</sup> such as analgesia,<sup>55</sup> reward,<sup>26-31</sup> anxiety,<sup>56</sup> memory,<sup>57</sup> respiration,<sup>58</sup> and seizures.<sup>59</sup> Beyond the CNS, GIRK channels are critical in embryonic

development,<sup>60-62</sup> regulation of heart rate,<sup>63,64</sup> and hormone secretion.<sup>65,66</sup> Above, we discussed how different GIRK subunits are differentially expressed throughout the body. From here, we can assume certain combinations of these channels are therefore implicated in the functions of the tissues they are expressed in. Modulating these particular channels in their specific tissues may be a mechanism by which to modulate physiology. For example, GIRK1/4 channels are critical to establishing a stable heart rate; therefore, inhibition of GIRK1/4 in the heart is considered a prime mechanism for the inhibition of atrial fibrillation.<sup>67</sup> Further, GIRK1/2 channels have been demonstrated to be critical for opioid-induced analgesia,<sup>68</sup> and recently our laboratory has demonstrated that GIRK1/2 activation with selective activators can modulate opioid-induced analgesia (unpublished results).

One early example of GIRK channel malfunction due to a specific GIRK subunit was identified by researchers through the study of the *weaver* mouse, a mutant mouse with a neurologic phenotype. The *weaver* mouse has been studied extensively since its generation over 50 years ago.<sup>69</sup> This mouse was found to have a mutation in the pore of GIRK2 such that the channel was no longer K<sup>+</sup> selective and allowed a Na<sup>+</sup> conductance.<sup>70</sup> The main phenotype of this mouse was ataxia, which implicated GIRK2 involvement in control of movement. Since then, specific GIRK channel knockouts have been generated and studied. Using direct genetic manipulations of GIRK channels in animal models, researchers have demonstrated that GIRK subunit manipulations do indeed alter the physiology of animals. For example, various GIRK knock-out mice have been tested in models related to locomotor activity and self-administration of drugs such as cocaine, ethanol, and morphine. The various GIRK subunit manipulations exert different effects on animal behavior while decreasing GIRK currents.<sup>71</sup> However, no unifying hypothesis can yet be proposed due to variable responses that depended on whether whole-body or cell-specific manipulations of

GIRK subunits were conducted and that also depended on which specific compound was tested.<sup>71</sup> Nevertheless, this work has demonstrated that GIRK channels are important to CNS functioning and that further investigations are warranted.

The manner by which the GIRK channels are altered through genetic mutations is important in understanding the physiological implications. When GIRK channels are knocked out, cells lose the ability to respond appropriately to GPCR signaling. However, if a mutation creates a GIRK channel with altered properties, such as a failure to correctly rectify currents or conductations, cellular signaling may have unexpected and detrimental results. In either case, cellular membrane excitability becomes dysregulated and normal cellular signaling becomes disrupted. This leads to breakdown of normal physiological functioning and may result in disease.

Observations by the medical community confirm that proper GIRK channel function is important in human physiology. Recently, several patients with GIRK2 subunit mutations have been reported. These individuals presented with Keppen-Lubinsky Syndrome<sup>60</sup> (KLS), which occurs when the GIRK pore is modified by a deletion or mutation. The resulting clinical features are characterized by severe developmental delay, intellectual disability, microcephaly, facial malformation, and an aged appearance.<sup>60</sup> The authors note these are all features consistent with a generalized lipodystrophy disorder. While the overall phenotype of KLS is likely the result of the multifaceted utility of GIRK channels in physiology and one of many disease processes stemming from inappropriate GPCR signaling, further study of KLS is warranted to determine the impact of the channel malfunction. Furthermore, since the mutation is in the GIRK2 subunit, modulators of GIRK2-containing channels, such as GIRK2 homotetrameric channels described in our work herein, may be of use and potential therapeutic value.



In summary, GIRK channels are essential for normal human functioning and cause potentially severe pathology if altered. To better understand GIRK channel function and the potential value of GIRK channel-modulating therapies, we proposed and pursued the development of potent, efficacious, and subunit- or channel-specific pharmacological probes. We focused our efforts on describing the role that GIRK2 channels and their potential modulators may play in drug addiction and abuse.

### **A Brief Overview of Opioid and Alcohol Drug Abuse in the United States of America**

Two major drug classes are causing widespread concern throughout the USA. Opioid and alcohol addiction and abuse have led to the deaths of >160,000 Americans in 2017 alone. In 2016, approximately 15 million Americans had an alcohol use disorder while approximately 2 million people had an opioid use disorder.<sup>72</sup> To assess drug abuse from a monetary perspective, excessive drinking alone cost Americans \$249 billion in 2010.<sup>73</sup> Of the 15 million Americans with an alcohol use disorder, 1.1 million reported very heavy alcohol use.<sup>72</sup> Deaths attributable to excessive alcohol use number >88,000 people each year, and this statistic is now almost a decade out of date.<sup>74</sup> Over the past several years, however, opioid abuse has quickly become an epidemic of its own in the USA.

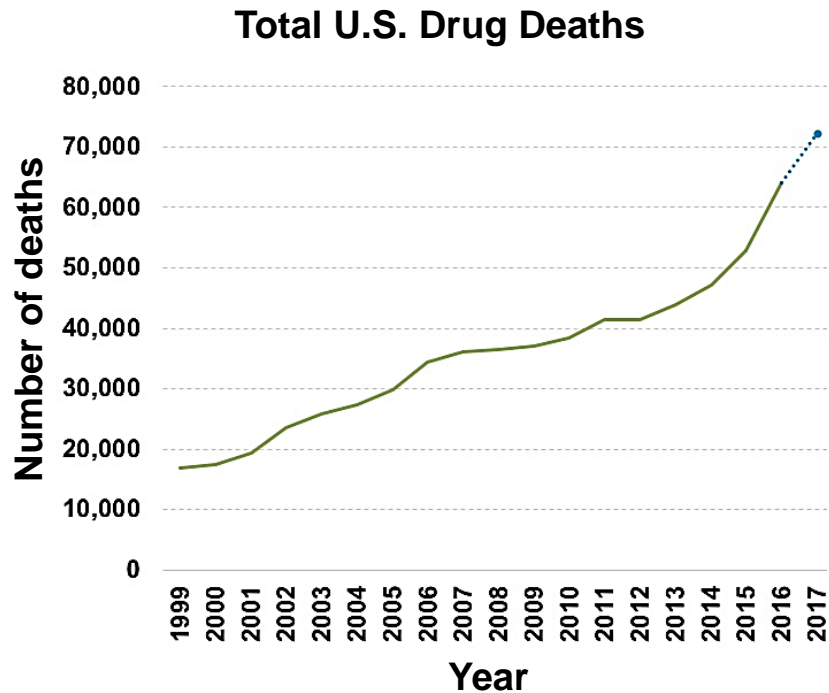
Opioids are some of the most effective pain medications, but they are also extremely addictive. Hydrocodone is the most commonly prescribed<sup>75</sup> opioid for temporary and chronic neuropathic pain; it is also the most abused. In 2016, an estimated 1.8 million Americans had a prescription pain reliever use disorder, while 11.5 million people were estimated to have misused a prescription pain reliever at least once in the year.<sup>72</sup> When abused, these medications serve as gateway drugs to heroin or illegally-obtained pills when legal means of obtaining opioids are

exhausted. Both of these alternatives are illegal and have shown to be incredibly dangerous. Heroin use more than tripled since 2000<sup>76</sup> and deaths from heroin overdose have doubled since 2012, to 16,000 individuals per year.<sup>77</sup> However, fentanyl and its analogs have truly revealed the extent of the opioid epidemic in the USA.

Synthetic opioids, namely fentanyl and its analogs, are often illegally pressed into pills and disguised as the other, less potent opioids that people are accustomed to abusing. However, due to the incredible potency of fentanyl and its analogs, they are now responsible for >40% of opioid overdose deaths, an increase of ~25,000 deaths in only five years (*Figure 7b*).<sup>77</sup> Before 2012, opioids claimed ~25,000 lives each year, half of which were due to prescription opioids. However, that number has risen to >50,000 deaths in 2017,<sup>77,78</sup> a staggering increase of >100% (*Figure 7a*). The unfortunate reality is that opioid overdose deaths occur upon ingestion of a much higher dose of the drug than an individual's neural circuitry is accustomed to or capable of handling. In these cases, respiratory depression occurs, breathing is inhibited, and the individual passes away.<sup>79</sup> Very likely, a large proportion of these deaths were due to illegal narcotic supplies tainted with synthetic opioids.

Taken together, these sobering statistics indicate a widespread problem with addictive substances throughout the USA. The difficulty in combating these issues is demonstrated by the large numbers of substance abusers and the unrelenting number of deaths. Tennessee is one of the states hit hardest by the opioid epidemic. Substance abusers and addicts need relief from their addictions, either by preventing addiction from the onset or by helping to cure existing addictions; however, the current available treatments are not sufficient. Fortunately, research into understanding the underlying mechanisms of addiction has intensified and aims to illuminate new paths for the prevention and treatment of addiction. One such area of focus involves GIRK

**a**



**b**

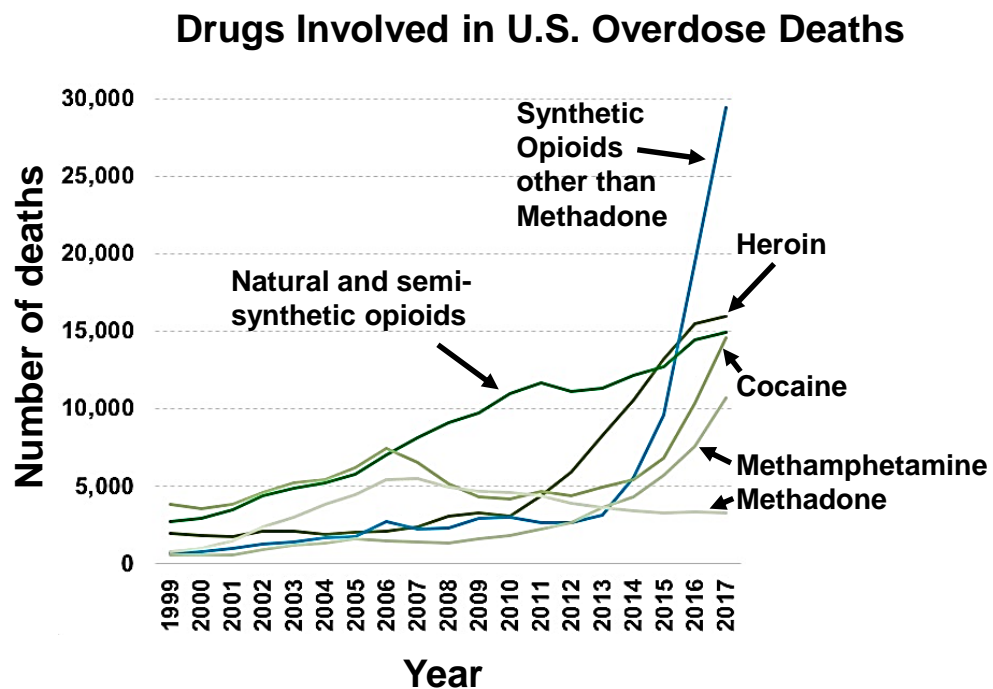


**Figure 7.** (a) More than 72,000 drug overdose deaths were estimated in 2017. (b) The breakdown of these deaths based on compound shows the greatest increase was those due to fentanyl and its analogs. Graphs adapted from: <https://www.drugabuse.gov/>. Data source: CDC WONDER.

channels.<sup>5,7,80</sup> Below, we describe the specific GIRK-based mechanisms critical to neuronal signaling underlying reward and addiction processes.

### **Non-GIRK1/X Channel Involvement in Processes Underlying Addiction and Drug Abuse**

GIRK1, GIRK2, and GIRK3 subunits are widely expressed throughout the CNS.<sup>4,20</sup> Non-GIRK1/X channels have been reported in a few discrete brain regions.<sup>4</sup> For example, the DA neurons of the VTA do not express GIRK1, but do express GIRK2 and GIRK3 subunits.<sup>24</sup> On the other hand, GABAergic (GABA<sub>B</sub>) neurons in the VTA express all 3 GIRK subunits.<sup>30</sup> When opioids and other drugs of abuse modulate the activity of the VTA, they alter the activity of these neurons in the VTA. Further, by altering the activity of VTA DA neurons, opioids alter DA signaling to the nucleus accumbens, a pathway critically involved in drug-induced seeking behavior.<sup>5</sup> Hence, VTA DA neurons became a target of immense interest when non-GIRK1/X channels became implicated as a specific target centrally involved in regulating key circuitry in reward and addiction.

Multiple laboratories are studying how GIRK2 and GIRK3 subunits regulate addiction and reward circuitry.<sup>26-32</sup> To date, researchers have demonstrated that the effect of addictive substances, such as ethanol,<sup>27</sup> opioids,<sup>30</sup> and methamphetamine,<sup>26</sup> on neuronal activity and animal behavior is indeed dependent on the expression of GIRK3 subunits in VTA DA neurons. Specifically for opioids, selective GIRK3 knockout in VTA DA neurons inhibited morphine-induced motor activity, a phenotype seen in mice given high doses of opioids.<sup>30</sup> On the other hand, morphine-induced motor activity was increased in animals with whole-animal GIRK2 knockout. Further, these researchers showed that the physiological effects of morphine were not due to the GABAergic population of VTA neurons. Considering the previous discussion surrounding GIRK3

as a negative regulator of surface GIRK channel expression, we propose a model in which increased GIRK2 expression and function decreases the negative effects of opioid abuse.

Altogether, past research suggests that modulation of non-GIRK1/X channels in the VTA may alter DA neuron activity and provide a mechanism for regulating the neuronal circuitry involved in reward and addiction. While future research focused on genetically modulating GIRK channels will continue to improve our understanding of GIRK channel involvement in drug abuse, we are excited about the development of pharmacological tools to help confirm whether non-GIRK1/X channels may be a top target for development of therapies to help combat the deadly opioid epidemic.

Alcohols, such as ethanol, bind and activate GIRK2 channels. While this evidence may suggest that GIRK channels play a critical role in generating the acute or chronic negative effects of alcohol abuse, alcohols also have many other targets throughout the CNS, the most famous one of which is GABA<sub>A</sub>R,<sup>81</sup> a Cys-loop receptor (discussed in detail in **Chapter 3**). GABA<sub>A</sub>R activation also generates IPSPs and exerts similar effects on neurons as GIRK channels. Therefore, studying the role of each in the alcohol addiction disease process is difficult. Hence, we describe the utility of selective GIRK channel modulators in the study of physiology.

### **The Utility of Selective GIRK Channel Modulators**

Genetic knockout studies are useful in determining the consequence of manipulating GIRK channel expression on tissue function or whole animal physiology. In order to determine the effect that changing the activity, but not expression, of a GIRK channel may have on animal physiology, scientists require molecular modulators of GIRK channel function. Further, due to the variety of GIRK channel combinations that are present throughout tissues, selective modulators of GIRK channel function are required. Ideally, subunit-specific pharmacological tools would enable the

identification of certain GIRK channel populations within tissues and cells. The ability to selectively activate a desired GIRK channel is useful first and foremost to probe whether any specific GIRK channel combination is expressed and functioning within the target of interest. In an ideal world, potent and efficacious small molecule ligands targeting specific channels would exist and such work would be possible. In order to create such compounds, our laboratory and others have expended much effort toward the discovery and development of GIRK channel modulators. Although we have made progress, only a few efficacious, potent, and selective compounds have been discovered and reported.

### **Previous Discoveries and Reports of GIRK Channel Activators**

Previously, our laboratory discovered and characterized a number of small molecule activators of GIRK1/X channels from a high-throughput screen. These modulators have proved highly useful as probes to investigate a variety of GIRK-expressing systems, i.e. the CNS.<sup>56,59,82–84</sup> They show extraordinary selectivity for GIRK1/X channels.<sup>85,86</sup> ML297,<sup>59,82</sup> was the first potent, effective, and selective GIRK1/X channel activator we reported (**Figure 8**). In brief, we found that ML297 activity was dependent on PIP<sub>2</sub> but independent of G<sub>i/o</sub>βγ protein activity.<sup>56</sup> We continued to study analogs of ML297 in an effort to discover more potent, efficacious, and selective molecules. From this work, we discovered VU0466551, which maintained selectivity for and demonstrated increased efficacy and potency on GIRK1/X channels (**Figure 8**).<sup>84</sup> Additional analogs of these compounds were identified to be GIRK1/X inhibitors, and we were further able to develop analogs that demonstrated selectivity between GIRK1/2 and GIRK1/4 channels.<sup>84</sup> We have also identified analogs that do not require the biaryl urea core for activity on GIRK1/X channels.<sup>87</sup> More recently and in collaboration with the laboratory of Dr. Dirk Trauner, we

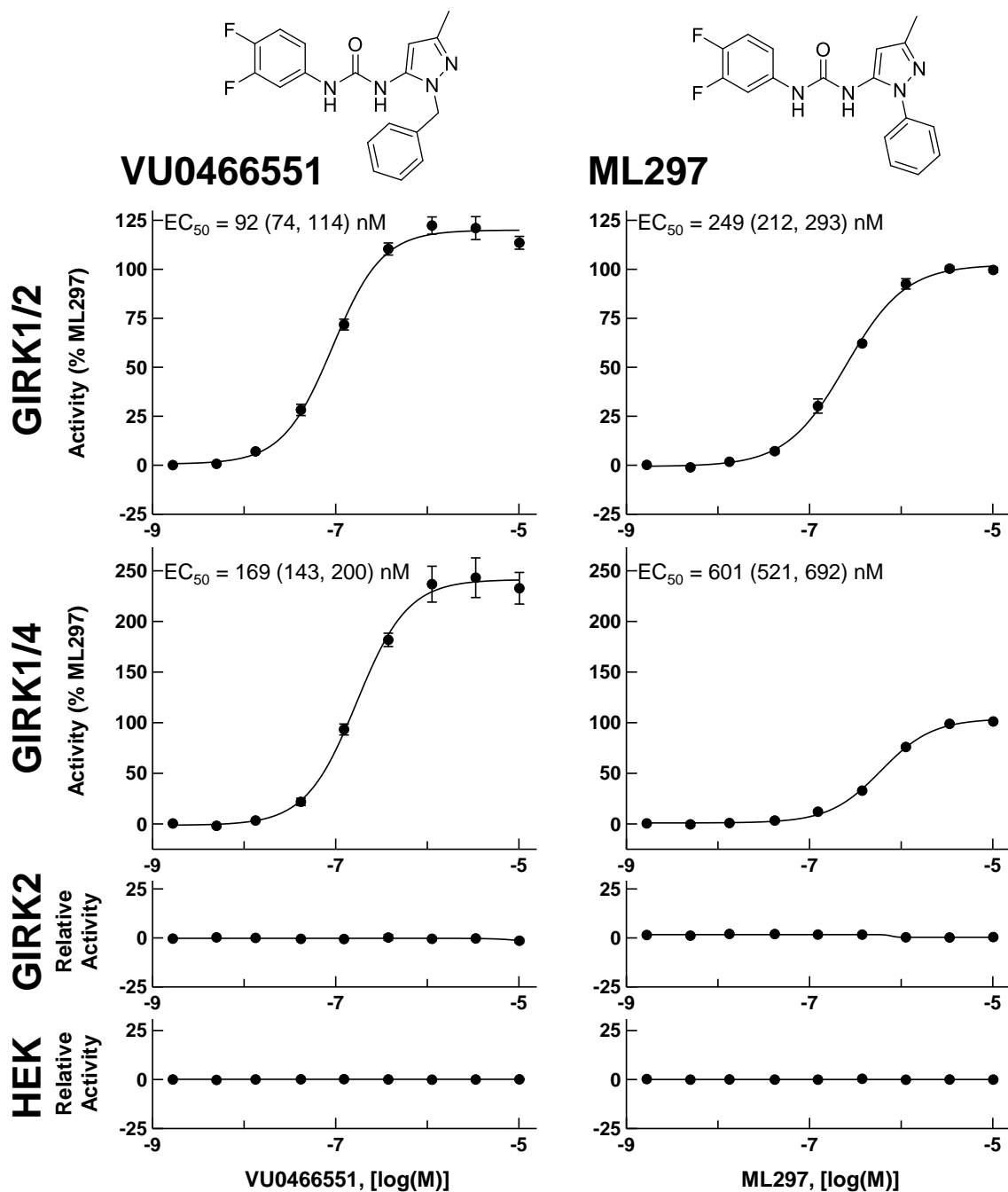


**Figure 8.** Characterization of VU0466551 and ML297 efficacy and potency using Tl<sup>+</sup> flux on untransfected HEK293 cells and HEK293 cells expressing GIRK1/2, GIRK1/4, and GIRK2. Potency (EC<sub>50</sub>) values were provided for active compounds along with 95% confidence intervals. GIRK1/2 and GIRK1/4 channel activity was normalized to a maximally-effective concentration of ML297. All data shown are averages of at least 3 independent experiments, and the error bars represent the standard error of the mean (SEM).

identified analogs that contain a photoswitchable azobenzene, which generated a light operated GIRK channel activator.<sup>83</sup> Such high utility from a single scaffold has been highly rewarding and required extensive medicinal chemistry efforts such that we have developed and tested nearly 800 analogs of ML297. In addition to this chemistry, we have studied the binding of these molecules. We discovered that the amino acids F137 and D173 of GIRK1 were necessary and sufficient for the selectivity of ML297 and its analogs.<sup>56</sup> However, even with such a tremendous amount of study surrounding these compounds, we never identified an analog that could activate non-GIRK1/X channels.

During the development and validation of a high-throughput assay designed to allow the discovery of GIRK2 modulators, we discovered that abamectin could activate GIRK1/2 and GIRK2 channels. Su *et al.*<sup>88</sup> and Chen *et al.*<sup>89</sup> have recently published and characterized the activity of ivermectin, an analog of abamectin, on GIRK1/2 and GIRK2 channels as well. Abamectin and ivermectin belong to the avermectin family of macrocyclic lactones, which have been utilized as insecticides<sup>90</sup> and antihelminthic medications<sup>91</sup> in human and veterinary medicine for decades. Most of these compounds contain a disaccharide moiety. Interestingly, many years prior, the compound naringin, which contains a similar moiety, was reported to activate GIRKs, but with very low potency (>100  $\mu$ M on GIRK1/X channels expressed in *Xenopus* oocytes),<sup>92</sup> and our laboratory has never been able to replicate these findings in GIRK-expressing HEK293 cells using thallium ( $Tl^+$ ) flux assays. All in all, we expect that our previous work will not be the end of efforts towards more potent and efficacious GIRK1/X channel activators. We will continue to report and improve the tools with which GIRK1/X channels can be studied.



## Previous Discoveries and Reports of GIRK Channel Inhibitors

The pharmacology of GIRK channel inhibitors has been more widely explored. K<sup>+</sup> channels in general are inhibited by a plethora of small molecules. Further, GIRK channels are inhibited by broadly-acting K<sup>+</sup> channel blockers, such as the barium (Ba<sup>2+</sup>) and cesium ions (Cs<sup>+</sup>),<sup>21,93</sup> and molecules that are known to modulate other targets, such as SCH-23390,<sup>94</sup> fluoxetine,<sup>95</sup> paroxetine,<sup>96</sup> ifenprodil,<sup>97</sup> NIP-142,<sup>67,98,99</sup> and VU573.<sup>100</sup> A plethora of antidepressant molecules have been demonstrated to be GIRK channel inhibitors,<sup>101,102</sup> which is an interesting observation that is unfortunately outside of the scope of this work. Nevertheless, these compounds all have significant activities on at least one other target, i.e. N-methyl-D-aspartate receptors, voltage-gated calcium channels, dopamine receptors, and other K<sup>+</sup> channels. A short peptide, the bee venom tertiapin-Q,<sup>103,104</sup> was identified to target GIRK1/X channels fairly selectively, with additional activity shown only on K<sub>ir</sub>1.1 channels from among many tested (**Figure 5c**). However, tertiapin-Q activity on non-GIRK1/X channels has not been demonstrated, to our knowledge. Nevertheless, many of these molecules have additional activity on non-GIRK targets, and they may be difficult to utilize as probes to study GIRK inhibition *in vivo* without confounded effects.

Among the more selective inhibitors with off-target effects only described among K<sup>+</sup> channels are NIP-142, VU573, and analogs of ML297. NIP-142 is an analog of NTC-801, a clinical candidate and result of a GIRK1/4 channel selective inhibitor drug discovery program conducted by Nissan Chemical Industries for the treatment of atrial fibrillation.<sup>99</sup> Unfortunately, NIP-142 was shown to also inhibit human ether a-go-go (hERG), K<sub>v</sub>7.1 channel, and K<sub>v</sub>1.5 channels.<sup>67,105</sup> Research conducted by the laboratory of Dr. Jerod S. Denton and our laboratory identified VU573,<sup>100</sup> a small molecule inhibitor of GIRK channels, among others. Although VU573 was not specifically selective for GIRK channels, it was selective for GIRK and certain

K<sub>ir</sub> channels over others within the K<sub>ir</sub> channel family. As mentioned above, analogs of ML297 have also been described to inhibit GIRK1/X channels,<sup>84,86</sup> although no follow-up has been done to validate the selectivity of these molecules among the wider family of K<sub>ir</sub> channels.

In general, non-selective compounds would be suspected of confounding activities when used *ex vivo* or *in vivo* to probe GIRK channel effects on physiology in tissues or in animals. However, these probes would be useful to study GIRKs in engineered cells *in vitro* where non-GIRK mediated effects could be recognized, addressed, and explored. Our laboratory has continued to explore GIRK1/X probes in search of compounds that are increasingly potent and efficacious GIRK channel inhibitors.

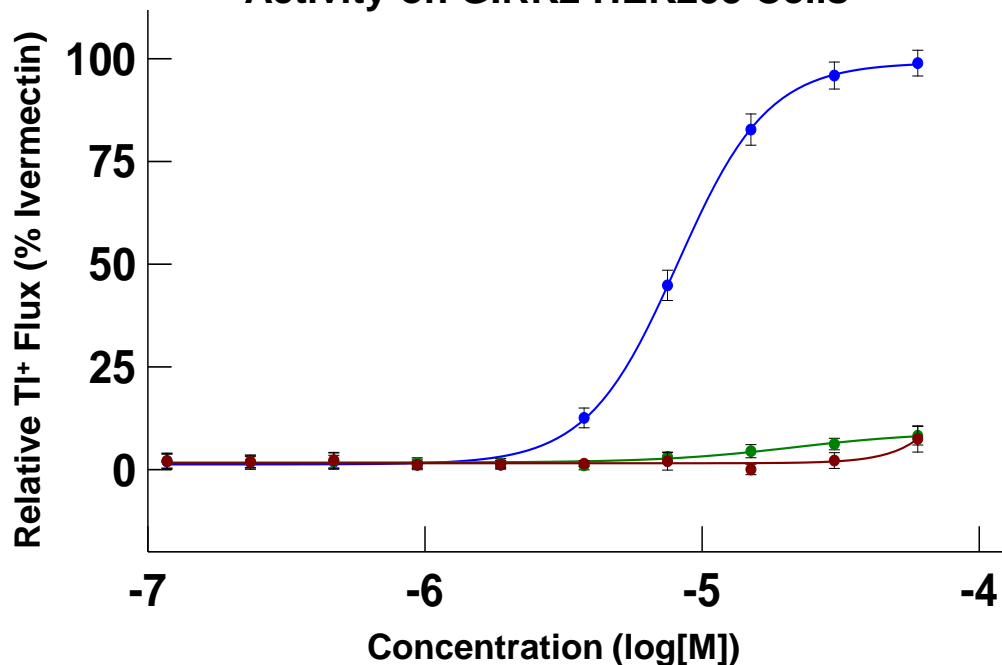
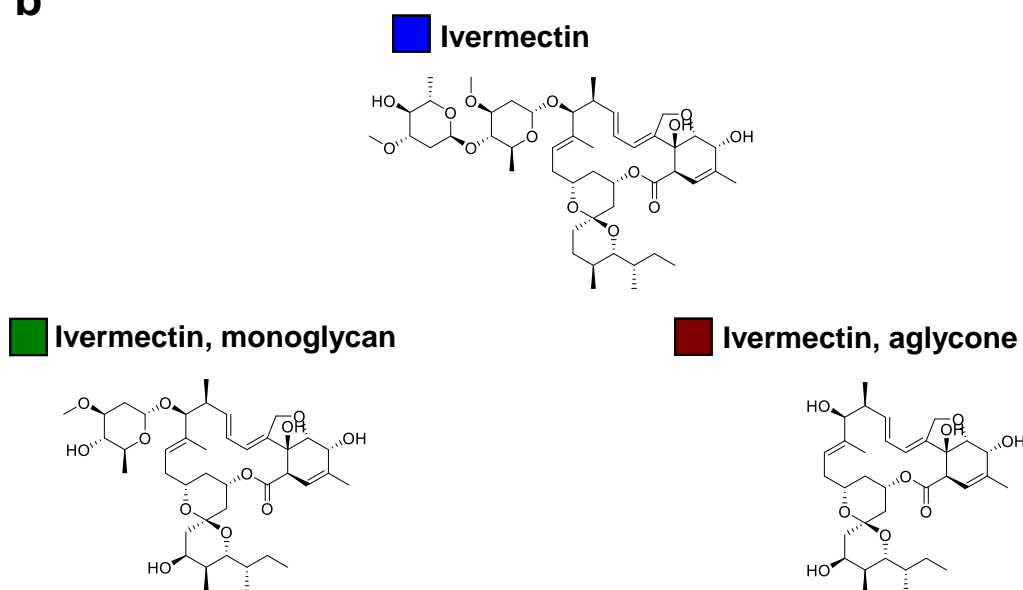
### **Previous Efforts Identifying Non-GIRK1/X Channel Activators**

To date, two other laboratories conducted screens that independently identified the same activator of non-GIRK1/X channels; both labs discovered that ivermectin (**Figure 9**) activated GIRK2 homotetrameric channels. Su *et al.*<sup>88</sup> briefly studied the ability of ivermectin to activate GIRK2 channels after discovering the molecule using a novel 100,000 compound high-throughput screen. Chen *et al.*<sup>89</sup> identified the compound through a smaller screen and conducted in-depth characterizations of ivermectin's propensity to activate GIRK1/2 channels and its inability to activate GIRK1/4 channels.

Ivermectin is one of the avermectin family of molecules, which include semisynthetic, naturally-derived, 16-membered macrocyclic lactones from the soil bacterium *Streptomyces avermitilis*.<sup>106,107</sup> Ivermectin and its analogs have been utilized as insecticides<sup>90</sup> and antihelminthic medications<sup>91</sup> for decades due to their ability to activate the insect glutamate-gated Cl<sup>-</sup> channel

**a**

### Ivermectin and its Aglycone Analog Activity on GIRK2 HEK293 Cells

**b**

**Figure 9.** (a) The activity on GIRK2 homotetrameric channels in TI<sup>+</sup> flux experiments of (b) ivermectin and ivermectin analogs synthesized through the Vanderbilt Synthesis Core, namely the monoglycan and the aglycone ivermectin analogs.

(GluR).<sup>108,109</sup> Since the discovery of the avermectins in 1979,<sup>106,107</sup> these compounds have been characterized extensively, both during their preclinical and clinical development. These studies identified that the analog ivermectin was both safe and efficacious during *in vitro* and *in vivo* studies,<sup>91</sup> which made it successful in clinical trials. Ivermectin has altered human health worldwide to such a great extent that half of the 2015 Nobel Prize in Physiology or Medicine<sup>110</sup> was granted to Drs. William C. Campbell and Satoshi Omura for their discovery of these compounds. The properties of ivermectin that made it a safe and efficacious antihelminthic medication also underly the reason why ivermectin is not a good non-GIRK1/X channel probe.

Ivermectin has multiple known important CNS targets that evoke a variety of known *in vivo* effects. This severely limits the utility of avermectins as probes to study the role of GIRK channels in the VTA and other brain regions. These CNS effects were not originally identified because the molecule does not cross the blood-brain-barrier effectively.<sup>111,112</sup> However, these compounds have been shown to modulate a wide variety of ion channels in humans, namely P2X purinoceptor 4 (P2X<sub>4</sub>R),<sup>113,114</sup> and a variety of Cys-loop, ligand-gated, ion channels, including  $\gamma$ -aminobutyric acid A receptor (GABA<sub>A</sub>R),<sup>115,116</sup> glycine receptor Cl<sup>-</sup> channel (GlyR),<sup>117</sup> and nicotinic acetylcholine receptors (nAChR).<sup>118</sup> The Cys-loop receptor superfamily is particularly damaging for the utility of ivermectin as a GIRK channel probe. The Cys-loop receptors are homopentameric and heteropentameric ion channels, which includes the aforementioned nAChR, GABA<sub>A</sub>R, and GlyR channels. This channel family was named Cys-loop because all the channels contain 13 highly-conserved amino acids that create a characteristic disulfide-bridged loop between two cysteine (Cys) residues near the N-terminal extracellular domain.<sup>119</sup> In the CNS, Cys-loop receptors are important mediators of synaptic transmission. Within this family, the different channels have evolved to be either cation- or anion-selective ion channels. Of note, GABA<sub>A</sub>R and

GlyR are both anion selective, and the neuronal consequence of activating these channels, membrane hyperpolarization and inhibition of action potential firing, is similar to that of GIRK channels. Ivermectin binding to these channels increases their activity, thus creating a confounding activity if attempting to study GIRK channels in neurons. These issues of poor selectivity are further compounded by a relatively low potency at the GIRK channel. Further, the avermectins are complex semi-synthetic natural products,<sup>120</sup> making synthesis and derivatization considerably more difficult than typical drug-like small molecules.

Our laboratory briefly investigated whether we could modify the avermectin structure to provide a synthetic route for the development of efficacious, potent, and selective activators of GIRK channels. For this, we aimed to identify whether removing the disaccharides from the ivermectin structure would improve its activity on GIRK channels. If we could eliminate these moieties, then maybe we could synthetically generate analogs to study. We partnered with the Vanderbilt Synthesis Core, in collaboration with Dr. Gary A. Sulikowski, to synthesize two commercially-unavailable analogs of ivermectin. These compounds either had one (monoglycan) or both (aglycone) of the sugar moieties of the disaccharide on ivermectin removed (*Figure 9b*). We studied the activity of these derivatives using  $\text{Ti}^+$  flux experiments and found that analogs of ivermectin missing the disaccharide were inactive on GIRK2 channels (*Figure 9a*). This concluded our brief investigation of avermectin analogs since the development of a library of natural product analogs was unrealistic. We realized that the discovery of potent and efficacious non-GIRK1/X channel modulators would be best approached using a high-throughput screen to identify small molecules that modulate non-GIRK1/X channels.

In light of the failures to discover synthetically tractable small-molecule modulators of non-GIRK1/X channels, we conducted a ~100,000 compound screen exclusively targeting

homomeric GIRK2 channels. In the following chapters, we describe in detail our efforts to identify small molecules capable of activating non-GIRK1/X channels. In **Chapter 2**, we describe the high-throughput  $\text{TI}^+$  flux assay-based screen we conducted in search of modulators of GIRK2 homotetrameric channels. In **Chapter 3**, we describe our efforts to characterize VU0529331, the first synthetic small molecule activator of homotetrameric and heterotetrameric GIRK channels. Finally, in **Chapter 4**, we conclude our discussions and provide insights into future experiments to be conducted following the discovery of VU0529331.

## CHAPTER 2

### **DISCOVERY OF NOVEL NON-GIRK1-CONTAINING GIRK CHANNEL MODULATORS USING HIGH-THROUGHPUT THALLIUM FLUX ASSAYS**

#### **Abstract**

GIRK channels are important regulators of cellular excitability throughout the body. Although the vast majority of GIRK channels contain a GIRK1 subunit, discrete populations of cells that express non-GIRK1/X channels do exist. For instance, DA neurons in the VTA of the brain, associated with addiction and reward, do not express the GIRK1 subunit. Targeting these non-GIRK1/X channels with subunit-selective pharmacological probes could lead to important insights into how GIRK channels are involved in reward and addiction. Such insights may, in turn, reveal therapeutic opportunities for the treatment or prevention of addiction. Therefore, we sought to discover synthetic small molecules that would serve as starting points for the development of non-GIRK1/X channel modulators. To accomplish this, we used a high-throughput  $Tl^+$  flux assay to screen a 100,000-compound library in search of activators of homomeric GIRK2 channels. Using this approach, we discovered a variety of scaffolds that activated GIRK channels in the  $Tl^+$  flux assay. Herein, we describe the high-throughput  $Tl^+$ -flux assay utilized to discover these molecules. Together, these structures represent the first steps towards the discovery of efficacious and modestly potent non-GIRK1/X channel probes. With future work, these compounds have the potential to be developed into more efficacious, highly potent, and potentially selective GIRK modulators. In the grand scheme, such molecules may help elucidate the role of GIRK channels in

addiction, potentially establishing a foundation for future development of addiction therapies utilizing targeted GIRK channel modulation.

## Introduction

GIRK channels are important regulators of cellular excitability throughout the body. GIRK channels are heterotetrameric and homotetrameric combinations of the  $K_{ir}3.1-4$  (GIRK1-4) subunits. Different subunit combinations are expressed throughout the CNS and the periphery, and most of these combinations contain a GIRK1 subunit. Although the vast majority of GIRK channels contain a GIRK1 subunit, discrete populations of cells that express non-GIRK1/X channels do exist. Due to the propensity of GIRK1 to form heterotetrameric channels, homotetrameric GIRK2 channels are difficult to study. Subunit-specific pharmacologic tools would help enable the study of certain GIRK channel populations. Unfortunately, such tools for non-GIRK1/X channels had not been identified until our work described herein.<sup>121</sup>

In an attempt to discover small-molecule modulators of non-GIRK1/X channels, we performed a high-throughput screen (HTS) of a collection of approximately 100,000 compounds using an HTS-compatible fluorescence-based  $Tl^+$  flux assay in a 384-well format. The  $Tl^+$  flux assay is based on three major principles: (1) extracellular  $Tl^+$  can permeate through  $K^+$  channels into cells (**Figure 10c** and **Figure 11c**),<sup>2</sup> (2) the fluorescent,  $Tl^+$ -sensitive dye precursor, Thallo-AM (**Figure 11a**), can be passively loaded HEK293 cells (**Figure 10b-e**), and (3) the fluorescence of Thallo (**Figure 11b**) increases dramatically when it interacts with intracellular  $Tl^+$  (**Figure 10c**).  $Tl^+$  is a heavy metal that is not normally encountered in human cells. Because  $Tl^+$  is not found in cells, the intracellular Thallo dye remains dim because it lacks  $Tl^+$  to bind to. However, once  $Tl^+$  is applied to the outside of cells, the  $Tl^+$  moves down its concentration gradient into the



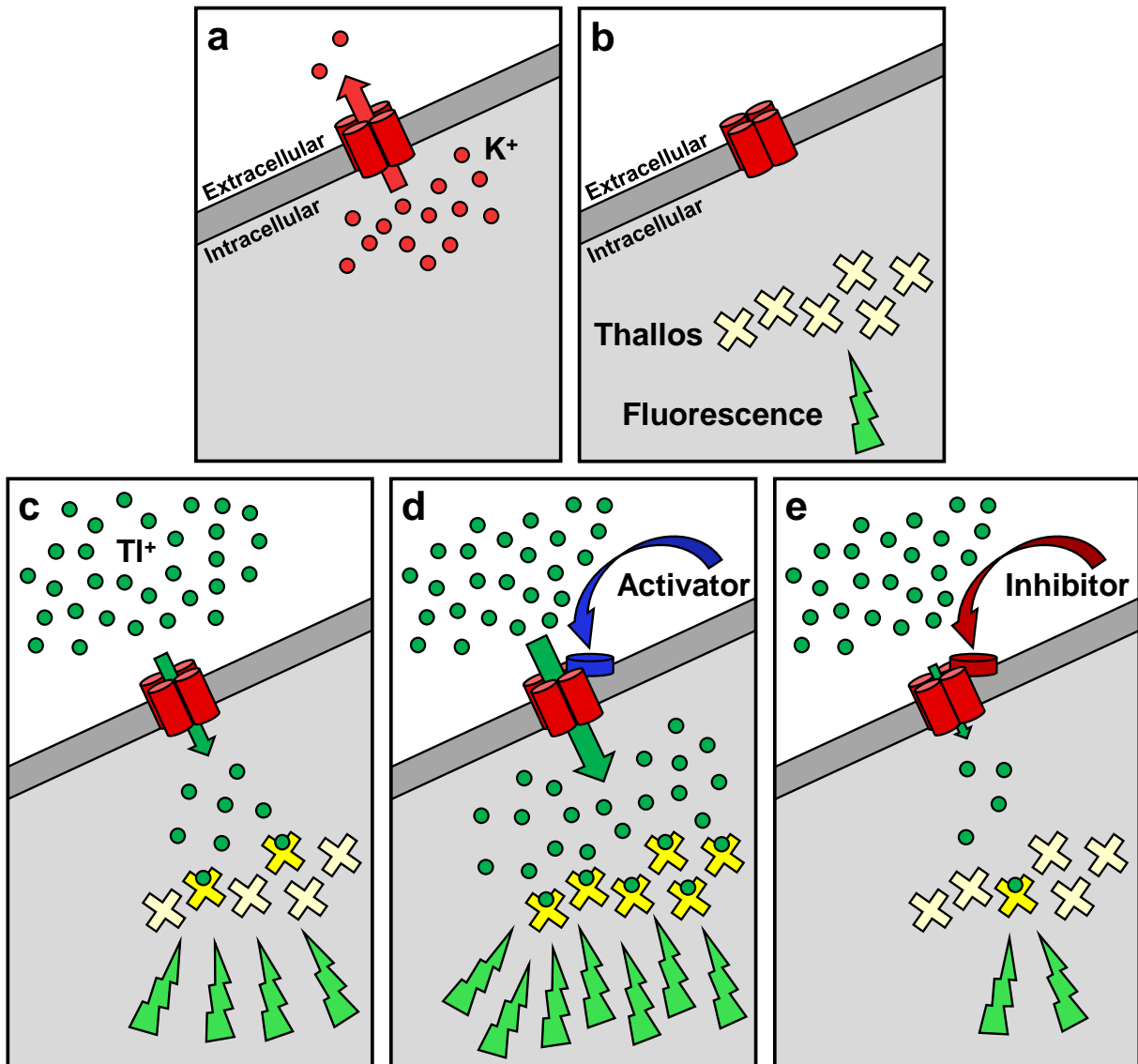


**Figure 10.** The TI<sup>+</sup> flux assay enabled identification of compounds that modulated TI<sup>+</sup> entry pathways on the cellular membrane. (a) When GIRK homotetrameric channels are expressed in a cell, they efflux potassium (K<sup>+</sup>) under normal physiological conditions. During a TI<sup>+</sup> flux assay, (b) an intracellularly-loaded TI<sup>+</sup>-sensitive dye, Thallos, enables (c) measurement of the influx of TI<sup>+</sup> via fluorescence (Fluo.). (d) Channel activators increase TI<sup>+</sup> influx while (e) channel inhibitors decrease TI<sup>+</sup> influx, both of which change the fluorescence signal and enable compound identification.

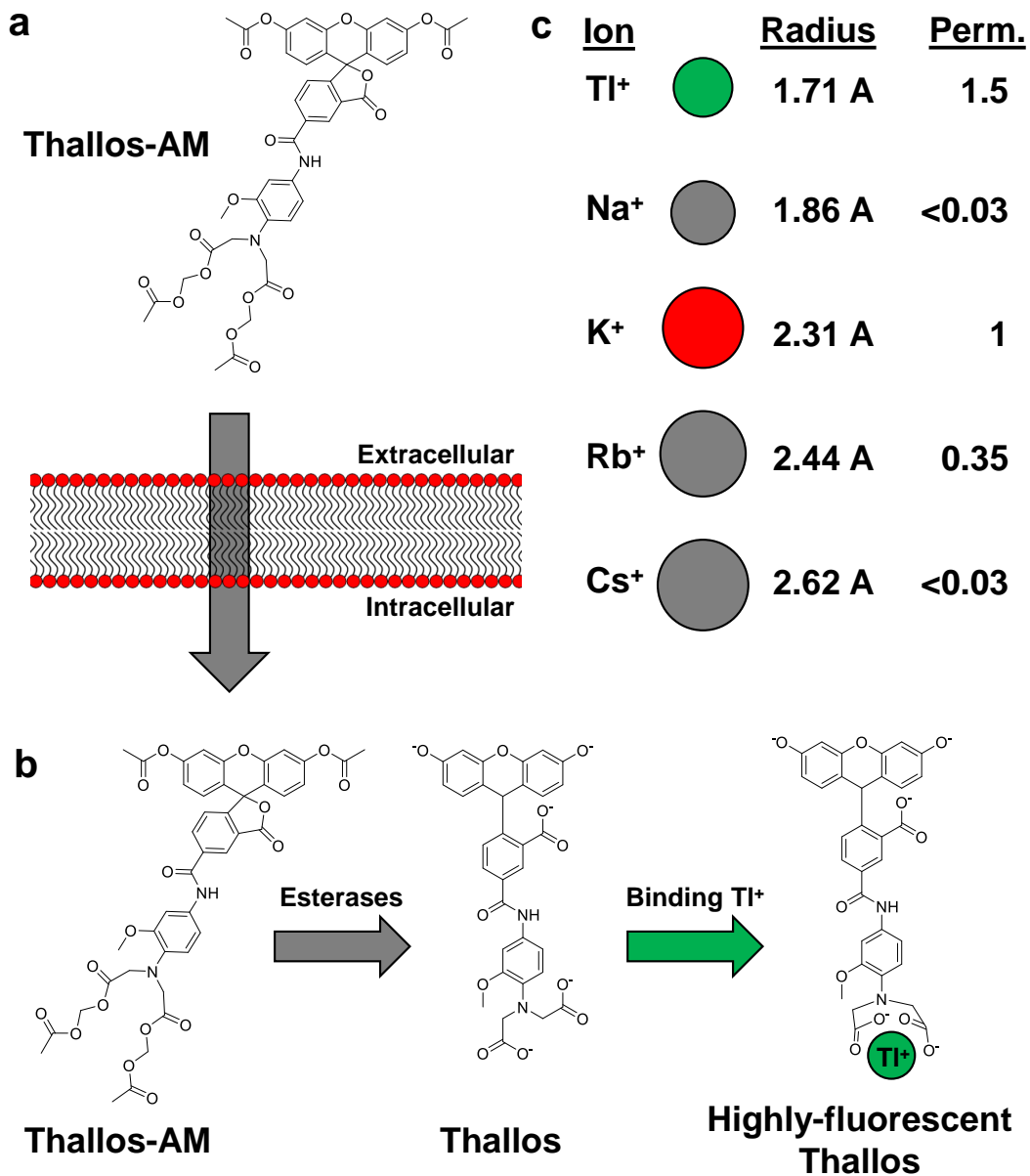


**Figure 11.** (a) The structure of Thallos-AM, which can cross the lipid bilayer to accumulate within cells. (b) Thallos-AM is catalyzed to Thallos by a variety of esterases. When Thallos binds thallium, its fluorescence greatly increases. (c) The ionic radii and the permeability (perm.) ratios through inward rectifier K<sup>+</sup> channels of the different monovalent cations, Na<sup>+</sup>, K<sup>+</sup>, Rb<sup>+</sup>, Cs<sup>+</sup>, and Tl<sup>+</sup>. Data adapted from Hille, B., *Ion Channels of Excitable Membranes*, 2001.

cells. In a system designed to highly express a channel of interest, the predominant  $\text{Ti}^+$  entry pathway is through that ion channel. When  $\text{Ti}^+$  influx occurs, Thallo binds the  $\text{Ti}^+$  and the Thallo dye undergoes a structural change, which unquenches the dye's fluorescein moiety and leads to a dramatic increase in fluorescence (**Figure 11b**). Compounds, both activators and inhibitors, that modulate the activity of the channel of interest, in this case GIRK2, are identified by the magnitude of increase, great vs small, respectively, in fluorescence that results from changes in  $\text{Ti}^+$  influx (**Figure 10d,e**). For over the last decade,  $\text{Ti}^+$  flux assays have been adapted and utilized at Vanderbilt University and elsewhere for HTS to screen and characterize compounds on targets such as  $\text{G}_{i/o}$  protein-coupled GPCRs<sup>122-126</sup>,  $\text{K}^+$  channels<sup>85,100,127,128</sup>,  $\text{Na}^+$  channels,<sup>129</sup> and electroneutral  $\text{K}^+$ -utilizing transporters.<sup>130</sup> These HTS efforts have often identified compounds for targets that had no known modulators prior to these efforts.

When designing our HTS to screen for GIRK2 homomeric channels, we chose to utilize the human embryonic kidney cells #293 (HEK293) due to their fast growth, immortality, ease of genetic manipulation, neuron-like gene expression,<sup>131</sup> and our laboratory's experience with this line. We engineered low-passage numbered HEK293 cells to express the GIRK2 channel and the neuropeptide Y receptor type 4 (NPY4R), a  $\text{G}_{i/o}$ -coupled GPCR. NPY4R is capable of increasing the activity of GIRK2 channels by signaling through the  $\text{G}_{i/o}\beta\gamma$ -subunit after receptor activation with its agonist, human pancreatic polypeptide (hPP). Henceforth, the HEK293 cell line expressing GIRK2 and NPY4R will be referred to as "G2Y4 cells".

Prior to beginning this HTS, our laboratory spent much time developing the  $\text{Ti}^+$  flux assay to generate a system sensitive enough to identify hits without generating a large number of false positives. In the HTS field, this is done by ensuring that the data is not noisy with a large separation between the activator controls and the negative controls. The assays herein are the final iterations

of our labors to optimize assay parameters and create an assay suitable for reproducible high-throughput  $\text{Ti}^+$  flux screening of GIRK2-expressing HEK293 cells.

Throughout this HTS, we utilized a three-addition protocol (*Figure 12a*) to provide multiple distinct analysis windows within which molecules with different behaviors, namely fluorescent molecules, activators, and inhibitors, could be identified (*Figure 12b*). We identified which compounds generated the greatest and least increases in fluorescence over the entirety of the assay. The best activators and inhibitors were ranked to determine which compounds would be most important to characterize, also known as the “hits” from this HTS. Within this chapter, we describe our process of hit confirmation and categorization through a gamut of secondary assays, which we call “counter screens” (*Figure 13*). These counter screens enabled us to elucidate whether compound activity was dependent on GIRK channels or another  $\text{Ti}^+$  entry pathway native to HEK293 cells.

Briefly, we will describe the order and logic behind the  $\text{Ti}^+$  flux-based counter screens. These assays quickly, yet robustly, identified which hits from our HTS were likely to be GIRK channel modulators and should be further characterized. First, we concurrently established which hits both replicated the activity that we observed during our HTS and did not require NPY4R expression for this activity. For this, we used HEK293 cells only overexpressing GIRK2 channels. With one experiment, we removed both compounds that were not active in our system in the first place and that were active but required NPY4R for activity. Activity of compounds on NPY4R was studied by other members of our laboratory and is not discussed herein.

Next, we identified whether GIRK2 channel expression was necessary for hit activity. Naturally, the GIRK2 HEK293 cells also express a variety of  $\text{Ti}^+$  influx pathways, such as other  $\text{K}^+$  channels,  $\text{Na}^+$  channels, transporters, and non-selective monovalent cation channels. To

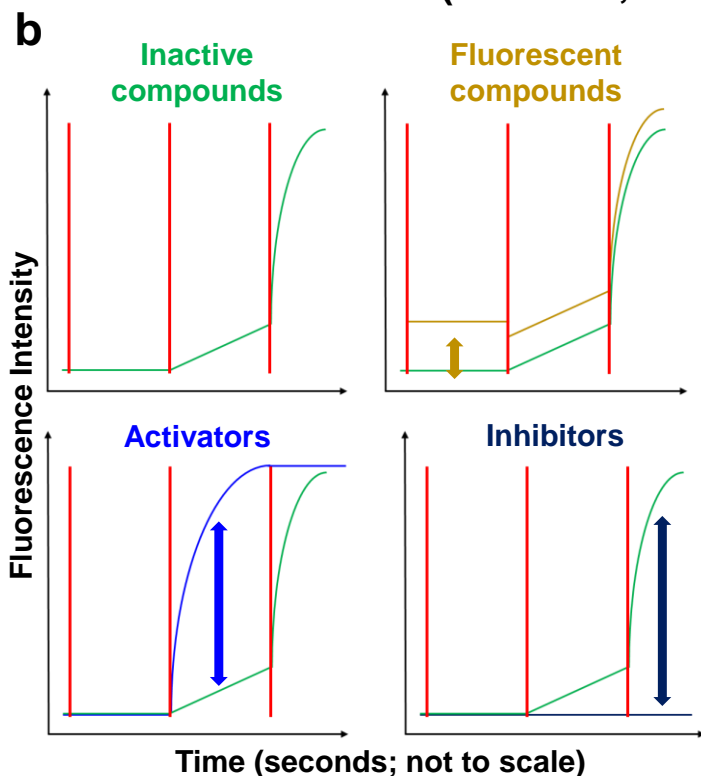
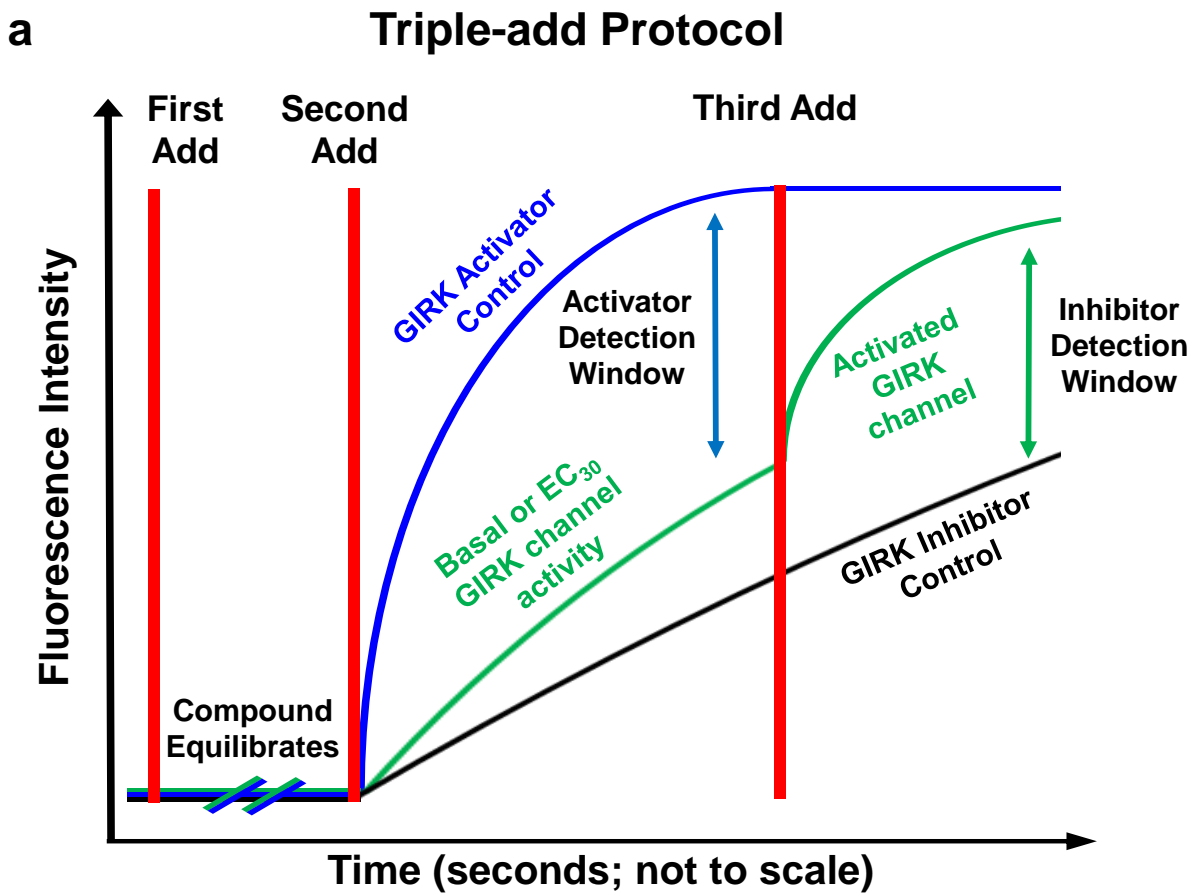


**Figure 12.** (a) The design of the triple-add protocol utilized during the GIRK2 HTS and executed using the WaveFront Biosciences Panoptic. (b) Examples of the different activities observed by compounds that would be classified as either inactive compounds, fluorescent compounds, activators, or inhibitors. Compounds displaying activity such as the “activators” would be chosen as hits and further studied.

eliminate hits that activated a  $\text{TI}^+$  influx pathway independent of the GIRK2 channel, we screened compounds using untransfected HEK293 cells. Hits that failed to increase fluorescence in these experiments indicated that the pathway through which they mediated  $\text{TI}^+$  influx required GIRK2 expression, while active compounds were identified as  $\text{TI}^+$  influx modulators of unknown origin and marked for future study. Additionally, hits that did not depend on the presence of GIRK2 could act as ionophores and transport  $\text{TI}^+$  across the cell membrane, or they could create pores in the cell membrane that allow  $\text{TI}^+$  influx. These mechanisms add a layer of complexity to any HTS, but can be identified and hits that act through these mechanisms can be easily eliminated. Although even these discoveries may be interesting and worthy of follow up, study of such compounds was outside the scope of this work.

While we already determined, above, that compounds did not require NPY4R for activity, the hits that continued to be active on GIRK2 cells could not yet be definitively identified as directly active upon GIRK2 channels. This was because HEK293 cells also natively expressed  $\text{G}_{i/o}$ -coupled GPCRs through which compounds could have been active. Compounds could target and bind a native  $\text{G}_{i/o}$ -coupled GPCR, which would signal downstream through  $\text{G}_{i/o}\beta\gamma$  and activate GIRK channels. To identify these off-target hits, we examined whether compounds maintained activity under conditions that inhibited  $\text{G}_{i/o}$  protein signaling.

Pertussis toxin (PTX) is a bacterial exotoxin that inhibits  $\text{G}_{i/o}$ -coupled GPCR signaling by catalyzing ADP-ribosylation of the  $\text{G}\alpha$  subunit of the trimeric G proteins.<sup>132</sup> Through this mechanism, PTX inhibits  $\text{G}_{i/o}\beta\gamma$  protein release and prevents signaling from any  $\text{G}_{i/o}$ -coupled GPCR expressed in HEK293 cells. Hits that were insensitive to PTX treatment indicated independence from  $\text{G}_{i/o}$  protein signaling. These compounds were suspected to act directly upon and modulate the GIRK channel to increase  $\text{TI}^+$  influx. In this way, we narrowed the potential

mechanisms through which compounds could be exerting activity in  $\text{TI}^+$  flux assays. We eliminated the off-target hits and determined which hits demonstrated the most promise as GIRK channel activators worthy of further extensive characterization. The following chapters detail our studies of the most efficacious and promising GIRK2 channel activators. A flowchart illustrating the experiments by which these compounds were filtered is provided in **Figure 13**.

Herein, we conducted an approximately 100,000-compound screen in search of small molecule modulators of homomeric GIRK2 channels.<sup>121</sup> We describe the screen and validation efforts of our studies within this chapter. In **Chapter 3**, we described the extensive characterization of the first small molecule activator of non-GIRK1/X channels, VU0529331, and our work with additional small molecules is elaborated upon in following chapters.<sup>121</sup> We describe our efforts at developing these scaffolds into more efficacious, potent, and selective non-GIRK1/x modulators. Altogether, we provided a detailed account of our GIRK2 channel HTS and the experiments that followed.

## **Methods**

### **General Equipment Utilized Throughout this Research**

Our laboratory maintains all equipment necessary to setup high-throughput assays outside shared cores. This includes an electronic balance, a pH meter, a water bath, a Thermo Nanopure water purification system, an ultrasonicator, vapor pressure osmometer, five complete sets of single channel pipettes, four complete (two Sartorius eLINE and two Eppendorf Xplorer) sets of 8-channel hand-held electronic pipettes, a Molecular Devices SpectraMax microplate reader, two microplate centrifuges, a microplate shaker, and two Thermo Multidrop non-contact liquid

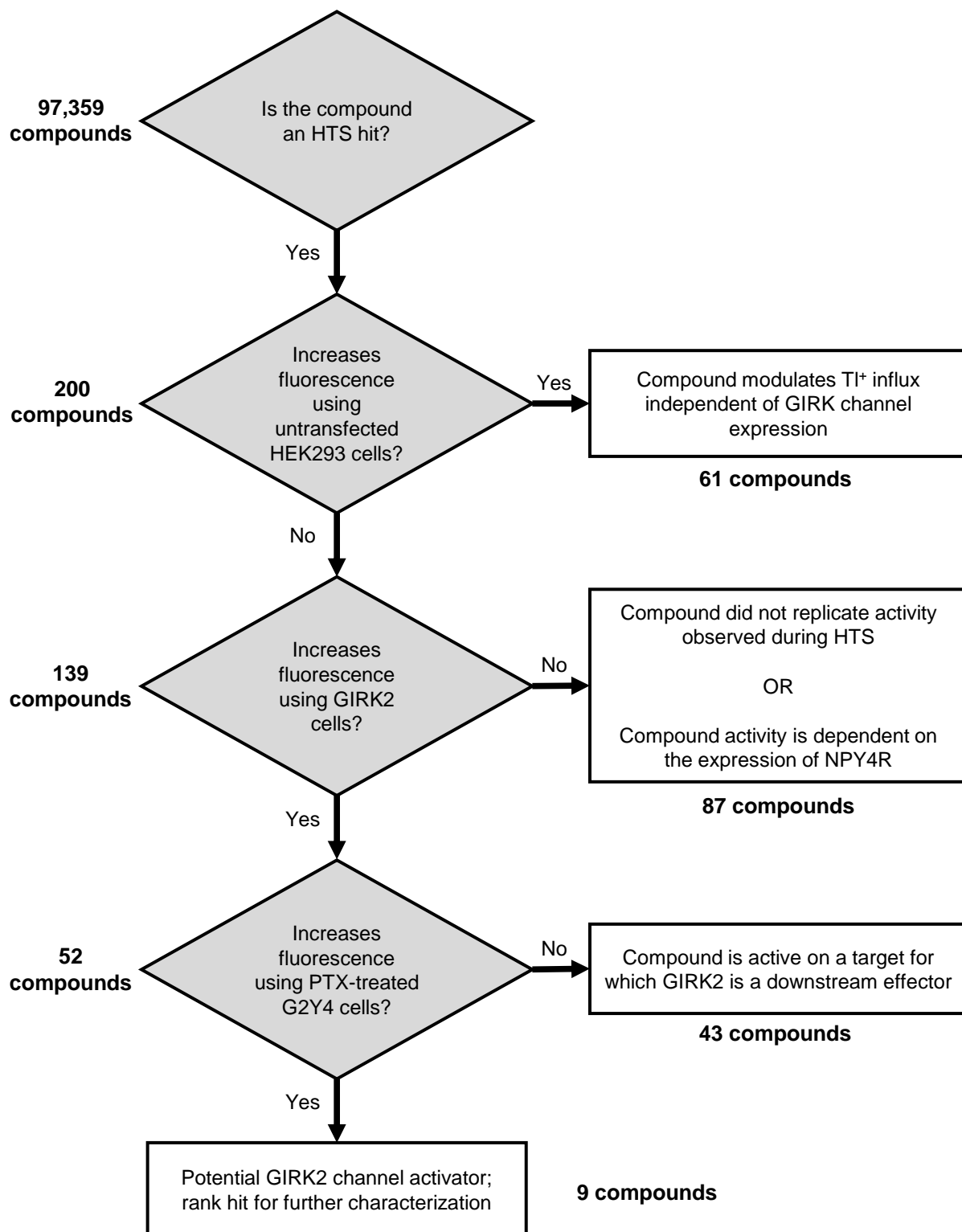


**Figure 13.** The counter-screening pipeline for GIRK channel activator discovery, with the different numbers of compounds filtered through each step during out GIRK2 high-throughput screen.



handlers for screening cell-plate preparation. The laboratory also maintains equipment for reagent and cell line preparation and storage, including block heaters, vortexes, minicentrifuges, Thermo S1 pipette fillers, hot plates, a Sorvall Pico microcentrifuge, a -20°C freezer, desiccators kept at various temperatures, and a Thermo Locator 6Plus liquid nitrogen storage device with a digital monitor. Further, our tissue culture room is fully stocked with plastics and disposables and includes all equipment needed for mammalian cell culture, including two direct heat Thermo Forma CO<sub>2</sub> incubators, a Forma Scientific Biological Safety Level (BSL) 2 rated isolation cabinet, an Eppendorf 5702 centrifuge, and a Zeiss PrimoVert cell culture microscope with image acquisition system.

### **Cell Line Generation**

HEK293 cells expressing human GIRK2 subunits were generated by transfecting a pCMV6-A-puro vector (Origene, Rockville, MD) carrying KCNJ6 into low-passage HEK293 cells (CRL-1573, ATCC, Manassas, VA). The FuGENE 6 (Promega, Madison, WI) transfection reagent and protocol, together with Opti-MEM (Thermo Fisher Scientific, Waltham, MA), were utilized in all transfections herein. Further, GIRK2 cells were transfected with a vector encoding human NPY4R, generously provided by the Dr. Annette Beck-Sickinger laboratory,<sup>133,134</sup> to create the G2Y4 cells used for HTS and PTX experiments.

### **Cell Culture**

Cell culture medium consisted of Minimal Essential Medium, Alpha Medium (Corning, Corning, NY) supplemented with 10% (v/v) heat-inactivated fetal bovine serum (Thermo Fisher

Scientific, Waltham, MA) and 1x GlutaGro (Corning, Corning, NY). When passaging cells, medium was supplemented with antibiotics, as appropriate, to maintain selection pressure.

### **Generation of Monoclonal Cell Lines**

Monoclonal cell lines were generated by limiting-dilution cloning, where polyclonal populations of cells were distributed in 384-well amine-coated plates at <0.8 cells per well and cultured till colonies grew to encompass at least a quarter of a well. These colonies were further tested and selected for expansion as described previously.<sup>129</sup> Selected clones were expanded for use in experiments and for cryopreservation.

### **Cell Plate Preparation for TI<sup>+</sup> Flux Experiments**

For use in TI<sup>+</sup> flux experiments, monoclonal HEK293 cells engineered to express proteins of interest were grown in cell culture medium on tissue-culture-treated and vented T75, T150, or T300 flasks (TPP, Trasadingen, Switzerland) in a humidified incubator at 37°C and 5% CO<sub>2</sub>. During screening, multiple T300 flasks were required to create upwards of 50 screening plates worth of cells. Cells were carefully grown to reach 90% confluence on the day before experimentation or screening. To prepare cells for transfer into 384-well plates, culture medium was removed from flasks, flasks were treated using TrypLE Express (Thermo Fisher Scientific, Waltham, MA) for 5 min at room temperature to dislodge cells, and single-cell suspensions were created through trituration. Cells were resuspended in antibiotic-containing medium at 1,000 cells/μL. To achieve a cell density of 20,000 cells/well, 20 μL of cellular suspensions were plated in Corning<sup>®</sup> PureCoat<sup>™</sup>, amine-coated, 384-well microtiter plates (cell plates; cat#354719, Corning, Corning, NY). Cell plates were incubated overnight in a humidified incubator at 37°C

and 5% CO<sub>2</sub>. Of note, an extra 2 empty cell plates were placed both above and below the cell plates containing cells while in the incubator to limit the effects of heat and moisture gradients on the reproducibility of our experiments.

### **Pertussis Toxin Treatment of Cells for TI<sup>+</sup> Flux Experiments**

In order to fully inhibit G<sub>i/o</sub>-coupled G protein-coupled receptor activity within HEK293 cells, cell plates were treated with PTX for 8 hours prior to the dye loading process described in the experiments below. For this, cell medium from cell plates was removed and replaced with fresh cell medium also containing 800 ng/mL PTX (Tocris, Bristol, United Kingdom). Cell plates were returned to the incubator and incubated for 8 hours in a humidified incubator at 37°C and 5% CO<sub>2</sub>.

### **Compound Plate Preparation for High-throughput Experiments**

The compounds utilized as controls during the HTS included 30 mM SCH-23390, 100 mM ivermectin, and 100 mM eprinomectin dissolved in DMSO. All compounds received from the Vanderbilt HTS Core Facility were 10 mM stocks in DMSO. Until the time of use, all compounds and compound plates were stored in desiccators at either room temperature, 4°C, or -20°C as instructed by the originating source.

To generate high-throughput compatible compound plates during counter screening for TI<sup>+</sup> flux experiments, 10 µL aliquots of stock compounds were plated into 384-well, Echo qualified, low dead volume microplates (Labcyte, Sunnyvale, CA). As needed, these stock compound plates were copied or reformatted to generate a desired compound layout using an Echo555 plate reformatter (Labcyte, Sunnyvale, CA) into 384-well, round-bottom, polypropylene microplates (compound plates; Greiner, Monroe, NC). In this way, compounds were dispensed as 2.5-500 nL

aliquots from stocks and backfilled with DMSO, also using the Echo555, to generate 80-500 nL/well compound samples. These samples were dissolved to 40-100  $\mu$ L/well with assay buffer comprising Hanks Balanced Salt Solution (Thermo Fisher Scientific, Waltham, MA) and 20 mM HEPES pH 7.3 (Corning, Corning, NY). Each compound plate was designed to provide solutions at concentrations twice the final concentration of compound. This was because solutions were diluted 2-fold during the assay, which resulted in the desired final concentration being applied to cells during imaging (*Figure 14*).

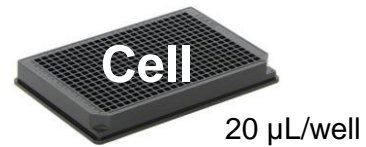
To help solubilize compounds into assay buffer, compound plates were sealed using a PlateLoc Thermal Microplate Sealer (Agilent, Santa Clara, CA), briefly ultrasonicated in a bath sonicator (Cole-Parmer, Vernon Hills, IL), and shaken vigorously using a Teleshake (Inheco, Martinsried, Germany) for at least 30 min prior to use. Compounds were used within an hour of preparation, and the final DMSO concentrations in all assays were  $\leq 0.25\%$  (v/v). Our laboratory has found that DMSO  $< 0.3\%$  (v/v) does not elicit any effects on untransfected or GIRK2-expressing HEK293 cells in our experiments. However, DMSO concentrations of  $> 0.6\%$  (v/v) increased GIRK channel activity (unpublished data). For all experiments, compounds were DMSO-matched to eliminate any differences that may have been due to DMSO concentrations.

### **Conducting a $\text{TI}^+$ Flux Experiment**

The  $\text{TI}^+$  flux assay was mainly conducted as previously described.<sup>135,136</sup> Here, we detail the specifics of the assays as it was utilized throughout this work. Cells were prepared 1 day before an experiment, as described above. At 1 hour directly prior to imaging, assay buffer containing the  $\text{TI}^+$ -sensitive dye Thallo, namely the dye-loading buffer, was applied to cells. For this, culture

**a** 1 hour prior to screening

- Medium is removed from cell plates
- Cell plates are loaded with Thallos-containing assay buffer



**b** 30 minutes prior to screening

- Assay buffer is added to the compound plate



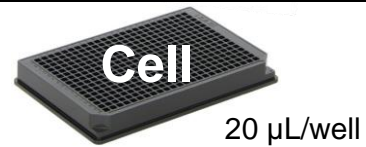
**c** 10 minutes prior to screening

- Stimulus plate 1 is prepared
- Stimulus plate 2 is prepared



**d** Immediately prior to screening

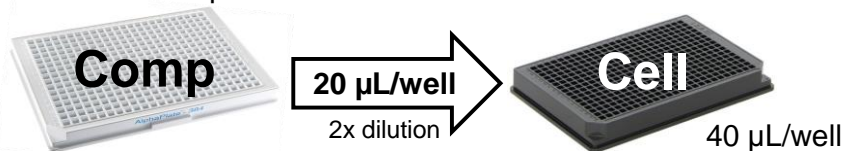
- Dye buffer is removed from cell plates
- Cell plates are loaded with assay buffer
- All plates are loaded onto the WaveFront Pantopic



**e** 10 seconds into imaging

- Compounds are added to the cell plate

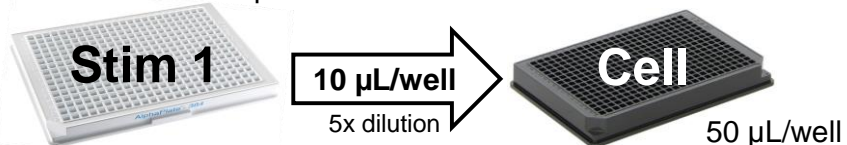
**FIRST ADDITION**



**f** 130 seconds into imaging

- The first stimulus is added to the cell plate

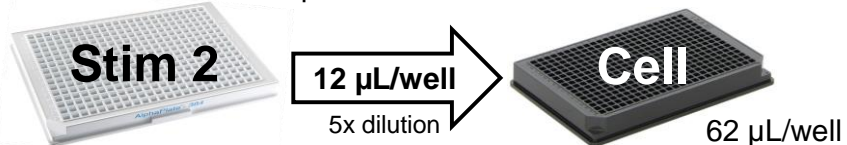
**SECOND ADDITION**



**g** 160 seconds into imaging

- The second stimulus is added to the cell plate

**THIRD ADDITION**



**h** 220 seconds into imaging

- Imaging is concluded

**Figure 14.** The screening paradigm utilized for this GIRK2 HTS. (a) Cell plates, (b) compound (Comp) plates, and (c) stimulus (Stim) plates were prepared in advance of imaging. (d) For imaging, cells were prepared in assay buffer. During the first addition, (e) compounds were added to the buffer. During the second addition, (f) the first stimulus was added to the solution. For the third and final addition, (g) the second stimulus plate was added to the solution. (h) Imaging was completed at 220 seconds.

medium was replaced with 20  $\mu\text{L}$ /well of dye-loading buffer comprising assay buffer with 0.6  $\mu\text{M}$  Thallos. Thallos was stored dry in 20  $\mu\text{g}$  aliquots and resuspended with 30  $\mu\text{L}$  of DMSO (Sigma-Aldrich, St. Louis, MO) containing 6.7% (w/v) Pluronic F-127 (Sigma-Aldrich, St. Louis, MO) immediately prior to dilution. After incubating cells in dye-loading buffer for 1 hour at room temperature, dye-loading buffer was replaced with assay buffer and loaded onto the WaveFront Biosciences Panoptic (Franklin, TN). For all  $\text{Ti}^+$  flux experiments, data were acquired at 5 Hz using a  $482 \pm 35$  nm excitation filter and a  $536 \pm 40$  nm emission filter. Data were first collected for 10 s, at which time 20  $\mu\text{L}$ /well of test compounds was added and allowed to equilibrate for 120 s. Next, 10  $\mu\text{L}$ /well of  $\text{Ti}^+$  stimulus buffer (125 mM  $\text{NaHCO}_3$ , 1.8 mM  $\text{CaSO}_4$ , 1 mM  $\text{MgSO}_4$ , 5 mM glucose, either 2 or 4 mM  $\text{Ti}_2\text{SO}_4$ , and 20 mM HEPES pH 7.3) was added. Imaging was concluded after an additional 120 s. This process is illustrated in *Figure 14*. When preparing hPP for testing, 100  $\mu\text{M}$  hPP stock solutions were diluted to 5-fold over the desired final concentration in  $\text{Ti}^+$  stimulus buffer additionally containing 0.0025% fatty acid free, low endotoxin, lyophilized, powdered bovine serum albumin (Sigma-Aldrich, St. Louis, MO).

Of note, the  $\text{Ti}^+$  stimulus buffer described above is not the same as the assay buffer we used for compound dilution.  $\text{Ti}^+$  readily interacts with  $\text{Cl}^-$  and precipitates into insoluble  $\text{TiCl}$  if added into assay buffer, which contains  $\text{Cl}^-$ . For this reason,  $\text{Ti}^+$  stimulus buffer comprises of salts with anions other than  $\text{Cl}^-$ , maintaining the integrity of the assay and enabling higher concentrations of  $\text{Ti}^+$  to be utilized for screening.

### **Data Analysis for $\text{Ti}^+$ Flux Experiments**

$\text{Ti}^+$  flux assay data were collected using WaveGuide (WaveFront Biosciences, Franklin, TN) and analyzed using Excel (Microsoft, Redmond, WA). For analysis of the HTS and also for

day-to-day analysis of fluorescence-based assays, we utilized macros written using Microsoft Visual Basic for Applications (VBA) within Microsoft Excel to automate data analysis using custom-build Excel Spreadsheets. For all experiments, data reported were averages of at least 3 independent experiments, unless otherwise stated. Compound activity was extracted from normalized and control-subtracted fluorescence waves generated through imaging. The wave for each well was normalized by dividing by the average fluorescence from the first 8 s of imaging ( $F/F_0$ ), which accounted for non-uniformity in cell number, dye loading, and illumination in the plate reader. Next, each wave was control-subtracted, and the change in wave amplitude ( $\Delta A$ ) due to stimulus buffer addition was calculated. At the time of stimulus buffer addition ( $T_s$ ), the  $\Delta A$  of active wells increased dramatically.  $\Delta A$  was calculated as the difference in amplitude between time points  $T_s-5$  s and  $T_s+15$  s for the untransfected, G2Y4, and GIRK2 HEK293 cells utilized herein. This time frame was chosen to provide a high signal-to-noise ratio while measuring nearest the linear portion of the initial  $TI^+$  influx.

### **High-throughput Screen using the $TI^+$ Flux Assay**

With the help of the Weaver laboratory members in the execution of this HTS, namely Dr. Yu (Sunny) Du, Dr. Brittany D. Spitznagel, and Francis J. Prael III, we created a workflow using which we screened up to 50 compound plates (16,000 unique compounds) per screening day. Our HTS relied on the ability of the kinetic-imaging plate reader, the WaveFront Biosciences Panoptic (Franklin, TN), to conduct 3 separate additions of 3 different buffer solutions into a 384-well cell plate containing G2Y4 cells. In brief, the first addition comprised of adding compounds to cells and allowing the solutions to equilibrate. The second addition comprised of adding a  $TI^+$ -containing stimulus buffer to each compound-containing cell well, which evoked a change in

fluorescence from the system. After a short wait, the third addition comprised of adding a GIRK channel activator to each well, activating the GIRK2 channel and facilitating the discovery of inhibitory compounds. We utilized activator and inhibitor control compounds to validate the quality of the  $\text{TI}^+$  flux protocol for each plate. Example data traces expected from screening are shown in *Figure 12*.

More specifically, this GIRK2 channel HTS was conducted in 2 parts, which mainly differed in the method by which we activated GIRK channels to identify inhibitory compounds. Our rationale for this change is provided in the **Discussion** below. For the first part of this HTS, the second addition comprised of activating GIRK2 channels to approximately 30% of maximum activity using hPP and the third addition comprised of activating GIRK2 channels maximum activity using hPP.

For the second part of this HTS, we modified our protocol and no longer used hPP to activate GIRK channels through NPY4R. Instead, we utilized an alcohol, 2-methyl-2,4-pentanediol (MPD), to activate GIRK channels to approximately 20% of maximum activity during only the third addition. MPD directly binds to the alcohol-binding pocket of GIRK2 channels to open the channels and allow  $\text{TI}^+$  influx, as described in **Chapter 1**. Additionally, the avermectin analog utilized as a positive control differed between the first portion of the screen and the second, with eprinomectin used during the first part and ivermectin used during the second part. The results of both of these HTS parts have been published in the PubChem BioAssay Database, with the first part of the screen recorded under Assay ID = 1259324,<sup>137</sup> and the second part under Assay ID = 1259325.<sup>137</sup>

On the day of screening, our protocol for this HTS was as follows. At 1 h prior to imaging a cell plate, cell plate medium was replaced with 1.5  $\mu\text{M}$  Thallos-containing assay buffer and



stored in the dark at room temperature. Compounds for this HTS were provided by the Vanderbilt HTS Facility Core and received on the day of screening as 80 nL aliquots of 10 mM compound stocks stored in dimethyl sulfoxide (DMSO). Compounds were received already formatted in 384-well compound plates with 1 compound/well for a total of 320 compounds/plate. At 30 min prior to imaging, 40  $\mu$ L of assay buffer was added to each of the 320 wells containing a compound, which generated 20  $\mu$ M compound solutions. Controls were loaded in the remaining empty wells in a predetermined pattern by hand. During the first and second parts of our screen, we used 16.6  $\mu$ M eprinomectin and 30  $\mu$ M ivermectin, respectively, as positive activator controls. For both part of this screen, we utilized 30  $\mu$ M SCH-23390 as positive inhibitor controls and assay buffer without compounds as negative controls.

The stimulus plates for the second and third additions throughout both parts of this HTS were prepared within 10 min of screening. During the first part of this HTS, the first stimulus plate (second addition) contained 2 mM  $\text{Ti}^+$  stimulus buffer and 3.5 nanomolar (nM) hPP, which was added to all wells. This solution was generated by a two-step dilution from 100  $\mu$ M stocks of hPP using  $\text{Ti}^+$ -free stimulus buffer additionally containing 0.0025% fatty acid free, low endotoxin, lyophilized, powdered bovine serum albumin. Because of the 5-fold dilution that occurs during imaging, the final  $\text{EC}_{30}$  hPP concentration was 0.7 nM. The second stimulus plate (third addition), delivered 2 mM  $\text{Ti}^+$  stimulus buffer together with 1  $\mu$ M hPP, which generated a 200 nM hPP solution after the 5-fold dilution during imaging. This was a maximally-activating concentration ( $\text{EC}_{\text{Max}}$ ) of hPP on NPY4R and generated a large activation of GIRK2 channels. Different from the first part of this HTS, the second part of this HTS had only 2 mM  $\text{Ti}^+$  stimulus buffer plated into the first stimulus plate and delivered during the second addition. During the third addition, instead of using hPP, we delivered a solution of 2 mM  $\text{Ti}^+$  stimulus buffer containing 250 mM

(3.2% v/v) MPD. Due to the 5-fold dilution, this generated 50 mM MPD at the time of imaging. Each of these solutions was vortexed vigorously before plating out onto the 384-well compound plates, ensuring thorough mixing.

For the duration of imaging, data were acquired at either 1 or 5 Hz (excitation  $482 \pm 35$  nm, emission  $536 \pm 40$  nm). Immediately before imaging, the Thallo-containing buffer was removed from the cell plate and replaced with 20  $\mu$ L/well of assay buffer. After the first 10 s of imaging, 20  $\mu$ L/well from the first compound plate was added and allowed to equilibrate for 120 s. The next two additions differed between the first and second parts of the screen. During the first part of the screen, 10  $\mu$ L/well of the first stimulus buffer was added and imaged for 120 s, and this was followed by a 12  $\mu$ L/well addition of the second stimulus buffer with data collection lasting another 120 s. During the second part of the screen, 10  $\mu$ L/well of the first stimulus buffer was added and imaged for 30 s, and this was followed by a 12  $\mu$ L/well addition of the second stimulus buffer with data collection lasting at least another 60 s. A total of 34,131 compounds were screened during the first part of this HTS, while a total of 63,228 compounds were screened during the second part of this HTS. The HTS protocol for this HTS was illustrated in *Figure 14*.

### **Screened Compound Library**

The compound collection that we screened for this work was composed of the following libraries: Vanderbilt Discovery Collection, which is selected from the Life Chemicals collection for HTS. The compounds in this collection were chosen by Vanderbilt medicinal and computational chemists to provide lead-like motifs, minimum pan-assay interference, and maximum diversity; NIH Clinical Collection I and II, which are small molecules that have history of use in human clinical trials; NCI Focused Natural Product Collection, which is comprised of

pure compounds acquired by the NCI from Analytical and MerLion; Cayman Lipid Library, which is a broad variety of bioactive lipids; Ion Channel Library, which is a collection from Life Chemicals targeted to ion channels compiled using 2D fingerprint similarity methodology; Epigenetics Collection, which is a group of small molecule modulators with biological activity for use in epigenetic research; Marnett Collection, which contains NSAID derivatives that contain cyclooxygenase inhibitors, PPAR $\gamma$  activators, and apoptosis inducers; and the Enzo Kinase Inhibitor Library, which is the Screen-Well™ Kinase Inhibitor Library containing 80 known kinase inhibitors of well-defined activity.

### **Western Blot**

Untransfected and engineered GIRK1/2, GIRK2, and G2Y4-expressing HEK293 cell lines were grown to 100% confluence in tissue culture treated 150 cm<sup>2</sup> dishes. The growth medium was aspirated and plates were twice washed with 5 mL phosphate-buffered saline (PBS) pH 7.4 (Thermo Fisher Scientific, Waltham, MA). Cells were scraped from the dish and triturated. Cell suspensions were then centrifuged at 500 g for 5 min at RT. Next, the supernatant solution was removed, and the pellet was resuspended in 1 mL of PBS and centrifuged once more. After removal of the supernatant solution, cells were resuspended in 1 mL of RIPA buffer (Sigma-Aldrich, St. Louis, MO) containing Halt™ Protease Inhibitor Cocktail (Thermo Fisher Scientific, Waltham, MA) and stored on ice. Suspensions were then ultrasonicated in 4 brief 5 s pulses and allowed to cool on ice for 15 min before centrifugation at 6,000 g for 10 min in a 4°C room. The supernatant was recovered, and the protein concentration was determined using the Pierce™ BCA Protein Assay Kit (Thermo Fisher Scientific, Waltham, MA) with a SpectraMax Plus 384 Microplate Reader (Molecular Devices, San Jose, CA). Samples were diluted to contain 30  $\mu$ g of protein in 25

$\mu$ L of Laemmli Sample Buffer (Bio-Rad, Hercules, CA) containing 355 mM  $\beta$ -mercaptoethanol (Sigma-Aldrich, St. Louis, MO). Samples were heated at 55 °C for 10 min before loading, and the gel was run according to the NuPage Bis-Tris/MOPS protocol using NuPage buffers and gel (Invitrogen, Carlsbad, CA). 25  $\mu$ L/well of each sample was loaded onto a precast NuPAGE 4-12% Bis-Tris Gel and separated for 50 min at 200 V in NuPAGE MOPS SDS Running Buffer. The gel was transferred onto Odyssey Nitrocellulose Membrane (LI-COR Biosciences, Lincoln, NE) for 1 h at 30 V in NuPAGE Transfer Buffer. The membrane was rinsed using Tris-buffered Saline (TBS; Corning, Corning, NY) before blocking with 25 mL of TBS containing 5% (w/v) Blotting Grade Blocker Non-fat Dry Milk (Bio-Rad, Hercules, CA) at RT for 1 hour. For the remainder of the membrane treatments, 0.05% Tween 20 was added to the milk-containing TBS buffer and will be referred to as TT20. Next, the membrane was incubated overnight at 4°C in TT20 containing a 1:2,000 dilution of a monoclonal IgG2b mouse anti-GIRK1 antibody (cat#TA504152, Origene, Rockville, MD) and a 1:1,000 dilution of monoclonal IgG rabbit anti-GIRK2 antibody (cat#25797, Cell Signaling Technology, Danvers, MA). On the next day, the membrane was washed 3 times with 5 mL of TT20 for 5 min each before incubating for 1 h at RT in TT20 containing a 1:20,000 dilution of fluorescent IRDye 800CW donkey anti-rabbit antibody (LI-COR Biosciences, Lincoln, NE) and a 1:20,000 dilution of fluorescent IRDye 680LT donkey anti-mouse antibody (LI-COR Biosciences, Lincoln, NE). Afterwards, the membrane was washed 3 times in 5 mL of TT20 for 5 minutes before a final rinse with TBS. Fluorescence from secondary antibodies was detected using the Odyssey CLx (LI-COR Biosciences, Lincoln, NE).

## Results

### Validating the Expression of GIRK2 and NPY4R in HEK293 Cells

We confirmed the expression of the GIRK2 protein in HEK293 cells by western blot (*Figure 15a*). As expected, the GIRK2 homomeric protein was identified as a band at approximately 46 kDa. Further, we confirmed NPY4R expression using a functional assay. This assay involved testing hPP activity in G2Y4 cells using  $TI^+$  flux and utilizing PTX to inhibit the activity of NPY4R on GIRK2 channels. This experiment and its results were nearly identical to the experiment reported in *Figure 18b*.

### Selection and Counter Screening of Hits from the GIRK2 Channel High-throughput Screen

We have deposited the outcomes of our HTS to the publicly-available PubChem BioAssay Database accessible at <https://pubchem.ncbi.nlm.nih.gov/> under the Assay IDs 1259324 (first portion of this HTS) and 1259325 (second portion of this HTS). The available data include the structures and lists of the compounds we tested, descriptions of the screened parameters for each part of the screen, the results of each counter screen, and the final hit list with relative compound efficacies. Herein, we describe these results.

In total, we screened 97,359 compounds for activity on GIRK2 channels. Of these, 34,131 compounds were screened during the first phase of the HTS. During the second part of this HTS, we screened 63,228 compounds. For data analysis of this HTS, compound activity was calculated by analyzing time-dependent fluorescence data on a plate-to-plate basis as described briefly below, and in more detail in the **Methods** above. For hit picking after completion of screen and of the compound analyses, we recorded fold-changes in fluorescence as well as the percentage change

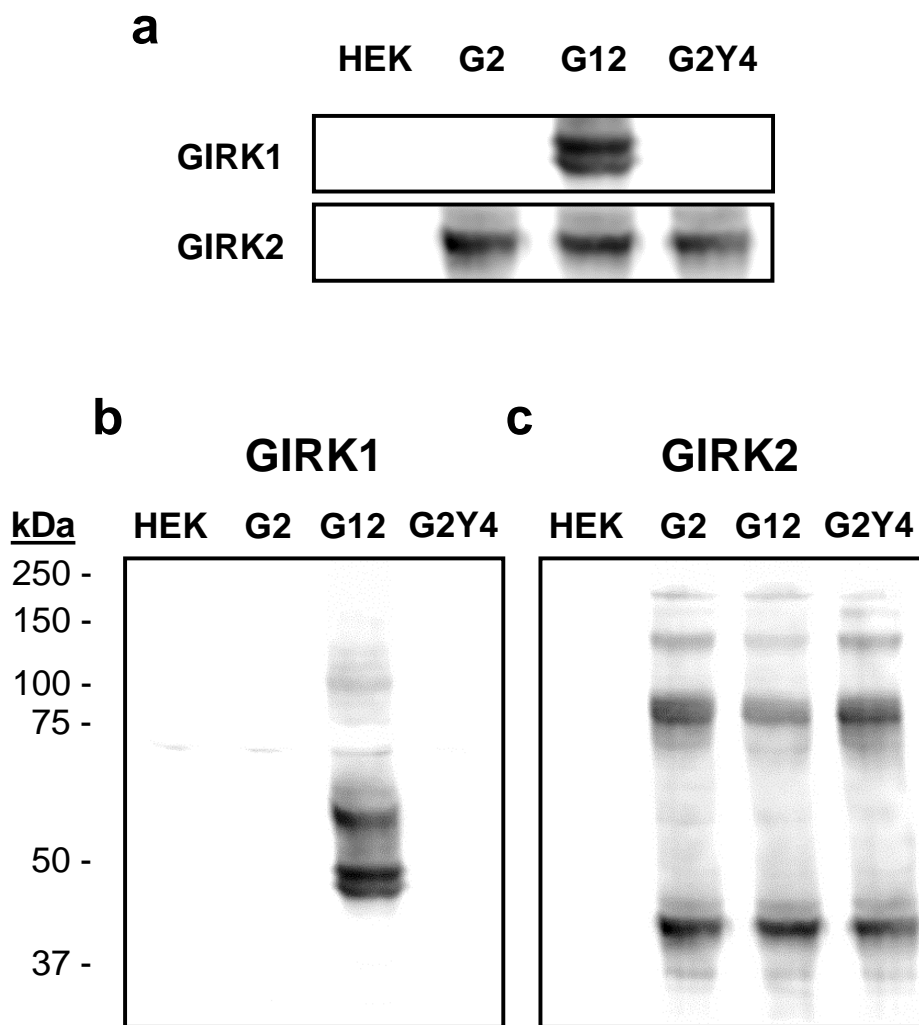
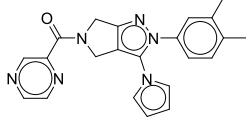
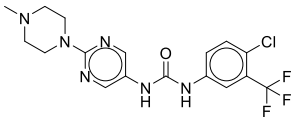
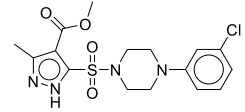
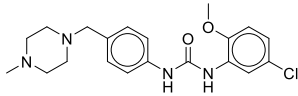
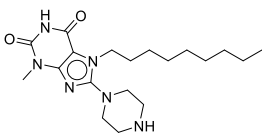
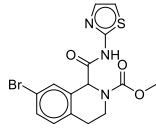
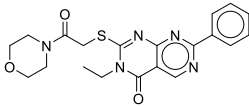
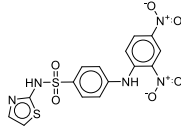
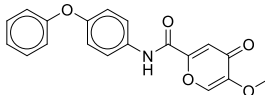


Figure adapted from Kozek, K.A. et al., *ACS Chemical Neuroscience* **2018**.

**Figure 15.** (a) GIRK1 and GIRK2 protein expression levels shown in untransfected HEK293 cells (HEK) or cells engineered to express GIRK2 (G2), GIRK1/2 (G12), or GIRK2 and NPY4R (G2Y4). Complete western blots of the data in (a) were imaged with (b) anti-GIRK1 antibody and (c) anti-GIRK2 antibody, revealing bands for GIRK1 at ~56 kDa and for GIRK2 at ~46 kDa, as expected.

relative to the avermectin analog controls, per plate. These values were combined to generate a single measure of compound activity, which was then used to rank the compounds. In this way, compounds were ranked based on their ability to generate an increase in fluorescence as well as how the compound performed as compared to our controls. Combining this information provided a robust method for capturing active molecules. From this list, we chose the top 200 compounds to test for activity on GIRK2 channels in search of the most efficacious, and promising, channel activators.

After selecting these top 200 molecules to test for activity against GIRK2 cells. We learned that that 61 of these molecules increased fluorescence in HEK293 cells without GIRK channel expression, generating  $\text{Ti}^+$  influx by a GIRK2-independent pathway. We also found that only 52 of these compounds displayed activity on GIRK2 cells. When we tested these molecules in the presence of PTX, we found 9 compounds that did not lose efficacy due to inhibition of GPCR signaling. We determined the relative efficacy of these 9 scaffolds as compared to VU0529331, our most efficacious hit, and generated a ranked list (*Table 1*). These molecules were the only candidates for further characterization from our entire ~100,000 compound screen. Curious to see whether the activity of these molecules differed when tested in a GIRK1/X channel, we briefly investigated the activity of these compounds on GIRK1/2 channels; one of these molecules demonstrated differential activity for GIRK2 and GIRK1/2, but the efficacy of this compound was too low to warrant future characterization.

Compound Structure	VU Number	GIRK2 Efficacy	GIRK1/2 Efficacy
	VU0529331	++++	++++
	VU0537695	+++	+++
	VU0620931	++	+++
	VU0648786	++	++
	VU0510988	+	Inhibitor
	VU0541289	+	+
	VU0627321	+	+
	VU0510748	+	+
	VU0643342	+	++

**Table 1.** (a) 9 scaffolds of hits from the GIRK2 channel high-throughput screen that activated GIRK2 channels in a  $G_{i/o}$  protein-coupled receptor independent manner.



## Discussion

Throughout both parts of this HTS, we utilized a three-addition protocol in order to provide multiple distinct analysis windows from within which molecules with different behaviors, i.e. fluorescent molecules, activators, or inhibitors, could be identified (*Figure 12a*). Comparison of the screened compounds against our positive activator controls, namely eprinomectin, ivermectin, MPD, or hPP, and against our positive inhibitor control, SCH-23390, provided us with a measure of compound activity in either direction. About a third of the way through this HTS, we changed the design of this HTS changed significantly, but in the end, it did not greatly affect the manner in which we would discover activators.

Initially, the purpose of NPY4R overexpression was to promote modest activation of GIRK2 channels through the  $G_{i/o}\beta\gamma$  pathway using an  $EC_{30}$  concentration of hPP throughout the screen. We had chosen this approach in order to enable discovery of inhibitors and activators of GIRK2 channels and, potentially, potentiators of hPP activity on NPY4R. However, a third of the way through the screen we adjusted our methodology to exclude use of hPP, as outlined in the **Methods** section above. This removed the  $EC_{30}$  activation with hPP during the second addition and replaced the hPP added in the third addition with a partially-activating concentration of MPD. Further, we decreased the time window between the second and third additions from 120 s to 30 s and decreased the final waiting time after the third addition.

These changes were done for multiple reasons. First, we became concerned that the bovine serum albumin we used to protect hPP from being absorbed to the many plastics used throughout screening was actually affecting the concentration of the screened compounds. The majority of drug-like small molecules can be absorbed >90% by albumin, and we grew concerned that we might be missing a number of hits. Second, we desired a more consistent method of activating

GIRK channels; even with the use of albumin to limit the effects of plastic containers on hPP concentration, the hPP activity demonstrated greater well-to-well and plate-to-plate variability than we desired and expected. We found that using MPD, provided more consistent plate-to-plate activation of GIRK2 channels. Finally, since we shortened the length of each assay by 40%, from ~370 s to ~220 s, we were able to increase the rate of completion of this HTS. In fact, this change was one of the key factors that enabled our group to screen upwards of 16,000 compounds per day.

After our work identifying the 9 scaffolds that were efficacious on GIRK2 channels, we pursued in-depth characterization and development of the most promising compounds. This work involved analog acquisition and testing, medicinal chemistry, off-target screening, and characterization via whole-cell voltage-clamp electrophysiology (EP). We aimed to identify the most potent and efficacious GIRK activators. Because these studies are costly with regards to both laboratory resources and time, we aimed to budget our time and resources most efficiently. We wanted to confirm that our most efficacious hits would be amenable to medicinal chemistry, and we asked our collaborator Dr. Corey R. Hopkins to confirm that the most promising candidates would be worthwhile of pursuit through medicinal chemistry efforts. Dr. Hopkins confirmed that from among the hits, VU0529331, VU0537695, and VU0648786 (*Table 1*) would be valuable scaffolds to synthetically explore. Further he was eager to learn more about VU0537695 and VU0648786 due to the biaryl urea-based scaffold each compound presented. These molecules, were structurally reminiscent of ML297, the first potent, efficacious, and selective GIRK1/X activator discovered by our laboratory. Together with our collaborator Dr. Hopkins, we had already synthesized and characterized over 800 analogs of ML297 over the last half decade. However, none of those biaryl urea analogs had shown any activity on non-GIRK1/X channels. Our laboratory has extensive knowledge of biaryl urea analogs that cannot activate non-GIRK1/X

channels, so we were pleasantly surprised to discover new biaryl urea structures that appeared to activate GIRK2 channels. Unfortunately, through further investigation of these molecules we learned that while their performance in the  $\text{TI}^+$  flux assays was repeatable, although with low efficacy relative to our ML297 controls against GIRK1/2 channels, evaluation with EP assays produced confounding results where exposure to the compound initially appeared to result in brief increased channel activity, but upon continued exposure the molecule demonstrated clear and complete inhibition of GIRK currents. While interesting, we choose not to further evaluate these compounds. We had been conducting experiments in parallel, and we had identified that VU0529331 was more potent and more efficacious on GIRK channels with robust activity demonstrated by  $\text{TI}^+$  flux and EP assays. In **Chapter 3**, we describe our thorough characterization of VU0529331.

## CHAPTER 3

### CHARACTERIZATION OF VU0529331 ACTIVITY ON GIRK CHANNELS

#### Abstract

With the completion of a high-throughput  $\text{TI}^+$  flux assay-based screen for activators of GIRK2 channels, we selected for further characterization the most efficacious and potent compound, namely VU0529331. We studied this molecule using a multitude of assays, including  $\text{TI}^+$  flux assays,  $\text{Cl}^-$  influx assays, and whole-cell voltage-clamp EP to study a variety of channels. We confirmed that VU0529331 acted independently of G protein-coupled receptor signaling and that it required GIRK channel expression for activity. Further, we discovered that this compound was broadly active on GIRK channels, including GIRK2, GIRK1/2, GIRK1/4, and GIRK4 channels. To our knowledge, VU0529331 is the first moderately potent and efficacious small molecule reported to activate homotetrameric GIRK4 channels, in addition to being the first potent and efficacious synthetic small molecule activator of homotetrameric GIRK2 channels. We confirmed the activity of VU0529331 on GIRK2 and GIRK1/2 channels using EP and discovered that this compound generated a larger activity in GIRK2 channels as compared to GIRK1/2 channels. Using  $\text{Cl}^-$  influx assays, we determined that VU0529331 was inactive on a representative anion-selective Cys-loop receptor; these receptors were a suspected target of VU0529331 because they are activated by ivermectin, a compound previously shown to also activate GIRK1/2 and GIRK2 channels. Further, by testing the activity of VU0529331 on a broader selection of  $\text{K}^+$  channels, we discovered that this compound was also a potent and efficacious activator of  $\text{K}_{\text{ir}}6.1/\text{SUR2a}$  and  $\text{K}_{\text{ir}}6.1/\text{SUR2b}$  channels. To our knowledge, VU0529331 is also the first

reported small molecule activator of  $K_{ir}6.1/SUR2a$  channels. These results suggest a yet undiscovered structural and pharmacological homology between the GIRK and  $K_{ir}6$  families. Unfortunately, our studies with analogs of VU0529331 did not generate any compounds with improved potency or efficacy on GIRK channels. Herein, we detail our extensive efforts toward characterizing VU0529331.

## Introduction

Upon discovering that VU0529331 (*Figure 16*) was the most efficacious hit from the GIRK2 HTS, as described in **Chapter 2**, we sought to characterize the activity of this molecule more thoroughly. In brief, we confirmed the results from our initial counterscreens, explored VU0529331 analogs for improved activity on GIRK channels, characterized the activity of VU0529331 on a broad variety of ion channels, and studied its ability to modulate GIRK channels using EP. By combining the knowledge gained through these experiments, we were able to determine with confidence that VU0529331 binds directly to GIRK channels and increases the ion current through the channel. Below, we introduce the process and logic behind the characterization of VU0529331's activity using  $Tl^+$  flux assays, fluorescence resonance energy transfer (FRET)-based  $Cl^-$  influx assays, and whole-cell voltage-clamp EP.

To begin, we sought to validate the results from our HTS and to measure the potency and efficacy of VU0529331 on the various GIRK channels, namely GIRK1/2, GIRK2, GIRK1/4, and GIRK4. We also aimed to confirm that PTX did not modify the potency and efficacy of VU0529331. If the potency or efficacy of VU0529331 changed with PTX application, then we would be concerned that the activity of VU0529331 may not be on the GIRK channel, but

potentially interacting with the  $G_{i/o}\beta\gamma$  subunit. Next, we aimed to study the activity of VU0259331 on GIRK channels using EP.

We wanted to identify the changes in GIRK channel activity due to VU0529331 using whole-cell voltage-clamp EP. This technique enables the measurement of currents generated through the various ion-permeant pathways on the membrane of a single cell. In cells that overexpress a channel of interest, such as GIRK2, the dominant current corresponds to the overexpressed GIRK2 channel. We first aimed to investigate whether the activity of VU0529331 observed via  $TI^+$  flux assays could be replicated with EP. For this, we would generate current-voltage (IV) relationship curves from multiple series of current recordings over a range of membrane potentials. IV curves illustrate the different currents evoked through GIRK channels over this range of membrane potentials for a cell. Further, IV curves would allow us to identify and measure the extent of any VU0529331-evoked changes in the inward rectification, the and  $K^+$  selectivity. The importance of these properties to the function of GIRK channels was described in **Chapter 1**. Briefly, alteration of the reversal potential would indicate that the compound disrupted the  $K^+$  selectivity of GIRK channels. Changes in rectification would indicate that the VU0529331 altered the characteristic inhibition of outward  $K^+$  currents through GIRK channels.

If we determined that VU0529331 did not drastically alter the characteristic properties of GIRK channels, we would then study the effect of this compound on GIRK currents recorded at one membrane potential. For this, we would keep the membrane at a specific potential and record how the channels reacted to the presence of VU0529331. We would hold the membrane at a potential more negative than that of the  $K^+$  reversal potential because the inward rectification of GIRK currents makes the inward currents more linear with respect to membrane potential. Outward currents are inhibited, and we would like to observe changes in GIRK channel  $P_o$  and not

any potential disinhibition evoked by a compound. In this way, we sought to observe changes in GIRK currents with increasing concentrations of VU0529331. This way, we could study the concentration-dependence of VU0529331 with EP and compare this to our measurements using  $\text{TI}^+$  flux. Additionally, we sought to use  $\text{Ba}^{2+}$ , a non-selective  $\text{K}_{\text{ir}}$  channel inhibitor, to investigate whether an increase in current evoked by VU0529331 could be inhibited. This would further support that the VU0529331-evoked currents were mediated through GIRK channels and that VU0529331 does not dramatically alter the channel's sensitivity to  $\text{Ba}^{2+}$ . Taken altogether, the information gleaned from such EP studies could help understand the mechanism by which VU0529331 increased  $\text{TI}^+$  influx and whether this molecule would be useful for studying GIRK channels in native cells. If VU0529331 dramatically changes the properties specific to GIRK channels, VU0529331's utility as a probe for *in vitro*, *ex vivo*, and *in vivo* studies will be limited. Typically, such studies aim to maintain the inherent characteristics of a channel. That is, unless one were to study the compound-induced dysregulation of a specific property of a channel that may otherwise only be naturally-occurring with a genetic mutation. Our efforts characterizing VU0529331 through EP are reported in the **Results** below.

Next, we aimed to study the selectivity of VU0529331 among a variety of ion channels. We previously discussed how the lack of selectivity of ivermectin for GIRK channels was a significant deficiency limiting its use as a GIRK probe (see **Chapter 1**). We wanted to determine whether VU0529331 would have similar issues with selectivity and have an undesirable pharmacological profile similar to the avermectins. First, we wanted to identify whether VU0529331 was capable of activating closely or distantly-related  $\text{K}^+$  channels using  $\text{TI}^+$  flux assays. Next, we sought to test the activity of VU0529331 on a member of the Cys-loop receptor superfamily. We focused our attentions on the glycine receptor  $\alpha 1$  ( $\alpha 1$  GlyR) Cys-loop receptor,

which ivermectin has been demonstrated to activate and potentiate.<sup>117</sup> To study whether VU0529331 activated  $\alpha 1$  GlyR, we developed and conducted a SuperClomeleon FRET-based  $\text{Cl}^-$  influx assay. This assay is described in detail in the **Methods** below.

In addition to investigating the activity of VU0529331 on a variety of ion channels, assays in which the compound was kept constant and the targets changed, we wanted to switch around the variables. We wanted to study how modifying the structure of VU0529331 would alter its activity on GIRK2 channels. This is known broadly as the study of the structure-activity relationship (SAR). Ideally, SAR studies inform the development of compounds with improved efficacy and potency against a target. Sometimes, the SAR may reveal structural substitutions that grant a compound selectivity for one target versus another, i.e. among different GIRK channels. Other times, the SAR may reveal substitutions that drastically alter the activity on a target, i.e. inhibitors may be identified from substitutions on an activator. Both such phenomena have been observed in our laboratory while studying the SAR of ML297 (see **Chapter 1**). Herein, we described our efforts to illuminate the SAR of VU0529331.

## **Methods**

### **Cell Line Generation**

GIRK1/2, GIRK2, and G2Y4 cells were created as previously described in **Chapter 2**. The FuGENE 6 (Promega, Madison, WI) transfection reagent and protocol, together with Opti-MEM (Thermo Fisher Scientific, Waltham, MA), were utilized in all transfections herein. Further, all transfections were conducted in low-passage HEK293 cells. To study GIRK4 channels, HEK293 cells were transiently transfected with a pCMV6-A-Neo vector (Origene, Rockville, MD)



containing human KCNJ5. HEK293 cells stably expressing human  $\alpha 1\beta 2$  MaxiK and  $\alpha 1\beta 4$  MaxiK channels were generated by transfecting a pCMV6-A-puro vector (Origene, Rockville, MD) with human KCNMA1 and a pcDNA3.1(+)/zeo vector (Genscript, Piscataway, NJ) with either human KCNMB2 or human KCNMB4, respectively. HEK293 cells expressing human Slack channels were generated by transfecting a pCMV6-Entry vector (Origene, Rockville, MD) containing the KCNT1 gene. HEK293 cells expressing human  $K_v 2.1$  channels were generated by transfecting a vector encoding the KCNB1 gene, generously provided by the Dr. Jennifer Kearney laboratory.<sup>138</sup> HEK293 cells expressing both human  $K_{ir}6.1$  and rat SUR2a were generated by transfecting a pBUDCE4.1 vector (Invitrogen, Carlsbad, CA) containing KCNJ8 and ABCC9 isoform A. HEK293 cells expressing both human  $K_{ir}6.1$  and rat SUR2b were generated by transfecting a pcDNA5/TO vector (Origene, Rockville, MD) containing KCNJ8 and a pcDNA3.1 vector, generously provided by the Dr. Colin Nichols laboratory, containing ABCC9 isoform B. Stably-transfected monoclonal T-REx-HEK293 cell lines expressing human  $K_{ir}2.1$ ,<sup>139</sup>  $K_{ir}4.1$ ,<sup>140</sup> or  $K_{ir}6.2/SUR1$ <sup>141</sup> under a tetracycline-inducible promoter were previously generated and provided by the laboratory of Dr. Jerod S. Denton. HEK293 cells stably expressing SuperClomeleon and KCC2 were generated in a T-REx-HEK293 background by transducing a pLenti CMV Puro DEST vector containing SuperClomeleon and transfecting a pcDNA4/TO vector containing human KCC2 isoform B. To study  $\alpha 1$  GlyR, this cell line was then transiently transfected with a pCMV6-A-hygro vector containing human GLRA1. All stably-transfected cells were maintained under antibiotic selection over their lifetime.

## Cell Culture Conditions

Cell culture was conducted as described in **Chapter 2**.

## **Generation of Monoclonal Cell Lines**

Monoclonal cell lines were generated as described in **Chapter 2**.

## **384-well Cell Plate Preparation for Fluorescence-based Experiments**

For use in  $\text{TI}^+$  flux experiments, HEK293 cells stably expressing a protein of interest were prepared as described in **Chapter 2**. Preparation of cell plates for experiments that utilized transient protein expression, as with GIRK4 and  $\alpha 1$  GlyR channels, is described below. HEK293 cells transiently transfected with channel-encoding plasmids were utilized to test the properties of GIRK4 channels using a  $\text{TI}^+$  flux assay and to test the properties of  $\alpha 1$  GlyR channels using a  $\text{Cl}^-$  influx assay. These cells were not processed for monoclonal selection. Instead, they were generated anew prior to each assay. To generate these cells, transfections were conducted when flasks were 40% confluent. Flasks were incubated overnight to reach 90% confluence in a humidified incubator at  $37^\circ\text{C}$  and 5%  $\text{CO}_2$ . To prepare cells for transfer into 384-well plates, culture medium was removed from flasks, flasks were treated using TrypLE Express for 5 min to dislodge cells, and single-cell suspensions were generated through trituration. Cells were resuspended in antibiotic-containing medium at 1,000 cells/ $\mu\text{L}$ . 1  $\mu\text{g}/\text{mL}$  of tetracycline (Sigma-Aldrich, St. Louis, MO) was added to suspensions in which cells expressed a protein under a tetracycline-inducible promoter. 20  $\mu\text{L}$  of cellular suspension was plated in each well of 384-well plates to achieve a cellular density of 20,000 cells/well. Cell plates were incubated overnight in a humidified incubator at  $37^\circ\text{C}$  and 5%  $\text{CO}_2$ .

## **Pertussis Toxin Treatment of Cells for $\text{TI}^+$ Flux Experiments**

See **Chapter 2**.

## **Compound Dissolution and Maintenance**

All commercially purchased dry compounds were dissolved in DMSO, unless otherwise specified, to generate 100 mM stocks. If compound solubility was an issue, the concentration was decreased until compounds were completely soluble. Dissolution was attempted at a concentration by adding DMSO to dry powder, vortexing the solution, ultrasonicated the compound, and checking for a completely transparent solution. Compounds from collaborators that were received as dry powders were also solubilized in this way. Otherwise, compounds from collaborators were generally received at 10 mM in DMSO. Commercially-acquired compounds and analogs not available through conventional purchasing methods were ordered through AldrichMarketSelect (Sigma-Aldrich, St. Louis, MO). All compounds received from the Vanderbilt HTS Core Facility were stored as 10 mM stocks in DMSO. Stock compounds for these experiments included 33.3 mM VU0529331, 30 mM ML297, 30 mM VU0466551, 30 mM SCH-23390, and 100 mM ivermectin. All compounds were stored as instructed by the originating source in desiccators at either room temperature, 4°C, or, -20°C. Compound aliquots of <100 µL were generated when compounds were used often in order to limit freeze-thaw cycles of the larger stocks.

## **Compound Plate Preparation for High-throughput Experiments**

To generate high-throughput compatible compound plates for all TI<sup>+</sup> flux experiments and FRET experiments described below, 10 µL aliquots of stock compounds were dispensed by hand into 384-well, Echo qualified, low dead volume microplates (Labcyte, Sunnyvale, CA). These stock compound plates were then reformatted using an Echo555 plate reformatter (Labcyte, Sunnyvale, CA) to generate a desired compound layout containing one or more compounds/well in 384-well, round-bottom, polypropylene microplates (compound plates; Greiner, Monroe, NC).

In this way, compounds were dispensed as 2.5-500 nL aliquots from stocks and backfilled with DMSO all within the same Echo555 protocol to generate 80-500 nL/well compound samples. These samples were dissolved to 40-100  $\mu$ L/well with assay buffer comprising Hanks Balanced Salt Solution (Thermo Fisher Scientific, Waltham, MA) and 20 mM HEPES pH 7.3 (Corning, Corning, NY). Each compound plate was designed to provide compound solutions at concentrations twice the final concentration. Solutions were then diluted 2-fold during the assay such that the desired final concentration was applied to cells during imaging. When creating concentration-response curves (CRCs), a.k.a. dose-response curves, compounds were distributed in 10-concentration, 3-fold dilution series in compound plates. Compound plates were solubilized as described in **Chapter 2** and used within an hour of preparation. The final DMSO concentration in all assays was  $\leq 0.25\%$  (v/v). For all experiments, compounds were DMSO-matched to eliminate any differences due to DMSO concentrations.

### **Execution and Analysis of $\text{Ti}^+$ Flux Experiments**

The  $\text{Ti}^+$  flux assays were conducted as previously described in **Chapter 2**. Below, we detailed the specifics of the assays pertaining to the characterization of VU0529331. Data for all experiments were acquired at 5 Hz (excitation  $482 \pm 35$  nm, emission  $536 \pm 40$  nm). The  $\text{Ti}^+$  stimulus buffer comprised of 125 mM  $\text{NaHCO}_3$ , 1.8 mM  $\text{CaSO}_4$ , 1 mM  $\text{MgSO}_4$ , 5 mM glucose, either 2 or 4 mM  $\text{Ti}_2\text{SO}_4$ , and 20 mM HEPES pH 7.3.

To better observe activity of certain channels, assay parameters were varied as follows: MaxiK-expressing cells were tested using a  $\text{Ti}^+$  stimulus buffer containing 3  $\mu$ M ionomycin, which elevated intracellular  $\text{Ca}^{2+}$  and promoted channel activity to approximately  $\text{EC}_{30}$ .  $\text{K}_v2.1$ -expressing cells were tested using a modified  $\text{Ti}^+$  stimulus buffer (87.5 mM  $\text{NaHCO}_3$ , 37.5 mM  $\text{KHCO}_3$ , 1.8

mM CaSO<sub>4</sub>, 1 MgSO<sub>4</sub>, 5 mM glucose, 4 mM Tl<sub>2</sub>SO<sub>4</sub>, and 20 mM HEPES pH 7.3) containing an elevated K<sup>+</sup> concentration to promote channel activity to approximately EC<sub>30</sub>. As described in **Chapter 2**, ΔA was calculated as the difference in amplitude between time points T<sub>s</sub>-5 s and T<sub>s</sub>+X s, where X ranges between 2 and 15 s depending on the particular cell line. For each cell line, this time point was chosen to provide a high signal-to-noise ratio while measuring nearest the linear portion of the initial Tl<sup>+</sup> influx. These values are inversely proportional to the overall measured activity of a specific channel. Specifically, X=15 for untransfected HEK293, GIRK2, K<sub>ir</sub>6.1/SUR2a, K<sub>ir</sub>6.1/SUR2b, K<sub>ir</sub>6.2/SUR1, α1β2 MaxiK, and α1β4 MaxiK cells, X=5 for GIRK1/4, Slack, K<sub>v</sub>2.1, K<sub>ir</sub>2.1, and K<sub>ir</sub>4.1 cells, and X=2 for GIRK1/2 cells. ΔA values for each compound at different concentrations were used to generate fits to a four-parameter logistic equation in XLfit (IDBS, Guildford, Surrey, United Kingdom). Statistical analyses were performed using Prism 7 (GraphPad, La Jolla, CA).

### **SuperClomeleon Cl<sup>-</sup> Influx Assay of Cys-Loop Receptor Activity**

Our laboratory developed a SuperClomeleon FRET-based Cl<sup>-</sup> influx assay to study activation of anion-selective Cys-loop receptors. Briefly, SuperClomeleon is a genetically-encoded fluorescent (optogenetic) sensor designed to monitor intracellular Cl<sup>-</sup> concentrations.<sup>142</sup> Structurally, SuperClomeleon consists of two linked fluorescent proteins, a Cl<sup>-</sup>-sensitive yellow fluorescent protein (YFP) and a Cl<sup>-</sup>-insensitive cyan fluorescent protein (CFP). The Cl<sup>-</sup>-sensitive YFP was engineered to exhibit high affinity for Cl<sup>-</sup> and possesses a Cl<sup>-</sup> binding pocket that quenches YFP fluorescence when occupied.<sup>142</sup> During a SuperClomeleon fluorescence assay, the intensity of both YFP and CFP fluorescence is measured over time. With the CFP energy donor and YFP energy acceptor, SuperClomeleon undergoes CFP-YFP FRET that enables ratiometric

determination of  $\text{Cl}^-$  concentrations. This feature eliminates multiple confounding factors to yield higher reproducibility within assays.<sup>142</sup> This is because fluorescence acquired using ratiometric measurement of  $\text{Cl}^-$  concentrations is not affected by differences in indicator concentration, optical path length, or excitation intensity, effectively making the experiments more reproducible. In addition to expressing SuperClomeleon in a HEK293 cell line, we engineered these cells to express the  $\text{K}^+$ - $\text{Cl}^-$  transporter (KCC2). KCC2 is a neuron-specific  $\text{K}^+$ - $\text{Cl}^-$  symporter that maintains the low intracellular  $\text{Cl}^-$  concentration found in neurons. In this way, KCC2 is critical for establishing the proper  $\text{Cl}^-$  gradient in neurons, which is the gradient that favors inward  $\text{Cl}^-$  influx and provides the correct environment for this assay.<sup>143</sup> After establishing this cell line, we explored the activation of Cys-loop receptors with various compounds.

The design and validation of this FRET assay, as well as all the labor required to generate the reagent cell line, was conducted by Francis J. Prael III. Two days before an experiment, T-REx-HEK293 cells stably expressing SuperClomeleon and KCC2 were grown to 40% confluence in multiple tissue-culture-treated T25 flasks (Corning, Corning, NY). Half of these flasks were transfected with  $\alpha 1$  GlyR using FuGENE 6. All flasks were incubated overnight in a humidified incubator at 37°C and 5%  $\text{CO}_2$ . One day before an experiment, cell medium was treated with 1  $\mu\text{g}/\text{mL}$  tetracycline to enable KCC2 expression and cells were transferred onto 384-well cell plates as described above at 30,000 cells/well. Each cell plate contained at least 1 transfected and 1 untransfected cell type. On the day of an experiment, one compound plate containing VU0529331 and ivermectin (Sigma-Aldrich, St. Louis, MO) at two-fold the desired final compound concentrations was generated as described above. A second compound plate containing five times the desired final glycine concentrations was prepared by hand. Compound plates were used within an hour of preparation, and the final DMSO concentration in all conditions assayed was 0.25%

(v/v). 20 minutes prior to imaging, culture medium on cell plates was replaced with 20  $\mu$ L/well of assay buffer. At the time of imaging, the experiment was loaded into the WaveFront Biosciences Panoptic, and data were acquired at 1 Hz with alternating filters set to capture both the  $\text{Cl}^-$ -insensitive cyan fluorescent protein (CFP) signal ( $440 \pm 40$  nm excitation;  $480 \pm 17$  nm emission filters) and the  $\text{Cl}^-$ -sensing yellow fluorescent protein (YFP) signal ( $440 \pm 40$  nm excitation;  $536 \pm 40$  nm emission). After 10 s of imaging, 20  $\mu$ L/well from the first compound plate was added to the cell plate and imaged for 120 s. Next, 10  $\mu$ L/well from the second compound plate was added, and imaging was concluded after an additional 120 s. Fluorescence data was collected using WaveFront Biosciences WaveGuide and analyzed using Microsoft Excel. Statistical analyses were performed using GraphPad Prism 7. Data reported are the averages of at least 3 independent experiments. The potential of a compound to affect the movement of  $\text{Cl}^-$  across the cell membrane was calculated from normalized and control-subtracted measurements of the area under the curve of the FRET ratio ( $F_{\text{CFP}}/F_{\text{YFP}}$ ) generated throughout imaging. In this way, increased signal correlated with increased intracellular  $\text{Cl}^-$  concentrations.

### **Whole-cell Voltage-clamp Electrophysiology**

Serial dilutions of compounds were done by hand in DMSO, and DMSO stocks were diluted into a buffer consisting of 20 mM KCl, 140 mM NaCl, 0.5 mM  $\text{CaCl}_2$ , 2 mM  $\text{MgCl}_2$ , 10 mM glucose, and 10 mM HEPES (pH 7.4; 315 mOsm), named the 20K extracellular solution (KES). Cells were prepared by triturating flasks of engineered cells (cultured and dissociated as described above) to create single-cell suspensions. Cell suspensions were sparsely plated on 35 mm cell culture dishes (cat#83.3900, SARSTEDT, Nümbrecht, Germany) and incubated overnight in a humidified incubator at  $37^\circ\text{C}$  and 5%  $\text{CO}_2$ . Before patching, culture medium was removed

and each dish was washed twice with 1 mL of assay buffer (Hanks Balanced Salt Solution and 20 mM HEPES pH 7.3) before being filled with 1 mL of KES. Borosilicate glass electrodes (3-7 M $\Omega$  resistance) were filled with intracellular solution containing 130 mM KCl, 20 mM NaCl, 5 mM EGTA, 5.46 mM MgCl<sub>2</sub>, and 10 mM HEPES (pH 7.4; 305 mOsm). Whole-cell current recordings were conducted in KES using a system comprised of an EPC10 amplifier (HEKA Elektronik, Ludwigshafen am Rhein, Germany), an MP-285 micromanipulator (Sutter Instruments, Novato, CA), and an Axiovert 200 microscope (Zeiss, Oberkochen, Germany). HEKA PatchMaster software was used to control the amplifier, enabling semiautomatic signal compensation for electrode capacitance, cellular capacitance, and series resistance. Currents were filtered using the 6-pole Bessel prefilter with 10 kHz bandwidth, and signals were digitized at 20 kHz. Cells were exposed to solutions using a homemade, 8-channel, local superfusion manifold with manual solution switching. Sensitivity to Ba<sup>2+</sup> was measured by applying KES, +/- compound, containing 2 mM BaCl<sub>2</sub> during recordings. Current-voltage (IV) relationships were measured with cells held at -40 mV before switching between -100 mV and 10 mV in 10 mV steps lasting 250 ms and separated by 500 ms. Current density at ~200 ms into each pulse for each step was extracted and averaged for 3 consecutive pulse protocols conducted on an individual cell at each condition. Current density was calculated by dividing current amplitudes by each cell's cellular capacitance in picoFarads (pF). We reported averages of IVs for at least 3 different cells per channel. Data was analyzed using Microsoft Excel. Statistical analyses were performed using GraphPad Prism 7.



## Results

### **Dependence of VU0529331 Activity on GIRK2 Expression and $G_{i/o}$ -coupled G Protein-coupled Receptor Activity**

For these experiments, we utilized VU0529331 (*Figure 16a*) at various concentrations to generate concentration-response curves (CRCs). This enabled measurement of efficacy and potency of compounds on a variety of cell types. First, we tested VU0529331 using  $TI^+$  influx assays in untransfected HEK293 cells. We confirmed that VU0529331 activity was independent of  $TI^+$  influx pathways naturally occurring in HEK293 cells (*Figure 16d*). Next, we confirmed that VU0529331 activity was independent of NPY4R using HEK293 cells engineered to only overexpress GIRK2 channels. VU0529331 activity in the absence of NPY4R confirmed that activity was dependent on GIRK2 expression (*Figure 16b*). Examples of the raw  $TI^+$  flux assay fluorescence traces used to generate these CRCs are provided in *Figure 17*. Next, we confirmed that a natively-expressed  $G_{i/o}$ -coupled GPCR in HEK293 cell lines was not the target of VU0529331 by testing VU0529331 on G2Y4 cells treated with PTX. We confirmed that VU0529331 activity was independent of PTX treatment on G2Y4 cells (*Figure 18a*). In contrast, PTX treatment dramatically inhibited a maximally-effective dose of hPP from activating GIRK channels indirectly (*Figure 18b*), which indicated that the PTX was efficacious at inhibiting  $G_{i/o}$ -coupled GPCR signaling to GIRK2 channels in this system. In this way, we demonstrated that VU0529331 activity was dependent on the expression of the GIRK2 subunit and channel, and that VU0529331 activity was independent of  $G_{i/o}$ -coupled GPCR overexpression and activity.

Figure adapted from Kozek, K.A. et al., *ACS Chemical Neuroscience* 2018.

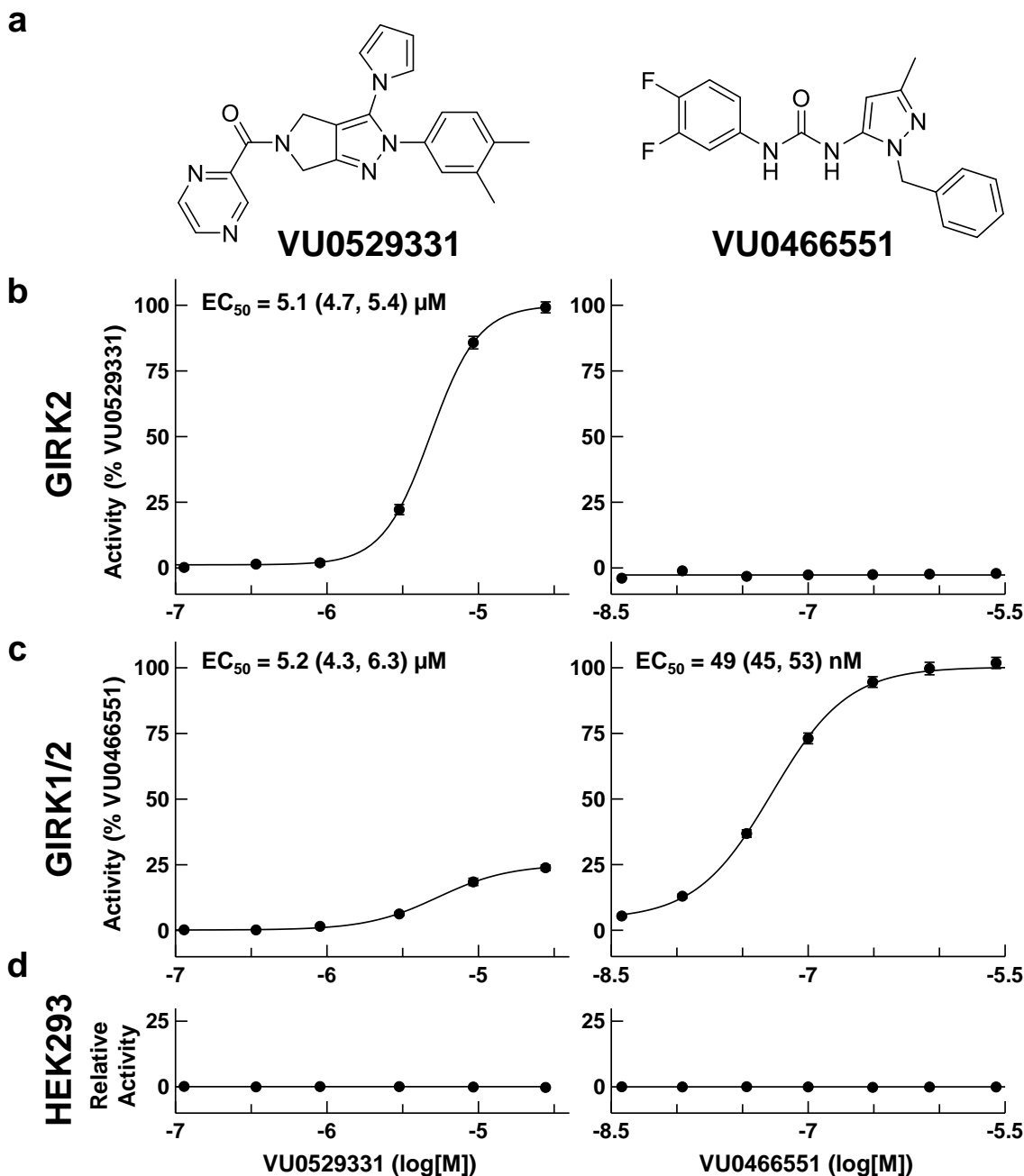


**Figure 16.** Characterization of VU0529331 efficacy and potency using  $\text{Ti}^+$  flux. VU0529331 activated GIRK2 and GIRK1/2 channels in a concentration-dependent manner. In contrast, VU0466551 only activated GIRK1-containing channels. Potency ( $EC_{50}$ ) values were provided for active compounds along with 95% confidence intervals. GIRK2 channel activity was normalized to a maximally-effective concentration of VU0529331, while GIRK1/2 channel activity was normalized to a maximally-effective concentration of VU0466551. All data shown are averages of at least 3 independent experiments, and the error bars represent the standard error of the mean (SEM).

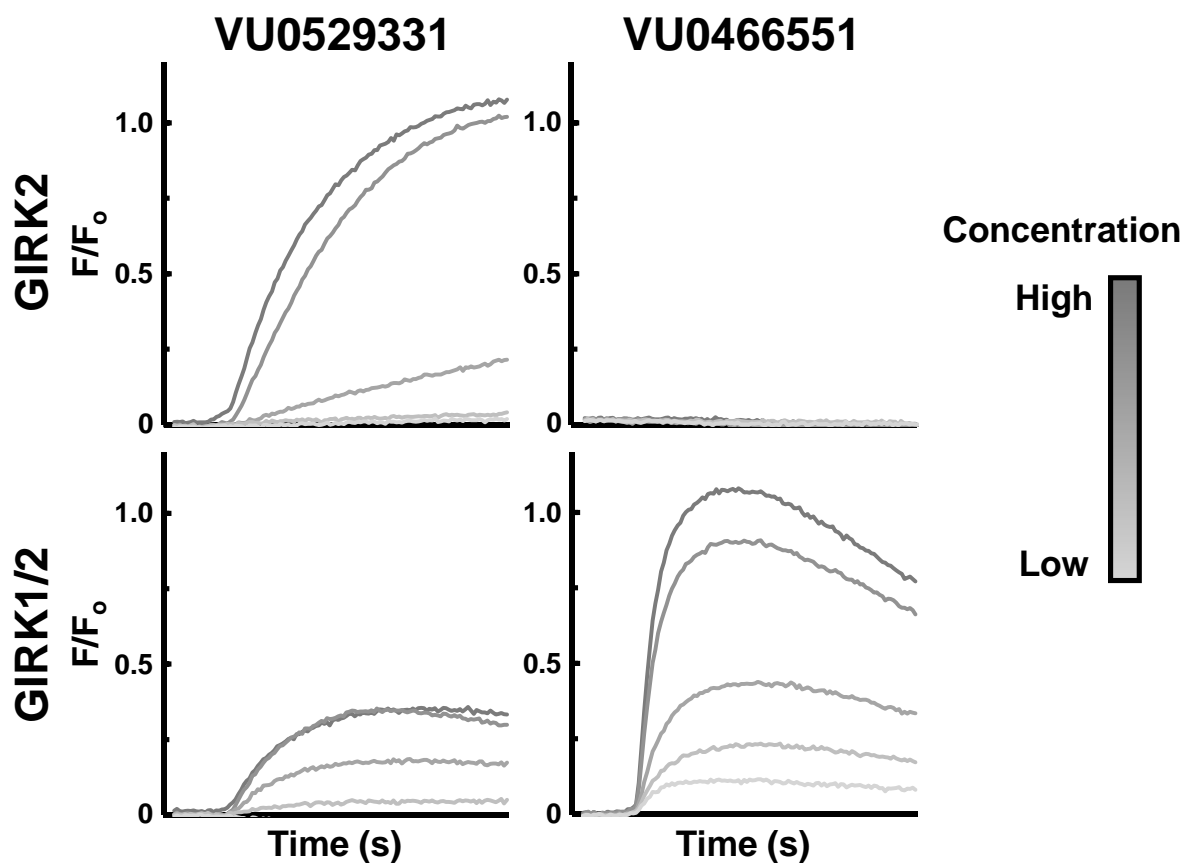
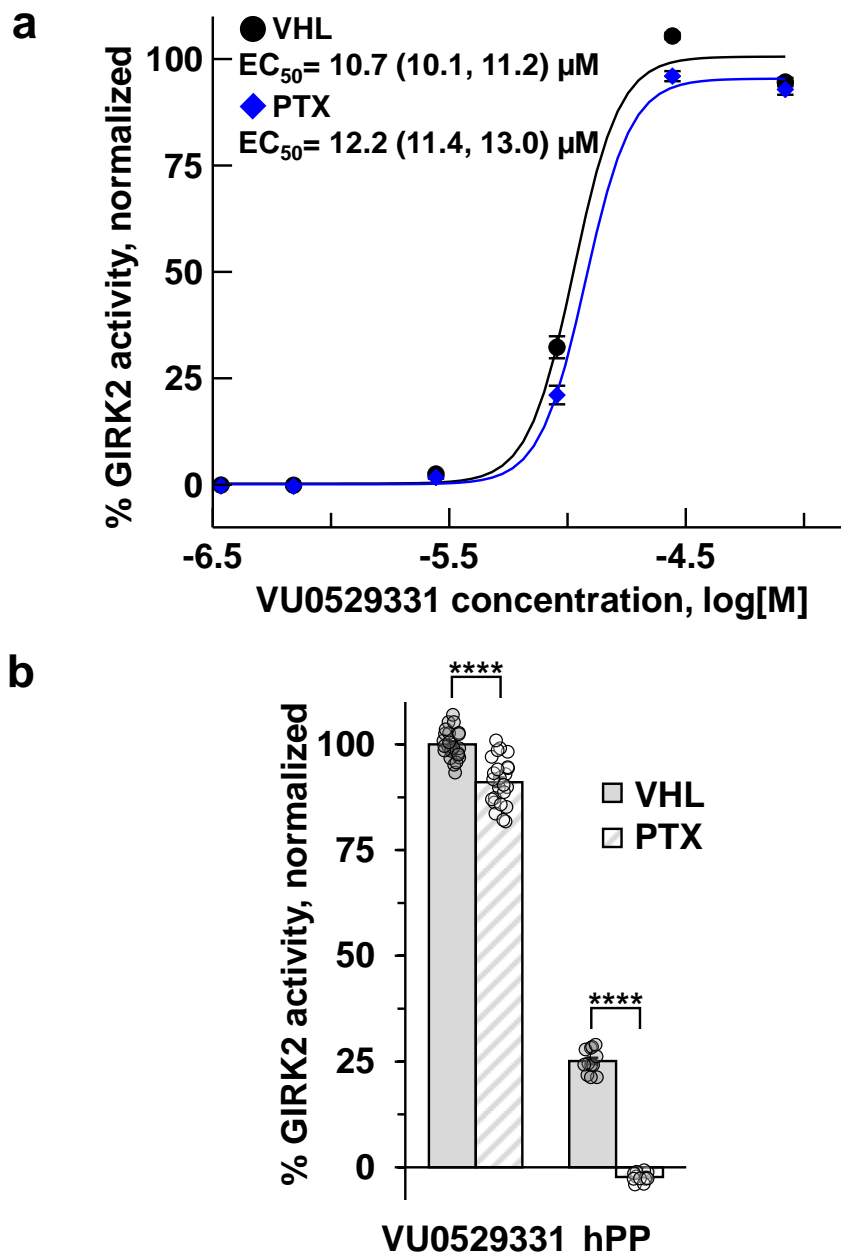


Figure adapted from Kozek, K.A. et al., *ACS Chemical Neuroscience* 2018.

**Figure 17.** VU0529331 increases the activity of GIRK2 and GIRK1/2 channels while VU0466551 increases the activity of GIRK1/2 channels. Channel activity is observed using fluorescence generated during a  $\text{TI}^+$  flux assay, and representative traces are vehicle control subtracted. Fluorescence (F) over time is normalized to initial fluorescence ( $F_0$ ) to yield  $F/F_0$ . The scaling for the  $F/F_0$  axis in all these graphs is relative and can be compared.



**Figure 18.** (a) Pertussis toxin (PTX) does not affect the activity of VU0529331 on G2Y4 cells while (b) activation of GIRK2 through the neuropeptide Y receptor type 4 (NPY4R), or any other  $G_{i/o}$ -coupled GPCR expressed in HEK293 cells, is fully inhibited. A maximally-effective concentration, 200 nM, of human pancreatic polypeptide (hPP) was used to activate NPY4. All values in (a) were normalized to the predicted maximum activity of VU0529331 under VHL conditions. VU0529331 activity in (b) is normalized data from the 30  $\mu\text{M}$  value in (a). 95% confidence intervals for the  $EC_{50}$  measurements were calculated using a 2-tailed Mann-Whitney test. \*\*\*\* indicates  $p < 0.0001$ . Error bars represent the standard error of the mean (SEM). Figure adapted from Kozek, K.A. et al., *ACS Chemical Neuroscience* **2018**.

### **Characterization of VU0529331 Selectivity Among GIRK Channels**

We aimed to determine whether VU0529331 activity was specific to homomeric GIRK2 channels or whether this molecule was also capable of activating other GIRK channels. Using  $\text{TI}^+$  flux assays, we observed that VU0529331 was able to activate GIRK1/2 (**Figure 16c**), GIRK1/4, and GIRK4 channels (**Table 2**) expressed in HEK293 cells. When studying the activity of VU0529331 on GIRK1/X channels, we compared our results against VU0466551, an efficacious, potent, and selective activator of GIRK1/X channels that was previously discovered by our laboratory.<sup>84</sup> We verified that VU0466551 was active on GIRK1/2 channels with a potency of ~50 nM and inactive on both untransfected and GIRK2-expressing HEK293 cells (**Figure 16b,c**). We found that the efficacy of VU0529331 on GIRK1/2 and GIRK1/4 was ~25% and ~20% of the maximum efficacy of VU0466551, respectively (**Table 2**). The raw  $\text{TI}^+$  flux traces (**Figure 17**) demonstrated that VU0529331 was capable of generating a much greater total fluorescence in cells expressing just GIRK2 as compared to cells expressing GIRK1/2 channels. We also examined the activity of VU0529331 in the presence of VU0466551 on GIRK2 and GIRK1/2 channels in order to determine whether one of the compounds affected the ability of the other compounds to modulate GIRK channel activity (**Figure 19**). Overall, these results suggest that VU0529331 is a modestly selective, non-GIRK1/X channel activator in addition to being the first synthetic small molecule known to activate both GIRK2 and GIRK4 homomeric channels.

### **Characterization of VU0529331 Selectivity Among a Broad Variety of Channels**

We assembled a group of engineered HEK293 cell lines that expressed a broad variety of  $\text{K}^+$  channels (**Figure 20**) and investigated the activity of VU0529331 on these cell lines. These

## VU0529331 activity on engineered HEK293 cell lines

Target	Efficacy, % (95% CI)	Potency, $\mu\text{M}$ (95% CI)
GIRK2	<sup>AD</sup> 100	5.1 (4.7, 5.4)
GIRK1/2	<sup>B</sup> 25.9 (+/- 2.4)	5.2 (4.3, 6.3)
GIRK1/4	<sup>B</sup> 18.1 (+/- 1.1)	4.8 (4.2, 5.4)
GIRK4	<sup>AD</sup> 100	22.3 (21.1, 23.7)
K <sub>ir</sub> 6.1/SUR2a	<sup>C</sup> 1418 (+/- 108)	15.7 (13.8, 17.8)
K <sub>ir</sub> 6.1/SUR2b	<sup>C</sup> 127(+/- 2)	12.3 (12.1, 12.5)
K <sub>ir</sub> 6.2/SUR1	Inactive	Inactive
K <sub>ir</sub> 4.1	Inactive	Inactive
K <sub>ir</sub> 2.1	Inactive	Inactive
Slack	Inactive	Inactive
K <sub>v</sub> 2.1	Inactive	Inactive
$\alpha 1\beta 2$ MaxiK	Inactive	Inactive
$\alpha 1\beta 4$ MaxiK	Inactive	Inactive
$\alpha 1$ GlyR	Inactive	Inactive
Untransfected	Inactive	Inactive

**Table 2.** VU0529331 was tested on an array of targets expressed in HEK293 cells. VU0529331 activated GIRK2, GIRK1/2, GIRK1/4, GIRK4, K<sub>ir</sub>6.1/SUR2a, and K<sub>ir</sub>6.1/SUR2b channels. The compound was inactive on all other listed targets. <sup>A</sup>Normalized to maximum VU0529331 activity; <sup>B</sup>Normalized to maximum VU0466551 activity; <sup>C</sup>Normalized to 250  $\mu\text{M}$  pinacidil activity; <sup>D</sup>Confidence interval (95% CI) cannot be calculated. Figure adapted from Kozek, K.A. et al., *ACS Chemical Neuroscience* **2018**.

Figure adapted from Kozek, K.A. et al., *ACS Chemical Neuroscience* 2018.

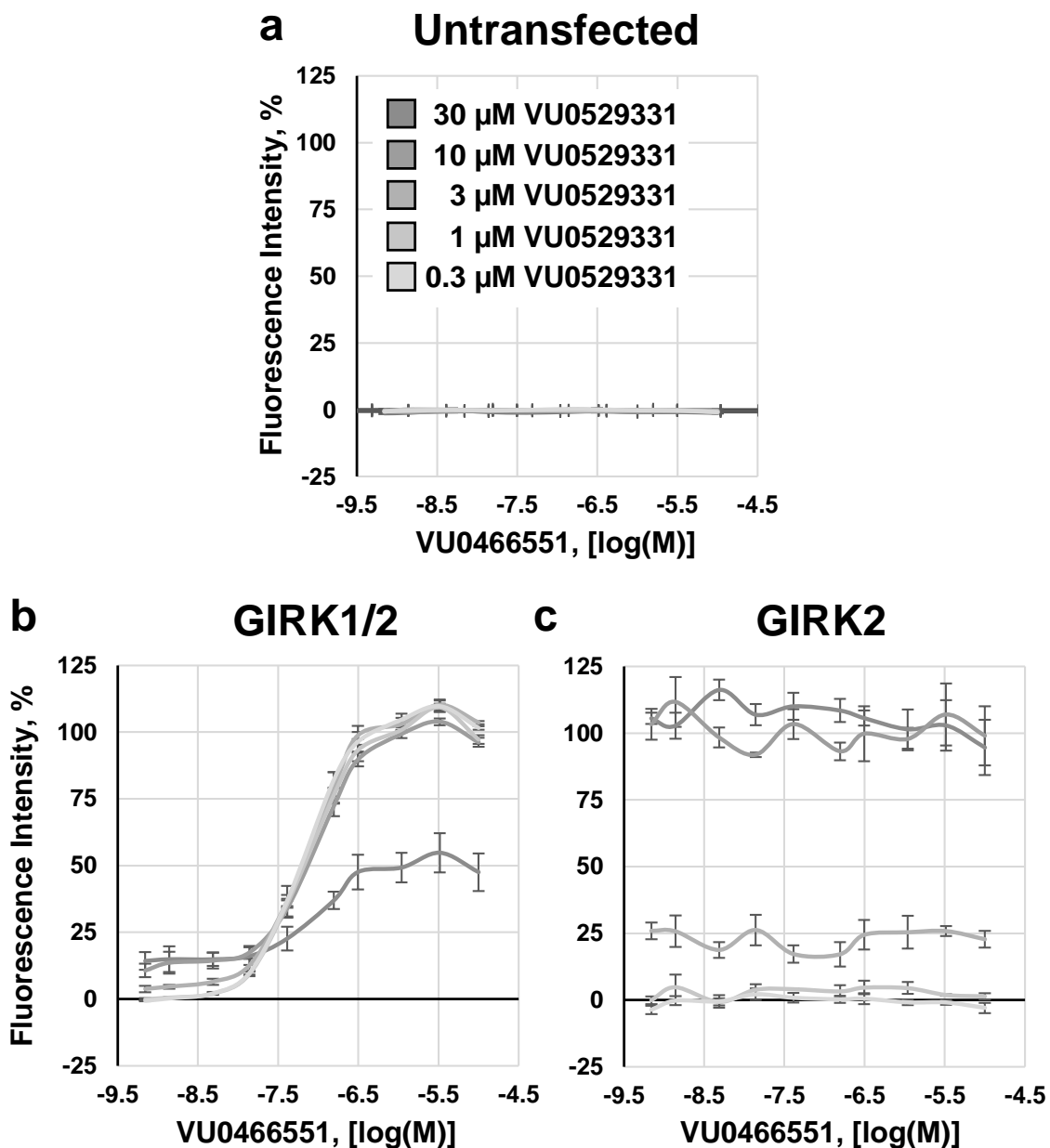


**Figure 19.** The activity of VU0466551 and VU0529331 when applied concurrently in  $\text{Ti}^+$  flux experiments using (a) untransfected HEK293 cells, (b) GIRK1/2-expressing HEK293 cells, and (c) GIRK2-expressing HEK293 cells. Error bars indicate the standard error of the mean (SEM).

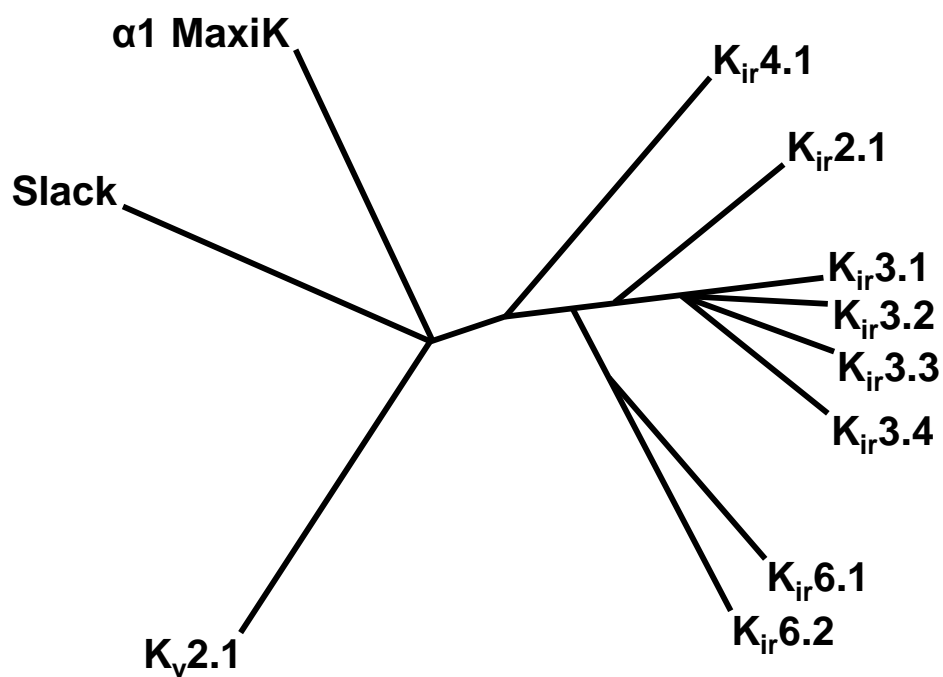


Figure adapted from Kozek, K.A. et al., *ACS Chemical Neuroscience* 2018.

**Figure 20.** A dendrogram depicting the genetic similarity between the different K<sup>+</sup> channels used to study the selectivity of VU0529331.



channels included a variety of  $K_{ir}$  channels as well as more distantly-related  $K^+$  channels (**Figure 20**). Using  $Tl^+$  flux assays, we found that VU0529331 was inactive on  $K_{ir}2.1$ ,  $K_{ir}4.1$ ,  $\alpha1\beta2$  MaxiK,  $\alpha1\beta4$  MaxiK,  $K_v2.1$ ,  $K_{ir}6.2/SUR1$ , and Slack channels. We did discover that VU0529331 activated  $K_{ir}6.1/SUR2a$  and  $K_{ir}6.1/SUR2b$  channels (**Table 2**). The activity of VU0529331 on these channels was compared to the activity of pinacidil, a known modulator of both  $K_{ir}6.1/SUR2a$  and  $K_{ir}6.1/SUR2b$  channel. VU0529331 proved to be more efficacious than pinacidil on both. Further, while our  $Tl^+$  flux experiments were unable to calculate the potency of pinacidil on  $K_{ir}6.1/SUR2a$  and  $K_{ir}6.1/SUR2b$ , we were able to measure a  $\sim 15 \mu M$  potency on  $K_{ir}6.1/SUR2a$  and  $\sim 1 \mu M$  potency on  $K_{ir}6.1/SUR2b$ . This demonstrated that VU0529331 is a moderately potent and efficacious activator of  $K_{ir}6.1/SUR2a$  and  $K_{ir}6.1/SUR2b$  channels.

In addition to testing VU0529331 selectivity amongst  $K^+$  channels, we also investigated whether VU0529331 modulated homomeric  $\alpha1$  GlyR,<sup>117</sup> one of the many Cys-loop receptors activated and potentiated by ivermectin. To test the activity of VU0529331 on  $\alpha1$  GlyR, we utilized a FRET-based assay which measured  $Cl^-$  influx using the SuperClomeleon sensor. While ivermectin demonstrated both activation of  $\alpha1$  GlyR and potentiation of glycine on  $\alpha1$  GlyR, VU0529331 neither activated  $\alpha1$  GlyR nor potentiated the activity of glycine on  $\alpha1$  GlyR (**Figure 21**). The selectivity results for VU0529331, including efficacies and potencies, are summarized in **Table 2**.

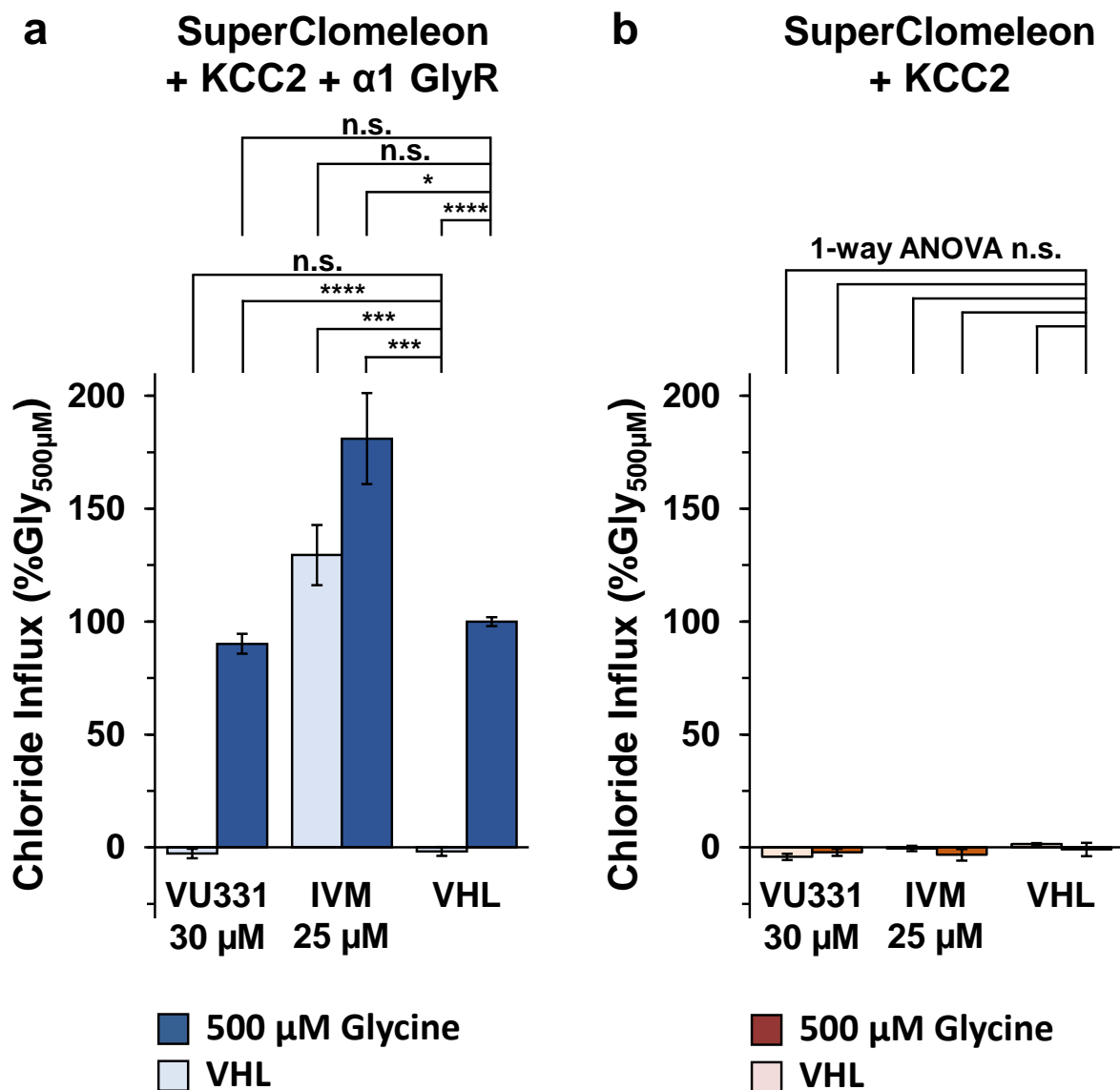


Figure adapted from Kozek, K.A. et al., *ACS Chemical Neuroscience* 2018.

**Figure 21.** (a) Ivermectin activates  $\alpha$ 1 GlyR and potentiates the activity of glycine on  $\alpha$ 1 GlyR, while VU0529331 does not affect the activity of  $\alpha$ 1 GlyR. VHL indicates solution comprising assay buffer with 0.25% (v/v) DMSO. (b) Neither compound has an effect on chloride flux in cells not expressing  $\alpha$ 1 GlyR. Chloride influx was calculated from the SuperClomeleon FRET ratio. To test for statistical significance of these results, conditions in each cell line were first compared using a 1-way ANOVA. Because the ANOVA identified significant differences between the condition in cells expressing  $\alpha$ 1 GlyR, we tested the significance of the pairs shown in (a) using 2-tailed Welch's t-tests. \*\*\*\* indicates  $p < 0.0001$ , \*\*\* indicates  $p < 0.001$ , \* indicates  $p < 0.05$ , and n.s. indicates no significance. Error bars represent the standard error of the mean (SEM).

## Characterization of VU0529331 Influence on the GIRK Channel Current-Voltage Relationship Using Whole-cell Voltage-clamp Electrophysiology

After establishing that VU0529331 increased  $\text{TI}^+$  flux in GIRK-expressing HEK293 cells through activity on GIRK channels, we explored the GIRK-activating properties of VU0529331 using whole-cell voltage-clamp EP. For EP results of  $\text{K}^+$  channels, convention dictates that negative current values indicate  $\text{K}^+$  moving intracellularly, while positive current values indicate  $\text{K}^+$  moving extracellularly. First, we investigated the effect of VU0529331 on the current-voltage (IV) relationship of GIRK channels. Here, we utilized the same engineered HEK293 cells expressing GIRK2 and GIRK1/2 channels that were used for  $\text{TI}^+$  flux assays. Currents were recorded in 12 increments of 10 mV, from  $-100$  mV to  $10$  mV, in the absence or presence of  $80$   $\mu\text{M}$  VU0529331, a maximally-effective concentration. Representative traces of the recordings used to generate these IVs are shown in **Figure 22**. IVs generated using GIRK2 (**Figure 23a**) and GIRK1/2 (**Figure 23b**) cell lines were consistent with inwardly-rectified  $\text{K}^+$  channels. Recordings demonstrated that inward and outward GIRK2 and GIRK1/2 currents were increased in the presence of VU0529331, while we did not record any changes in the currents of untransfected HEK293 cells (**Figure 23c**). The fold-increase in current magnitude over basal values upon activation with VU0529331 was greater for GIRK2 channels than GIRK1/2 channels (**Figure 23d**). We conducted this comparison on the outward GIRK currents, which would be relevant to the control over neuronal excitability that GIRK opening may evoke under normal physiological conditions. Because we utilized a high- $\text{K}^+$  external solution that shifted our  $\text{K}^+$  reversal potential to approximately  $-40$  mV, the outward current we chose to analyze was at  $-10$  mV, near the maximum outward currents GIRK can evoke. A greater modulation of GIRK2 than GIRK1/2 currents further supported the view that VU0529331 is a better activator of GIRK2 channels

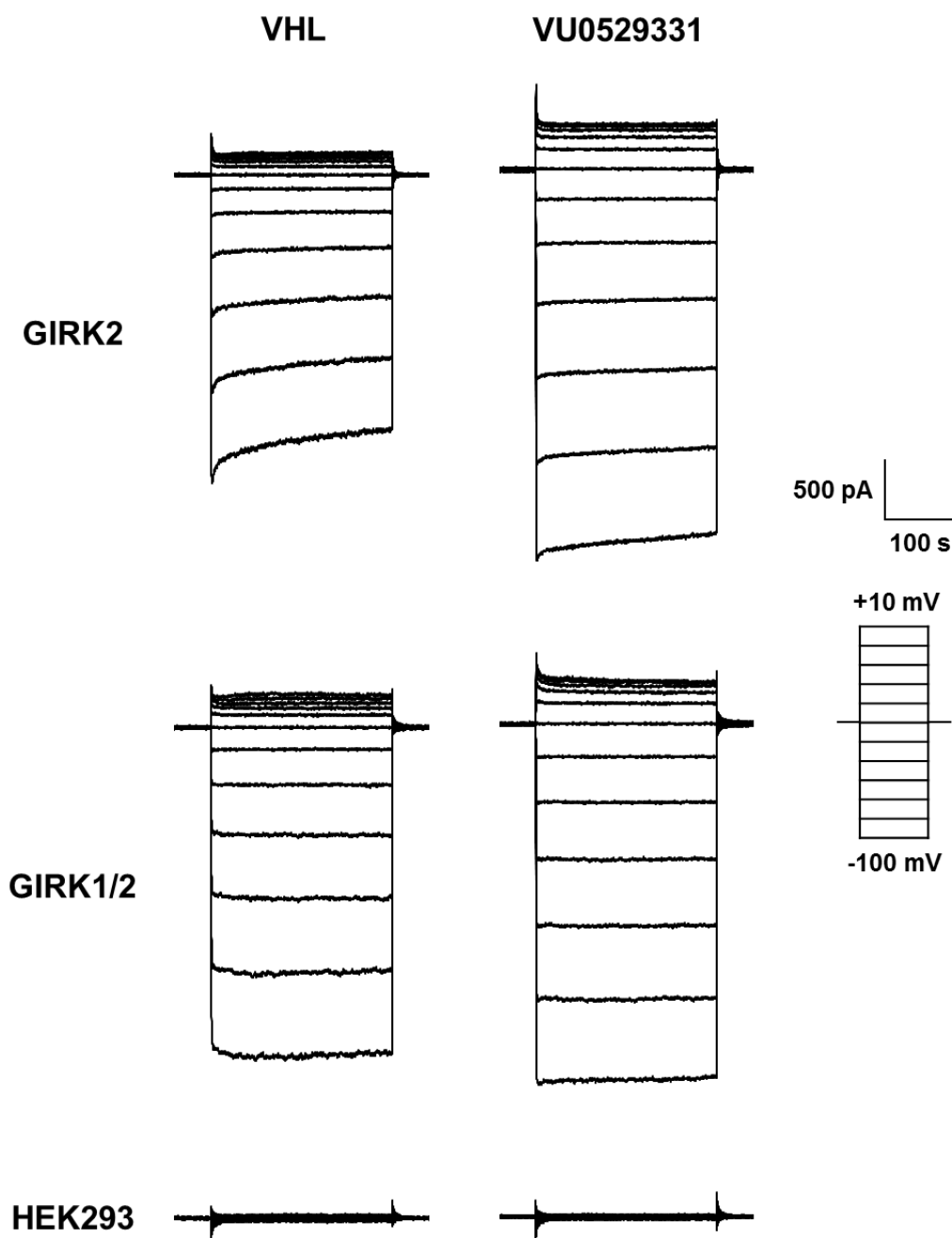
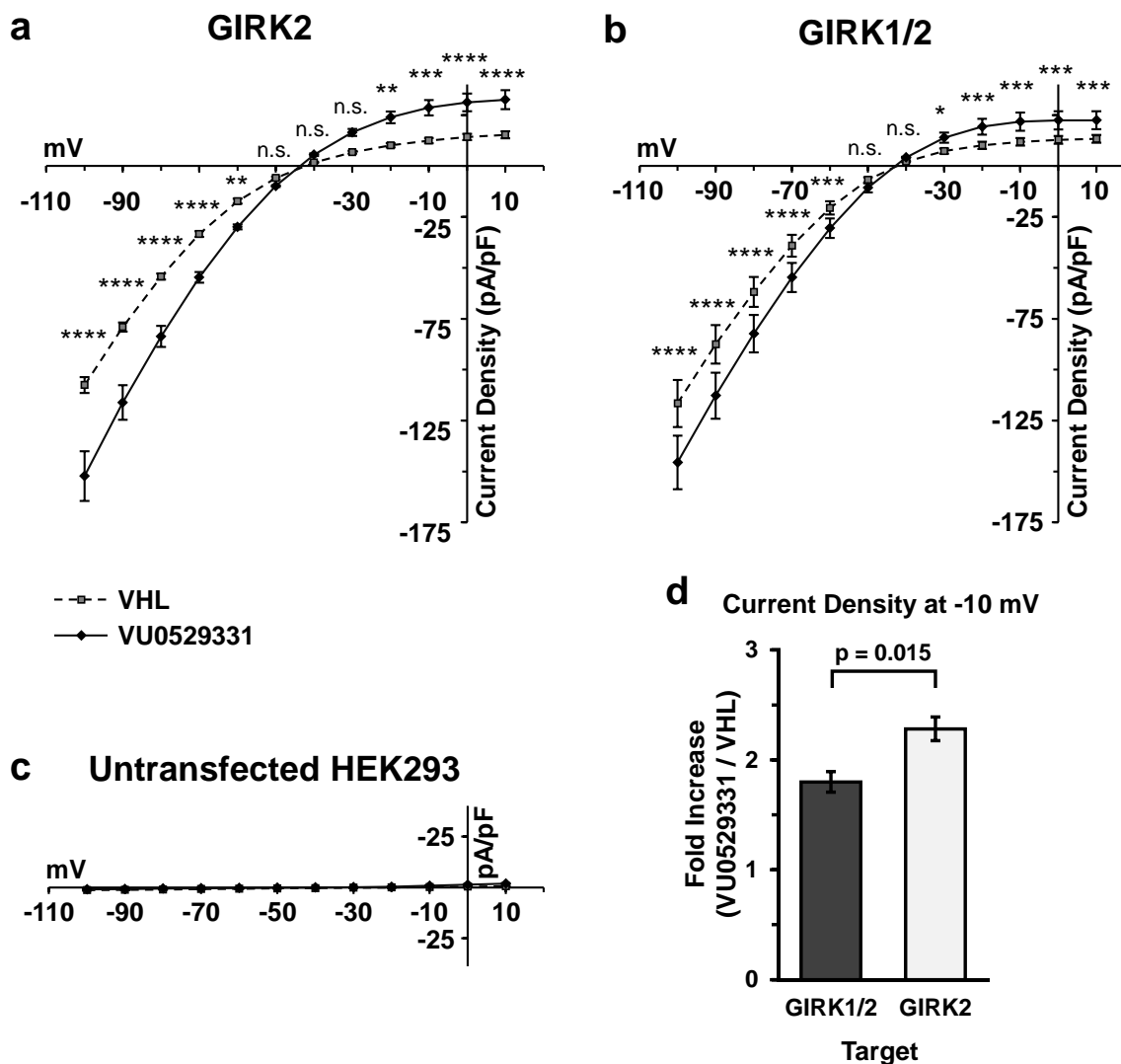


Figure adapted from Kozek, K.A. et al., *ACS Chemical Neuroscience* **2018**.

**Figure 22.** Representative raw traces of whole-cell patch-clamp electrophysiology recordings generated under 20 mM K<sup>+</sup> external buffer solution with 0.25% (v/v) DMSO (VHL). Consecutive recordings were generated on single cells bathed in VHL +/- 80  $\mu$ M VU0529331. Engineered GIRK2 and GIRK1/2 HEK293 cells and untransfected HEK293 cells were probed with sweeps generated from a holding potential of -40 mV and stepped from -100 mV to 10 mV in 10 mV steps.

Figure adapted from Kozek, K.A. et al., *ACS Chemical Neuroscience* 2018.



**Figure 23.** 80  $\mu\text{M}$  VU0529331 significantly increased both inward and outward currents in HEK293 cells expressing (a) GIRK2 and (b) GIRK1/2 channels. When examining these results, convention dictates that negative values for current indicate cations moving intracellularly, while positive values indicate cations moving extracellularly. VU0529331 did not evoke currents in (c) untransfected HEK293 cells. (d) The increase in current density for GIRK1/2 and GIRK2 cells at  $-10$  mV was significantly different. For each cell type in (a), (b), and (c), the conditions were compared using a 2-way ANOVA with Bonferroni's multiple comparisons test. \*  $p < 0.05$ , \*\*  $p < 0.01$ , \*\*\*  $p < 0.001$ , and \*\*\*\*  $p < 0.0001$ . The fold differences in (d) were compared using a Welch's t-test. Recordings were generated in 20 mM  $\text{K}^+$  external buffer solution containing 0.25% (v/v) DMSO (VHL). Error bars indicate standard error around the mean (SEM).

than GIRK1/2 channels. For both channels, inward rectification was maintained in the presence of VU0529331, and the rectification ratio (**Figure 24a**) was not significantly altered by VU0529331 (**Figure 24b**). Additionally, no significant change in the reversal potential was observed (GIRK2<sub>95%CI</sub>: (-43.9, -40.8) mV<sub>VHL</sub> vs (-44.4, -42.8) mV<sub>VU0529331</sub>; GIRK1/2<sub>95%CI</sub>: (-42.9, -42.0) mV<sub>VHL</sub> vs (-44.1, -41.9) mV<sub>VU0529331</sub>), indicating that K<sup>+</sup> selectivity was unaffected by VU0529331. Together, these data indicate that VU0529331 does not affect the inward rectification or the K<sup>+</sup> selectivity of GIRK2 or GIRK1/2 channels.

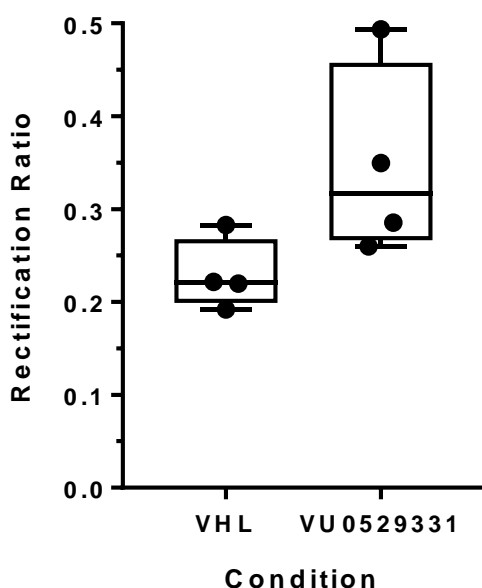
Next, we studied the effects of VU0529331 on GIRK channel currents held over time at a constant membrane potential. Using local superfusion, we were able to expose cells to a variety of solutions and observe the cellular responses. Specifically, we recorded currents in HEK293 cells expressing GIRK channels with the membrane potential clamped at -60 mV. We demonstrated that incrementally increasing concentrations of VU0529331 increased inward GIRK2 and GIRK1/2 currents (**Figure 25a,b**) while failing to induce changes in currents in untransfected HEK293 cells (**Figure 25c**). The onset of these currents was gradual, unlike the onset of currents previously recorded using ML297 on GIRK1/2 cells.<sup>56</sup> Changes in GIRK current due to VU0529331 could be reversed by washing the compounds off (**Figure 25a,b**). Further, repeated currents could be recorded on a single cell (data not shown). Application of an extracellular solution containing 2 mM Ba<sup>2+</sup> inhibits GIRK channel currents (**Figure 26a**) as it is a non-selective K<sub>ir</sub> channel inhibitor. Adding Ba<sup>2+</sup> to solutions containing VU0529331 was sufficient to block nearly all basal and VU0529331-evoked GIRK currents in GIRK2 channels (**Figure 26a**) and GIRK1/2 channels (**Figure 26b**). These data corroborated the results of the Tl<sup>+</sup> flux data that VU0529331 activity was concentration-dependent on GIRK channels and that the currents generated with VU0529331 were through the GIRK channels themselves.

**a**

$$\text{Rectification Ratio} = -1 * \frac{\text{Current Density at } -80 \text{ mV}}{\text{Current Density at } -10 \text{ mV}}$$

**b**

**GIRK2 Rectification Ratio**



**c**

**GIRK1/2 Rectification Ratio**

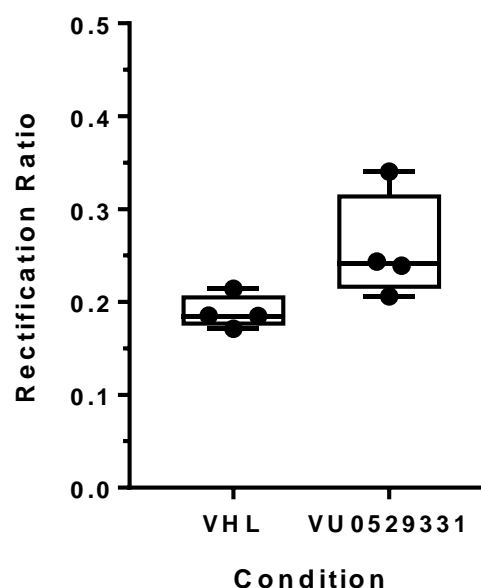


Figure adapted from Kozek, K.A. et al., *ACS Chemical Neuroscience* **2018**.

**Figure 24.** (a) The equation used to calculate the rectification ration (RR) in this work. 80  $\mu$ M VU0529331 had no effect on the rectification ratio of HEK293 cells expressing (b) GIRK2 and (c) GIRK1/2 channels. Whole-cell patch-clamp electrophysiology recordings were generated under 20 mM K<sup>+</sup> external buffer solution containing 0.25% (v/v) DMSO (VHL). A Wilcoxon matched-pairs signed rank test analysis indicated that there was not a statistically significant difference between the two conditions in (a) or (b).

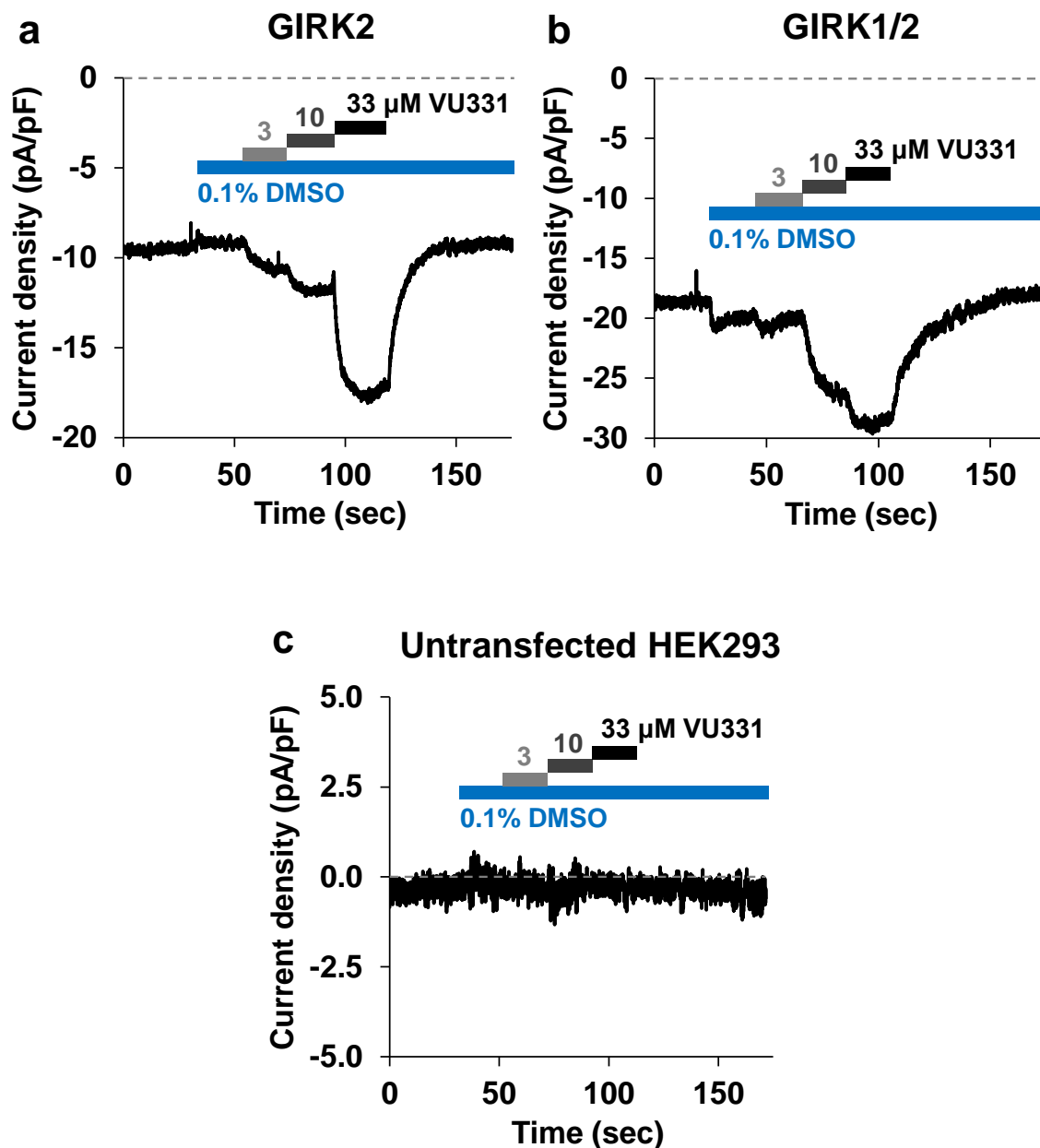
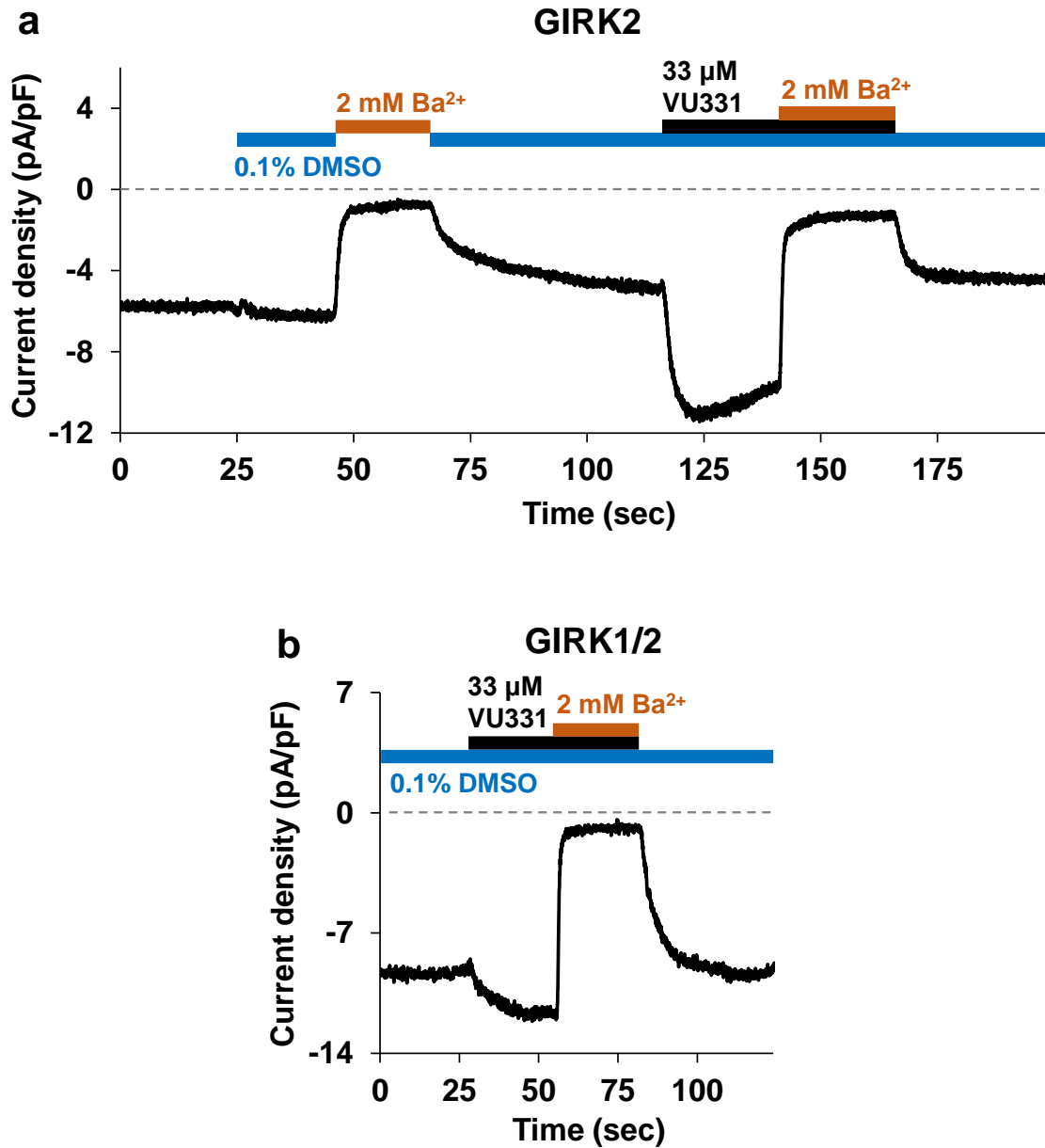


Figure adapted from Kozek, K.A. et al., *ACS Chemical Neuroscience* 2018.

**Figure 25.** Whole-cell patch-clamp electrophysiology using either untransfected HEK293 cells or cells engineered to express GIRK channels. Currents were held at  $-60$  mV while cells were bathed in 20 mM  $K^+$  external buffer. Exposure of (a) GIRK2 cells or (b) GIRK1/2 cells to escalating VU0529331 (VU331) concentrations showed concentration-dependent increases in inward current density. (c) Untransfected HEK293 cells did not show any changes in currents after VU331 exposure.



Figure adapted from Kozek, K.A. et al., *ACS Chemical Neuroscience* 2018.



**Figure 26.** Whole-cell patch-clamp electrophysiology using HEK293 cells engineered to express GIRK channels. Currents were held at  $-60$  mV while cells were bathed in  $20$  mM  $K^+$  external buffer. Both (a) GIRK2 and (b) GIRK1/2 currents evoked by maximally-active VU331 concentrations were blocked by exposure to extracellular solutions containing  $2$  mM  $Ba^{2+}$ , the non-selective inwardly-rectifying  $K^+$  channel inhibitor.

## Characterization of VU0529331 Analog Activity on GIRK Channels

Although VU0529331 represents a milestone for small-molecule-based modulation of non-GIRK1/X channels, the measured potency at GIRK2 channels of  $\sim 5 \mu\text{M}$  was not ideal for moving this compound into studies beyond *in vitro* experiments, such as those involving animals. We sought to identify analogs of VU0529331 with improved potency by studying the structure-activity relationship (SAR) between analogs and GIRK channels. To this end, we purchased 43 analogs from the Vanderbilt HTS Core Facility (**Figure 27**) and acquired 4 additional analogs with substitutions that were not commercially available (**Figure 28b**) for testing the SAR. The 4 commercially unavailable analogs were synthesized by the Hopkins laboratory (**Figure 28a**). None of the analogs from this limited analog library were active on GIRK2 or GIRK1/2 channels expressed in HEK293 cells when tested using  $\text{TI}^+$  flux experiments.

## Discussion

After identifying VU0529331 as the most efficacious hit from our GIRK2 HTS, we sought to further characterize the activity of this molecule. In this chapter, we characterized the activity of VU0529331 on GIRK channels using whole-cell voltage-clamp EP and fluorescent sensor-based assays. Through these efforts, we discovered that VU0529331 is a broadly-active GIRK channel activator that increases the currents of GIRK channels without affecting channel ion selectivity or inward rectification. Our efforts confirmed the results from our initial counterscreen and further revealed that VU0529331 is the first small-molecule activator identified for homotetrameric GIRK4 channels, as well as the first small synthetic molecule reported to activate homotetrameric GIRK2 channels. We were unable to improve the properties of VU0529331 with information gleaned from our SAR studies. From our selectivity efforts, we found that VU0529331

VU0529317		VU0529287		VU0529301		VU0529329	
VU0529318		VU0529288		VU0529302		VU0529330	
VU0529319		VU0529289		VU0529303			
VU0529320		VU0529290		VU0529304			
VU0529316		VU0529291		VU0529305			
		VU0529292		VU0529306		VU0529321	
VU0529324		VU0529293		VU0529307		VU0529322	
VU0529325		VU0529294		VU0529308		VU0529323	
VU0529326		VU0529295		VU0529309			
VU0529327		VU0529296		VU0529310			
		VU0529297		VU0529311			
VU0529328		VU0529298		VU0529312			
		VU0529299		VU0529313			
		VU0529300		VU0529314			

Figure adapted from Kozek, K.A. et al., *ACS Chemical Neuroscience* **2018**.

**Figure 27.** 43 analogs of VU0529331 purchased from Vanderbilt's compound collection or from AldrichMarketSelect. All of these compounds were inactive when tested on HEK293 cells expressing GIRK1/2 or GIRK2 channels using  $TI^+$  flux assays.

Figure adapted from Kozek, K.A. et al., *ACS Chemical Neuroscience* **2018**.

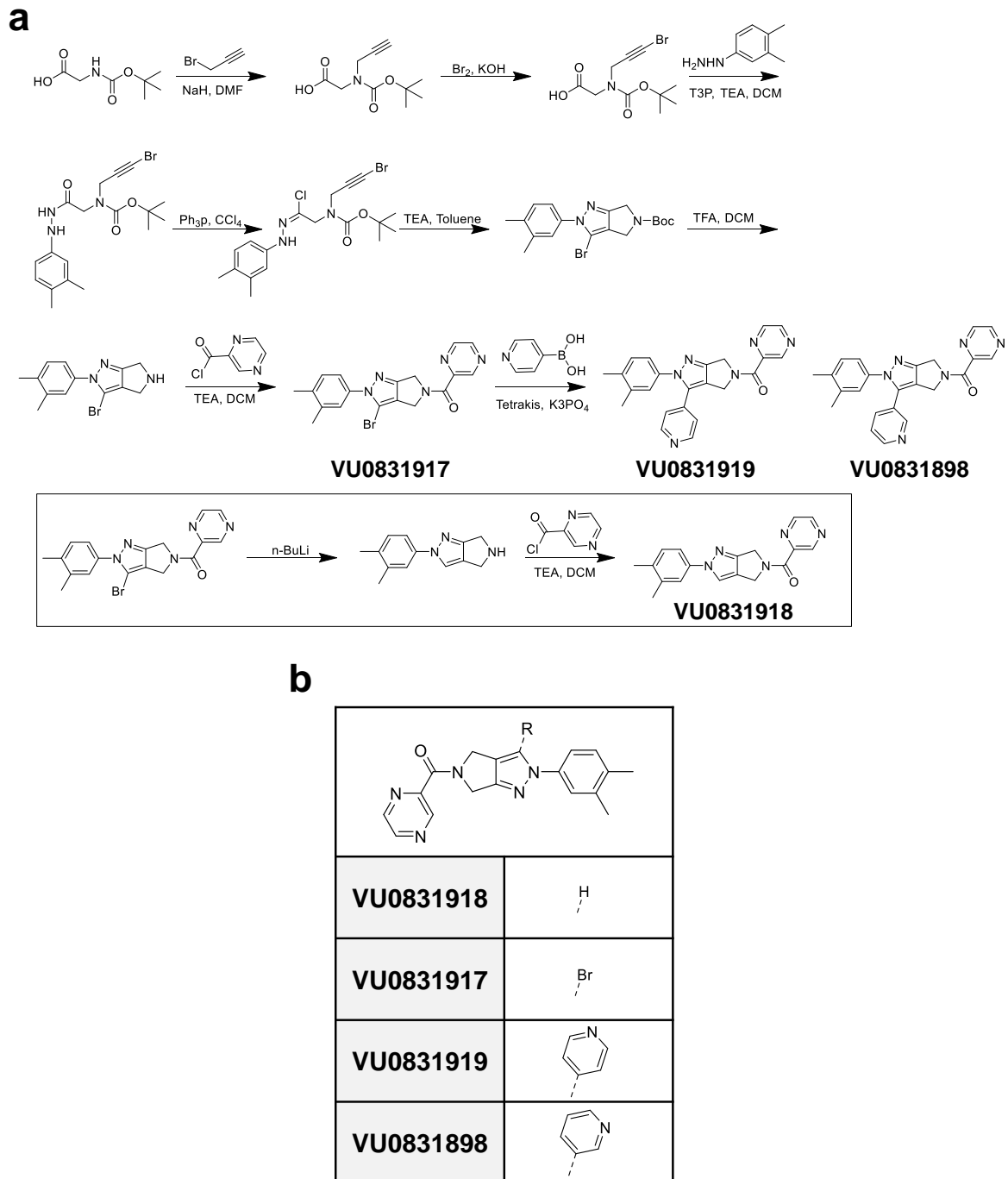


**Figure 28.** (a) Synthetic strategy for 4 commercially-unavailable analogs of VU0529331 developed by the laboratory of Dr. Hopkins. (b) These four analogs were inactive when tested on HEK293 cells expressing GIRK1/2 or GIRK2 channels using  $\text{Ti}^+$  flux assays.

also activated  $K_{ir}6.1/SUR2a$  and  $K_{ir}6.1/SUR2b$  channels, causing us to hypothesize that there is some yet unappreciated homology between the channels that may include the existence of a shared binding site. Below, we discuss in detail the findings from our **Results** above.

After completing our HTS counterscreens, we identified VU0529331 to be the most efficacious GIRK2 channel activator. To confirm our findings from **Chapter 2**, we aimed to investigate VU0529331 activity across multiple concentrations in various cell lines. Such measurements enabled us to generate concentration-response curves (CRCs) from which we measured the potency and record the maximum efficacy of VU0529331 under a variety of conditions. First, we confirmed that VU0529331 was inactive on untransfected HEK293 cells. Next, we confirmed that VU0529331 required GIRK2 channel expression in order to increase  $TI^+$  influx into HEK293 cells. Further, we validated that VU0529331 was insensitive to PTX, which allowed us to conclude that the activity of VU0529331 was independent of  $G_{i/o}$  protein signaling through any  $G_{i/o}$ -coupled GPCR that may be expressed in HEK293 cells. Altogether, these data confirmed our initial counterscreening results that VU0529331 exerted an effect on the GIRK channels engineered into HEK293 cells.

We began our selectivity studies by characterizing the activity of VU0529331 on channels within the GIRK channel family. Using  $TI^+$  flux assays, we discovered that VU0529331 was capable of activating GIRK1/2 and GIRK1/4 heterotetrameric channels and GIRK2 and GIRK4 homotetrameric channels. Considering that the GIRK subunits are highly homologous, we suspected that molecules from our screen could be broadly active on the many GIRK channels. However, because of our previous failures to generate non-GIRK1/X channel modulators, from our work with ML297, we did not expect pan-GIRK channel activity. Additionally, ivermectin has demonstrated a lack of efficacy on GIRK1/4 channels, with a single mutation between GIRK2 and

GIRK4 capable of governing this selectivity.<sup>89</sup> Hence, although the sequence homology of GIRK channels may be high, a single amino acid may make a difference in compound activity. Of all the GIRK subunits, GIRK4 is the most homologous with respect to GIRK2. Our finding that VU0529331 activates GIRK2 homotetrameric channels is exciting, since, to our knowledge, no other small molecule probes have been reported to activate homomeric GIRK4 channels, including ivermectin. VU0529331 is the first, most potent, and efficacious activator of homotetrameric GIRK4 channels. The only other known small molecules that activate GIRK4 are alcohols, which are broadly non-selective and for which potency cannot be measured.<sup>49</sup> For the remainder of our studies, however, we utilized GIRK2 and GIRK1/2 channels in order to enable the comparison between non-GIRK1/X and GIRK1/X channels relevant to neuronal physiology.

When we compared the fluorescence traces for GIRK1/2 and GIRK2 channel activation with VU0529331 (*Figure 17*), we observed differences in the overall fold-wise increase in fluorescence, and therefore  $Tl^+$  influx, over basal currents ( $F/F_0$ ) between GIRK2 and GIRK1/2 channels. This increase was larger for GIRK2 channels than for GIRK1/2 channels. For GIRK1/2 channels, VU0529331 was able to achieve only a fraction of the maximum fluorescence generated by VU0466551, a potent, efficacious, and selective activator of GIRK1/X channels. Meanwhile, on GIRK2 channels, VU0529331 achieved a maximum fluorescence similar to that of VU0466551 on GIRK1/2 channels. We did note, however, that the rate at which fluorescence increased for VU0466551 on GIRK1/2 channels, as compared to VU0529331 on both channels, was dramatically greater, illustrating the much greater ability of VU0466551 to activate GIRK1/X channels. Because both compounds had equal time to equilibrate across the cellular membrane, we did not suspect that access to a binding site, i.e. extracellular vs intracellular, would limit the rate of VU0529331. From these observations, we hypothesized that VU0529331 may be a more

effective activator of GIRK2 channels than GIRK1/2, but be less effective than VU0466551 at evoking activity.

Our laboratory had previously shown, using EP experiments, that GIRK2 channels generated approximately half as much current as GIRK1/2 channels when activated through the GABA<sub>B</sub>R GPCR using the agonist baclofen.<sup>56</sup> Here, we demonstrated, with Tl<sup>+</sup> flux, that VU0529331 was capable of activating GIRK2 channels to approximately 4 times the maximum attainable through the NPY4R GPCR using hPP (*Figure 18b*). Because GIRK2 channels are more difficult to activate via a GPCR, which is the physiologically-relevant response, the observed multifold increase in efficacy in response to VU0529331 on GIRK2 channels may evoke significant physiological effects. Although the EP and Tl<sup>+</sup> flux data we describe here may not be directly comparable, we note that the increase in GIRK1/2 currents due to ML297, an analog of VU0466551 and a selective GIRK1/X channel activator, was approximately 2.25-times greater than that through the GABA<sub>B</sub>R GPCR, less than the GPCR-compared increased using VU0529331 on GIRK2 channels. The manner in which to be able to compare VU0529331 activity on both GIRK1/2 and GIRK2 channels is through single-channel EP, discussed further below.

To evaluate whether VU0529331 and VU0466551 may have a similar binding site on GIRK1/2 channels, we assayed both of these compounds on HEK293 cells expressing GIRK1/2 channels at the same time. Combining these compounds in one experiment enabled us to generate graphs with intersecting CRCs and enabled us to determine how the presence of one molecule affected the activity of another. We discovered that on GIRK2 channels, VU0529331 activity was not affected by the presence of VU0466551. On GIRK1/2 channels, our results were slightly different. The presence of VU0529331 at the maximally-activating 10 and 30 μM concentrations affected the sensitivity of GIRK1/2 channel to VU0466551. At 10 μM VU0529331, the effect was

minor; however, at 30  $\mu$ M VU0529331 decreased the activity of VU0466551 at its higher concentration (**Figure 19**). From these graphs, we see that the potency of VU0466551 does not change yet the efficacy does, indicating that the mechanism by which these two compounds interact is non-competitive. This means that the binding sites of the two compounds are likely different. If the potency of VU0466551 upon addition of VU0529331 shifted towards greater values, then the two molecules could be competing for binding at a similar site. Further, we know that GIRK2 channels are not activated by VU0466551, and it was reassuring to see that VU0466551 did not affect the activity of VU0529331 in these cells. Again, if VU0466551 did not activate GIRK2 but was able to occupy a site that VU0529331 also occupied to evoke activity, then we would have observed competition in the curves. These data are the first glimpse into the mechanism of VU0529331 activity on GIRK channels. We continued to explore the potential binding of VU0529331 with GIRK subunit mutant channels.

We hypothesized that these molecules may have distinct binding pockets based on the non-competitive behavior of VU0529331 and VU0466551 on GIRK1/2 channels. To further explore whether the binding pocket of VU0466551 lends activity to VU0529331 on GIRK1/2 channels, we explored mutant GIRK channel lacking sensitivity to VU0466551. Our laboratory had identified that the F137A mutation in GIRK1 ablated sensitivity of GIRK1/X channels to VU0466551. We briefly examined whether GIRK1<sup>F137A</sup>/2 channels could be activated by VU0529331. We confirmed that GIRK1<sup>F137A</sup>/2 channels were not sensitive to VU0466551, and we learned that this mutation does not affect the activity of VU0529331 (**Table 3**). Further, Dr. Yu (Sunny) Du in our laboratory has recently identified a mutation, using random mutagenesis experiments, in the GIRK2 subunit, D86A, that caused GIRK1/2<sup>D86A</sup> channels to be unable to be activated with alcohols. This mutant is located very near to the PIP<sub>2</sub> binding site and is thought to



disrupt PIP<sub>2</sub> binding. However, this mutation retains response to VU0466551. Intrigued by this mutant, we examined whether this mutation also inhibited the activity of VU0529331 using GIRK1/2<sup>D86A</sup> and GIRK2/2<sup>D86A</sup> heterotetrameric and the GIRK2<sup>D86A</sup>/2<sup>D86A</sup> homotetrameric mutant channels (**Table 3**). We found that VU0466551 failed to activate GIRK channels that did not present at least 1 wildtype GIRK2 subunit. Throughout these experiments, we also tested the activity of ivermectin, and we found that it followed the activity of VU0529331 across all the GIRK channels we tested. While preliminary, these results indicate that we have identified at least 2 separate classes of GIRK channel activators, VU0466551 and its analogs in one class, and VU0529331 and the avermectins in another. These classes likely have distinct binding sites, and, because the D86A mutation is on the intracellular portion of the GIRK2 subunit, these compounds likely bind intracellularly. These results, while preliminary, provide the first glimpse into the mechanism of VU0529331, specifically the reliance of this compound on a wildtype GIRK2 subunit for activity. All in all, exploring the activity of VU0529331 on mutant channels and in the presence of VU0466551 has indicated that a separate binding site likely exists for each compound.

To further characterize the properties of VU0529331, we examined whether VU0529331 replicated its activity on GIRK channels using whole-cell voltage-clamp EP. With EP, we confirmed that this molecule did not evoke any currents in untransfected HEK293 cells and explored the currents evoked on both GIRK1/2 and GIRK2 channels. From our study of the current-voltage relationship, we learned that VU0529331 was capable of increasing current density through GIRK2 and GIRK1/2 channels without altering the K<sup>+</sup> selectivity or the inward rectification inherent to GIRK channels. When considering this data together with the results of our TI<sup>+</sup> flux experiments, our data demonstrated that VU0529331 acted upon and increased ion currents through homotetrameric and heterotetrameric GIRK channels. By measuring inward

	<b>GIRK1</b>	<b>GIRK1 F137A</b>	<b>GIRK1</b>	<b>GIRK2</b>	<b>GIRK2</b>	<b>GIRK2 D86A</b>
	<b>GIRK2</b>	<b>GIRK2</b>	<b>GIRK2 D86A</b>	<b>GIRK2</b>	<b>GIRK2 D86A</b>	<b>GIRK2 D86A</b>
<b>VU0466551</b>	Active	Inactive	Active	Inactive	Inactive	Inactive
<b>VU0529331</b>	Active	Active	Inactive	Active	Active	Inactive
<b>Ivermectin</b>	Active	Active	Inactive	Active	Active	Inactive

**Table 3.** The activity of VU0466551 (GIRK1-containing GIRK channel selective activator), VU0529331 (pan-GIRK channel activator), and ivermectin (GIRK2-containing GIRK channel preferring activator) on GIRK1/2 and GIRK2 channels expressed transiently in HEK293 cells. The GIRK1-F137A mutant was previously identified by our laboratory as necessary for ML297 activity, confirmed here. This mutation does not affect the activity of VU0529331 or ivermectin. The GIRK2-D86A mutant was recently identified by Dr. Yu (Sunny) Du in our laboratory. This mutant appears to not affect ML297 activity but inhibits the activity of VU0529331 and ivermectin if no wildtype GIRK2 subunits are present.

GIRK currents over time, we demonstrated that the activity of VU0529331 is also concentration-dependent in EP. Additionally, we showed that the currents we measured were unequivocally from GIRK channels when we inhibited nearly all GIRK currents, both basal and VU0529331-evoked, by batching cells in Ba<sup>2+</sup>-containing solutions. Unfortunately, none of these techniques were able to identify the precise manner by which VU0529331 increased the current through an individual GIRK channel. Future experiments that would be able to elucidate the mechanism by which VU0529331 increases currents through GIRK channels, such as single channel EP, are described in **Chapter 4**. Single channel EP would enable us to measure the effect that VU0529331 has on the frequency of channel opening, the length of time a channel remains open, and the magnitude of current that can pass through a single GIRK channel. Although highly meticulous, this technique would provide us detailed insight into how VU0529331 activity between the various GIRK channels, allowing us to determine if and how VU0529331 activity is different between them.

Considering our previous hypothesis that VU0529331 may be a more capable activator of GIRK2 channels than GIRK1/2 channels, we aimed to learn more from EP recordings. We examined whether VU0529331 activated GIRK2 homomeric channels to a greater extent than GIRK1/2 channels. We compared the physiologically-relevant outward currents at -10 mV between the two channels (**Figure 23d**). We discovered that the increase in current for GIRK2 channels was approximately 50% greater (~125% vs ~75% increase) than for GIRK1/2 channels. More interestingly, the physiologically-relevant outward basal current densities for GIRK2 channels were slightly larger than those of GIRK1/2 channels in these EP experiments (**Figure 23a,b**). This meant that GIRK2 channels generated a lightly larger outward current that increased to a greater extent upon exposure to VU0529331. One difference in the activity of VU0529331 on GIRK1/2 channels versus our previous observations with ML297 on GIRK1/2 channels is the

onset of activity upon dosing high concentrations of each compound. Our previous results with ML297 demonstrated an immediate increase in currents upon ML297 application, which the increase in currents in response to VU0529331 is gradual, even at high concentrations (*Figure 25*). While we discussed a similar phenomenon in  $\text{TI}^+$  flux, the compounds in those experiments had 2 min to equilibrate across the membrane. With superfusion in our EP experiments, we record the changes in currents while the compounds cross the cellular membrane. The slow onset of VU0529331 activity adds additional evidence to our hypothesis that the binding site of VU0529331 may be intracellular, supporting our mutagenesis studies. Overall, these results agreed with our  $\text{TI}^+$  flux findings and allowed us to address our hypothesis: VU0529331 is a more capable activator of GIRK2 channels than GIRK1/2 channels, demonstrating a modest selectivity for non-GIRK1/X channels. However, since these are channels were examined in engineered cells, we cannot be certain that these results accurately reflect GIRK channel activity in a neuron. To confirm these findings in a more physiologically-relevant setting, we propose testing VU0529331 in isolated neurons, as described in **Chapter 4**.

After studying VU0529331 activity among variations of the GIRK channel using both  $\text{TI}^+$  flux and EP, we explored the activity of various VU0529331 analogs on GIRK2 channels, namely the SAR. For this, we purchased commercially-available analogs and collaborated with the laboratory of expert medicinal chemist Dr. Corey R. Hopkins to synthesize commercially unavailable analogs. These analogs generally modified three substitutions around the core of the VU0529331 structure. Unfortunately, neither modifying nor removing these moieties was able to generate analogs with improved efficacy or potency. The analogs within this library could activate neither GIRK2 nor GIRK1/2 channels, indicating that none of the substitutions were tolerated. While beyond the scope of the present study, we remain hopeful that further medicinal chemistry

efforts may reveal compounds that can inform our understanding of VU0529331 SAR and lead to the generation of compounds with improved potency and efficacy.

After discovering that VU0529331 was capable of broadly activating the GIRK channel family, we expanded our selectivity studies to a variety of more distantly-related ion channels. From these selectivity experiments, we discovered that VU0529331 was an efficacious activator of channels within the  $K_{ir}6$  channel family. Specifically, we found that VU0529331 activated  $K_{ir}6.1/SUR2a$  and  $K_{ir}6.1/SUR2b$  channels; however, activity was not observed on  $K_{ir}6.2/SUR1$  channels. The two  $K_{ir}6$  subunits ( $K_{ir}6.1$  and  $K_{ir}6.2$ ) can combine with various subunits of the sulfonylurea receptor (SUR1, SUR2a, or SUR2b).<sup>144</sup> The various  $K_{ir}6$  and SUR subunits have differential expression throughout different tissues and cells, which creates tissue-specific channel expression and physiological importance. For example,  $K_{ir}6.2/SUR1$  is expressed in pancreatic  $\beta$  cells,<sup>145</sup> where it regulates insulin release; here, a channel malfunction can lead to diabetes, a life-altering and life-threatening disease.<sup>146</sup> We were eager to relate the physiological relevance of VU0529331 activating  $K_{ir}6.1/SUR2a$  and  $K_{ir}6.1/SUR2b$  channels to our work with GIRK channels. Specifically, we aimed to understand the potential complications that may occur in future *ex vivo* (e.g. brain slice preparations) and *in vivo* experiments. We learned that  $K_{ir}6.2/SUR1$  is expressed in neurons<sup>147,148</sup> and microglia,<sup>149</sup> whereas the  $K_{ir}6.1$  subunit expression has been shown in astrocytes.<sup>147</sup> Within the brain, SUR expression is still under investigation. While the expression of the SUR2a is generalized to cardiac and skeletal muscle cells and SUR2b to smooth muscle cells and the brain, recent work with rats demonstrated SUR2a in neurons and SUR2b glial cells, such as the astrocytes.<sup>150</sup> While explorations of SUR2 subunits continue, we speculate that  $K_{ir}6.1/SUR2b$  channels may be present in astrocytes and potentially confound experiments with animals by affecting neuronal physiology. The lack of activity of VU0529331 on  $K_{ir}6.2/SUR1$

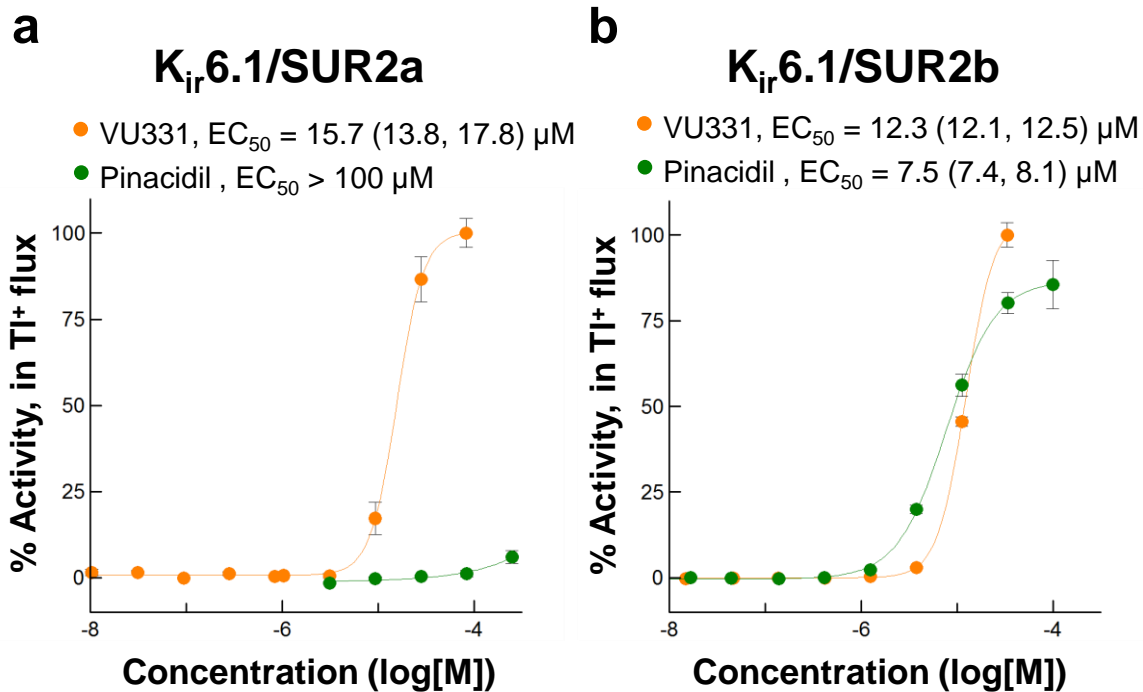
channels, which are expressed in neurons, provides one fewer confounding factor for such experiments. Nevertheless, we will remain cognizant of potential confounding activities in future work with VU0529331.

When we compared the activity of VU0529331 on  $K_{ir}6.1/SUR2a$  and  $K_{ir}6.1/SUR2b$  to pinacidil, our control compound pinacidil, we found VU0529331 to be both more efficacious on both channels. On  $K_{ir}6.1/SUR2a$  channels, the efficacy was >1000% as compared with pinacidil (**Table 2**) while the potency was approximately 15  $\mu$ M. For pinacidil, we were unable to calculate a potency, even when the highest concentration we tested was 250  $\mu$ M. However, when we studied VU0529331 activity on  $K_{ir}6.1/SUR2b$  channels, we were surprised to find a different profile. While VU0529331 displayed approximately 1  $\mu$ M potency, the same was true for pinacidil (**Figure 29**), which actually was slightly more potent. We note that VU0529331 is more potent on  $K_{ir}6.1/SUR2b$  channels than on any of the GIRK channels we tested. When comparing the efficacy of VU0529331 and pinacidil, VU0529331 was only approximately 25% more efficacious. Although beyond the scope of this report, we are pursuing characterization of VU0529331 on  $K_{ir}6.1/SUR2b$  channels through EP experiments to investigate further this activity, similar to what we have accomplished with GIRK channels. Considering our findings of VU0529331 activity on both  $K_{ir}6.1$  and the  $K_{ir}3$  channels, we hypothesize that these families share some as-of-yet unappreciated pharmacological homology.  $K_{ir}6$  and  $K_{ir}3$  are closely related  $K_{ir}$  families (**Figure 4**) and future experiments involving site-directed mutagenesis and chimeric channels will aim to elucidate the amino acids involved in VU0529331 binding and activity. It is possible, however, that the two channels do not share a common binding pocket, and that this discovery was a coincidence. Nevertheless, future work will aim to understand the dependence of VU0529331 activity on the  $K_{ir}$  subunit versus the SUR subunit, the beginnings of which we already presented.

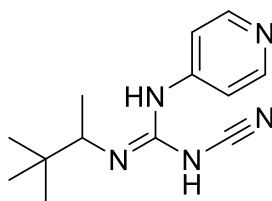
Altogether, VU0529331 was a noteworthy and efficacious activator of  $K_{ir}6.1/SUR2a$  and  $K_{ir}6.1/SUR2b$  channels.

In addition to studying the activity of VU0529331 on  $K^+$  channels, we aimed to determine whether this compound would be active on Cys-loop receptors. We were particularly curious about this because of the activity of ivermectin on both GIRK channels and Cys-loop receptors. We considered that the binding of ivermectin and VU0529331 may be similar, and if so, then a similar selectivity profile may be evident. To examine VU0529331 activity on anion-selective Cys-loop receptors, which are capable of passing  $Cl^-$ , we developed and utilized a FRET-based  $Cl^-$  influx assay. With this assay, we confirmed that ivermectin is an activator of  $\alpha 1$  GlyR, an anion-selective Cys-loop receptor; however, VU0529331 was inactive on this channel. While ivermectin and VU0529331 may share a binding pocket on GIRK channels, VU0529331 does not share ivermectin's activity on Cys-loop receptors. In light of these results, VU0529331 was shown to be a significantly more selective probe with which to study GIRK channels due to a smaller and less confounding population of ion channels.

As a GIRK channel probe, VU0529331 fills an important and unique pharmacologic gap. The same goes for the activity of VU0529331 on  $K_{ir}6.1/SUR2a$  and  $K_{ir}6.1/SUR2b$ , targets that continue to demand new probe molecules. We reported that VU0529331 did not activate Cys-loop receptors, unlike ivermectin, making it a more selective homomeric GIRK channel probe. We are eager to capitalize on the similarity between  $K_{ir}3$  and  $K_{ir}6$  channels to explore the amino acids important in VU0529331 activity. Such work may reveal opportunities to develop more potent and selective compounds for both  $K_{ir}3$  and  $K_{ir}6.1$  channels, alike. We did identify that the binding site of VU0529331 is likely independent of the binding site of VU0466551, but that it might overlap with the binding site of ivermectin. In either case, we have identified that potentially two different



**c**



**Pinacidil**

**Figure 29.** Activation of (a) K<sub>ir</sub>6.1/SUR2a and (b) K<sub>ir</sub>6.1/SUR2b channels with VU0529331 and pinacidil in TI<sup>+</sup> flux experiments. 95% confidence intervals are provided. Error bars represent the standard error of the mean (SEM). (c) The structure of pinacidil, utilized in (a) and (b).



classes of GIRK activators exist. In summary, VU0529331 was successfully identified through our GIRK2 HTS and revealed rich activity that had led to multiple interesting stories and many new questions.

## CHAPTER 4

### CONCLUSION AND FUTURE DIRECTIONS

#### Conclusion

Previously, our laboratory and collaborators had generated and tested nearly 800 compounds based on scaffolds discovered by screening >250,000 compounds on GIRK1/2 channels. The only compound active on non-GIRK1/X channels we had identified was abamectin, a compound closely related to ivermectin, which was recently described to activate GIRK channels by Su *et al.*<sup>88</sup> and Chen *et al.*<sup>89</sup> (discussed in **Chapter 1**). Although these avermectin analogs provided proof-of-concept for pharmacologic probes that activated non-GIRK1/X channels, they were far from ideal. These compounds activated and potentiated GlyR and GABA<sub>A</sub>R ion channels, which are often co-localized in the same neurons throughout the CNS and evoke a similar effect on neuronal excitability as GIRK channels. We sought to learn whether we could generate an ivermectin analog that would have a simpler synthesis than ivermectin for analog development. We learned that we could not remove the disaccharide moiety, the component that increased the difficulty of analog synthesis. We realized that in order to discover potent and efficacious non-GIRK1/X channel modulators, our laboratory would need to conduct its own high-throughput screen focused specifically on non-GIRK1-containing GIRK channels, which we described in **Chapter 2**.

Until this work, previous efforts to generate efficacious non-GIRK1/X channel activators, by our laboratory and others, have not been successful. In **Chapter 3**, we again demonstrated the difficulty of non-GIRK1/X channel modulator discovery. We sought to discover a synthetic small

molecule that would serve as a starting point for the development of potent, efficacious, and selective non-GIRK1/X channel modulators. When we set out, we screened a 100,000-compound library in search of activators of homomeric GIRK2 channels. We ended up with a single molecule, VU0529331, that we are confident activates GIRK2 channels. Whatever the mechanism by which VU0529331 increases the open channel probability, it appears to be rare. In limited, preliminary attempts, we were unable to identify any VU0529331 analogs that demonstrated activity on GIRK channels. Until the discovery of additional active analogs, VU0529331 alone is the first, synthetic, small-molecule, GIRK-channel activator capable of activating non-GIRK1/X channels. This discovery demonstrates that synthetic small molecules are capable of activating homotetrameric GIRK channels, even if they are difficult to identify or develop.

When we studied the activity of VU0529331 on a variety of  $K^+$  channels, we found that this molecule activated both homotetrameric and heterotetrameric GIRK channels. The activity of VU0529331 on GIRK4 was the first of its kind, but not surprising due to the close identity of the structure of GIRK2 and GIRK4 subunits. Additionally, we discovered that VU0529331 activated  $K_{ir}6.1/SUR2a$  and  $K_{ir}6.1/SUR2b$  ( $K_{ir}6.1/SUR2X$ ) channels from among a variety of  $K^+$  channels that were tested. VU0529331 efficacy on  $K_{ir}6.1/SUR2X$  channels was an unexpected, but not entirely unwelcomed, result. Few activators of  $K_{ir}6.1/SUR2X$  channels have been published,<sup>13</sup> which provides VU0529331 another avenue through which help researchers improve our understanding of the role of ion channels in physiology. Although the process of its discovery was daunting, the future work possible with this compound is exciting. In the **Future Directions**, we describe the many ways in which this compound will be useful to researchers in our laboratory and more.

## Future Directions

### Understanding the Mechanism of Action of VU0529331

Going forward, we would like to understand the mechanism by which VU0529331 activates GIRK channels. One of the first questions we can pursue is how the different factors that we know interact with GIRK channels affect VU0529331 activity. Already, we have tested whether VU0529331 activity was dependent on the activity of a GPCR by using PTX. However, many additional factors are known to modulate GIRK channel, as described in the **Chapter 1**, and they require investigation.

To study the effect of  $PIP_2$  and  $G_{i/o}\beta\gamma$  binding on VU0529331 activity, we can utilize EP and record cells engineered to express genetically-encoded tools. These cells would express proteins to limit the presence of  $PIP_2$  and  $G_{i/o}\beta\gamma$  subunits at the GIRK channel. We will be able to determine whether  $PIP_2$  and the  $G_{i/o}\beta\gamma$  subunits are required for the activity of VU0529331 on GIRK channels.<sup>56</sup> To study the effect that sequestering the  $G_{i/o}\beta\gamma$  subunit has on VU0529331 activity, we can express a  $G\beta\gamma$  sponge.  $G_{i/o}\beta\gamma$  can be sequestered intracellularly by expression of GPCR kinase 3 c-terminal fragment (GRK3ct),<sup>56</sup> and, therefore, GRK3ct will limit the amount of  $G_{i/o}\beta\gamma$  subunits able to bind to the GIRK2 channel. If the activity of a compound is not affected under this condition, then we can propose that VU0529331 acts independently of the  $G_{i/o}\beta\gamma$  subunit to activate GIRK channels. To investigate the dependence of a compound on  $PIP_2$ , we can deplete intracellular  $PIP_2$  with transiently-expressed the *Danio rerio* voltage-sensitive phosphatase (Dr-VSP).<sup>56</sup> Dr-VSP is activated by a strong depolarization which can be programmed into the experiential EP protocol. We can record whether compound activity is affected by the depletion of  $PIP_2$  after the stimulation of Dr-VSP.<sup>151</sup> While previous researchers have been confident in their

ability to demonstrate near-total depletion of PIP<sub>2</sub>,<sup>151</sup> we do worry that complete elimination of intracellular PIP<sub>2</sub> using this technique may not be achievable. Therefore, our results would not be able to say for certain whether the compound may be active in the absence of PIP<sub>2</sub>. We propose to further lower the availability of PIP<sub>2</sub> intracellularly by pretreating cells with wortmannin, a compound that inhibits the kinase required for PIP<sub>2</sub> synthesis.<sup>152</sup> With the inability to refill the PIP<sub>2</sub> stores, repeated activation using Dr-VSP may even further reduce the availability of PIP<sub>2</sub>. In either case, we would observe whether depleting PIP<sub>2</sub> affects the activity of VU0529331 on GIRK channels.

One additional factor that may affect the activity of VU0529331 and would be interesting to study is Na<sup>+</sup>. Increased Na<sup>+</sup> concentrations promote the activity of GIRK channels. Therefore, the presence of Na<sup>+</sup> may be important to the activity of VU0529331. We can determine the dependence of VU0529331 on Na<sup>+</sup> by studying the activity of the compound in Na<sup>+</sup>-depleted buffers using either TI<sup>+</sup> flux assays or EP experiments. Of note, TI<sup>+</sup> flux experiments may be confounding, since TI<sup>+</sup> is a congener of both K<sup>+</sup> and Na<sup>+</sup>. Therefore, TI<sup>+</sup> may bind to the Na<sup>+</sup> binding pocket and affect GIRK channel activity. To test this, we can record the response of GIRK channels to increasing TI<sup>+</sup> concentrations using Na<sup>+</sup>-depleted buffers, either in the presence or absence of VU059331. Whatever this result may be, it will further allow us to understand the mechanism by which VU0529331 is active on GIRK channels, and it may provide us with a new information regarding the effect of TI<sup>+</sup> on GIRK channels.

Ultimately, it may be required of us to conduct the aforementioned investigations in cell-free environments, as confounding factors for each of these experiments can be described. To be certain that a specific mediator of GIRK channels does or does not affect the activity of VU0529331, we would conduct these experiments using purified GIRK channels reconstituted in

lipid vesicles, as was utilized by Su *et al.* during their GIRK high-throughput screen at the laboratory of Dr. Roderick MacKinnon.<sup>88</sup> In these vesicles, we can be sure that only the factors that we supply into the system are present; therefore, we can observe the activity of VU0529331 on GIRK channels with and without the various factors in many different combinations. In this manner, we would be able to more definitively describe the mechanism by which VU0529331 activates GIRK channels.

Next, we propose to investigate the importance of known GIRK binding sites of the known GIRK activators to determine whether the binding site, and not the factors' binding, affects VU0529331 activity. This involves mutating the binding sites and examining the effect these mutations have on the activity of VU0529331. Specifically, the Na<sup>+</sup>, alcohol, PIP<sub>2</sub>, and G<sub>i/o</sub>βγ protein binding sites are known and may overlap with the binding sites of VU0529331. Because the binding sites for these factors are, many mutants have already been described in the literature and several have been generated by our laboratory. These mutant GIRK channels can be tested using TI<sup>+</sup> flux experiments in order determine the importance of intact binding sites for VU0529331 activity. Such experiments will rapidly inform whether the binding site was required or whether the factor that can no longer bind was required for activity. Coupled with the factor depletion experiments above, this can inform the reliance of VU0529331 activity on the presence of many GIRK channel modulators.

Through the above work, we may observe whether modifying the activity of the cellular factors has an effect on the activity of VU0529331. However, several amino acids have been reported to confer activity and specificity to other GIRK channel activators, such as ML297 and ivermectin. In order to investigate whether these mutations affect the activity of VU0529331, we will test the compound on channels containing one or both of the 2 amino acids involved in

providing ML297 specificity for GIRK1/X channels. We will also test the dependence of VU0529331 on the amino acid involved in providing ivermectin specificity between GIRK2 and GIRK4 channels. To date, our laboratory has conducted a brief investigation into one of these mutations. As discussed in **Chapter 3**, we identified that the GIRK1<sup>F137A</sup>/2 channel can be activated by VU0529331 while the GIRK1/2<sup>D86A</sup> and GIRK2/2<sup>D86A</sup> mutant channels ablate the activity of this compound. On the other hand, VU0466551 was active on GIRK1/2<sup>D86A</sup> channels, but fails to activate GIRK1<sup>F137A</sup>/2 channels. These preliminary results illustrated that there likely exist at least 2 different classes of GIRK channel activators, which likely have distinct binding sites. These results also provide the first glimpse into the mechanism of VU0529331 and its requirement of the presence of at least one wildtype GIRK2 subunit for activity.

Another manner by which to study the binding site of VU0529331 would be to investigate the similarity of K<sub>ir</sub>3 and K<sub>ir</sub>6 channels. These channels are the most related among the K<sub>ir</sub> channels, which provides them with a fairly high amino acid sequence identity. We would aim to identify individual amino acids or protein segments that are involved in enabling VU0529331 activity on either channel family. Elucidating the key amino acids involved in VU0529331 binding to GIRK channels and K<sub>ir</sub>6.1/X channels can be accomplished through site-directed mutagenesis and the generation of chimeric channels. If the required subunit for activity on K<sub>ir</sub>6 channels is the pore-forming K<sub>ir</sub>6 and not the accessory SUR subunit, then we can utilize the so-far inactive K<sub>ir</sub>6.2 subunit to determine which amino acids to mutate. Switching amino acids that differ between K<sub>ir</sub>6.2 and K<sub>ir</sub>6.1, GIRK2, and GIRK4 subunits will provide us with the first series of mutations to make. Additionally, we propose switching the intracellular amino and carboxyl termini of these channels, and possibly the transmembrane regions, to generate chimeric channels. Conducting TI<sup>+</sup> flux and EP experiments to determine the activity of mutant channels and their sensitivity to

VU0529331 may reveal the required structural portion of the proteins important to compound activity, and possibly binding. All of these investigations may come together to enable the discovery of the binding pocket of VU0529331.

Finally, we would like to understand the mechanism by which VU0529331 opens an individual GIRK channel by implementing single channel electrophysiology (SCEP) in excised patch experiments. Presently, the EP data we described in **Chapter 3** were observations about currents generated by the population of channels on a cell surface. Recording a single ion channel enables measurement of the individual current passing through that channel.<sup>73</sup> This will enable the identification of how the  $P_o$  of GIRK channels is modified to increase GIRK currents, or whether it stays the same and the current through a single channel increases. The changes to  $P_o$  will be informed by observations and analysis of the open time of a single opening event, the frequency of opening events, as well as the current amplitude through a single channel. On a single channel, we could then compare these properties in the presence and absence of a small molecule to discover the exact effect that is evoked on a given channel. For example, while we know that VU0529331 activates GIRK channels and increases GIRK currents, we do not know whether this is because channels open more frequently or whether channels remain open for longer periods of time. Using SCEP, we will be able to find out. Further, we would be able to compare VU0529331 activity on single ion channels against that of ivermectin and ML297. Our previous work with ML297 suggests that it increases the amount of time the channel stays open with each opening. In either case, we would demonstrate the effects of VU0529331 and compare them against the other known GIRK modulators.

Taken altogether, this mutagenesis and EP work would aim to further understand the mechanism by which VU0529331 activates GIRK channels.



## Characterizing the Activity of VU0529331 on the Kir6 Channel Family

In addition to characterizing VU0529331 further on GIRK channels, we could expand our efforts and characterize the activity of VU0529331 on the Kir6 channel family. Since we described robust activity using  $\text{TI}^+$  flux, we aim to determine whether the result replicates using whole-cell voltage-clamp EP. We would record the currents of Kir6.1/SUR2a and Kir6.1/SUR2b (Kir6.1/X) channels in engineered HEK293 cells and observe if they are affected by VU0529331 application. Next, we would determine whether VU0529331 activity is dependent on the SUR subunit or on the Kir6 subunit, since, as described in **Chapter 3**, we did not test channels with interchanged SUR1 and SUR2 subunits between the Kir6.1 and Kir6.2 subunits. In this way, we would determine whether SUR is required for the channel to open, as it is understood to be the case under normal physiological conditions.<sup>153</sup> After identifying the required subunits for channel activity, we would investigate the analogs of VU0529331 for their activity on all the Kir6 channels that could be activated by VU0529331. It may even be prudent to test these analogs on all the combinations as there may be analogs that activate the channels which VU0529331 may not. Such work has the potential to identify more efficacious, potent, and potentially selective activators on those channels, unlike our work with GIRK2, and develop a structure-activity relationship that could inform future analog development.

Altogether, such work would describe in more detail the activity of VU0529331 on the Kir6 family of channels and has the potential to described compounds with greater efficacy and improved potency. Further, if the activity of VU0529331 on Kir6 channels is found to be regulated by the SUR subunit, that may indicate the activity may be through binding to the SUR and not through a binding pocket on Kir6 subunit, making comparative mutagenesis between GIRK and Kir6 less valuable.

## Identifying Non-GIRK1-Containing GIRK Channels in Isolated DA Neurons

We foresee that VU0529331 and the other GIRK channel activators, namely ivermectin and ML297, or its analog VU0466551, will be useful in determining, for the first time, whether a specific cell expresses non-GIRK1/X channels. Initially, we had aimed to test whether VU0529331 could activate DA neurons of the VTA using *ex vivo* brain slice studies. These neurons have been shown to not express GIRK1 subunits, and our laboratory is eager to utilize our newfound compounds in order to confirm the surface expression of various GIRK channels. To date, neither ivermectin nor VU0529331 have been successful in evoking GIRK channel currents recorded in these neurons. Unknown yet is whether this is because of poor compound solubility or lack of efficacy at the target. For VU0529331, the reasons for this failure may be its poor potency; however, the solubility of VU0529331 above 100  $\mu\text{M}$  in our buffers is poor with visible precipitation, even when increasing DMSO to improve solubility. When conducting experiments in brain slices, concentrations of compounds are required to be at least multifold greater than the potency necessary for experiments *in vitro*, with higher concentrations being preferable to limit the effect of compound binding to proteins and fats in the brain slices. Considering VU0529331's relatively low potency *in vitro*, it is not surprising that we did not see activity in slices. For this same set of reasons, utilizing VU0529331 for *in vivo* experiments would be difficult, in addition to potential issues with compound binding to serum albumin (often >90%), which would further decrease the availability of compound at the target.<sup>154</sup> Future studies in brain slices and animals will first require development of compound analogs with improved potency, solubility, and selectivity.

Until the development of improved analogs, we propose to study VU0592331 compound activity in isolated DA neurons from rodents.<sup>155</sup> Specifically, we propose to use mice that express

green fluorescence protein (GFP) under the tyrosine hydroxylase (TH) promoter. These genetically-modified animals are available for purchase through the Jackson Laboratory, and a colony already resides at the laboratory of our collaborator Dr. Danny Winder. The way this mouse was designed, GFP is found in only neurons that also express TH, which is an enzyme that cells express to generate a dopamine precursor. Therefore, GFP expression is specific to cells that synthesize dopamine. Dopamine is a neurotransmitter that DA neurons utilize to communicate. Therefore, since DA neurons in this mouse are fluorescent, they can be visually identified, such as when neurons are isolated and cultured *in vitro*. This is especially relevant to EP, since choosing the correct cell to record is paramount, and now can be identified by eye. In this way, we can identify neurons that contain non-GIRK1/X channels and study the activity of VU0529331 on these channels in native cell populations.

During our experiments, we can test the overall population of GIRK channels on neurons by stimulating the response of GIRK channel through a GPCR, namely GABA<sub>B</sub>R using its agonist, baclofen. To identify whether the GIRK channels we probe contain GIRK1, we can record the activity of VU0466551 on such neurons. If neurons respond to VU0466551, then they contain GIRK1 subunits. If neurons do not respond, then we can determine whether VU0529331 or ivermectin activate the channels that may be present on the surface. As such, non-GIRK1/X channels may either be GIRK2 or GIRK2/3 channels, since we cannot be certain that either of these molecules does not activate GIRK2/3 channels. Finally, we would apply Ba<sup>2+</sup> while channels are activated in order to confirm that we were recording inward-rectifier currents. This would represent the first time that non-GIRK1/X channels would have been probed by a small molecule in neurons.

We have discussed that GIRK3 may potentially be a negative regulator of surface GIRK channel expression (see **Chapter 1**) and thus limiting the surface expression of GIRK2 or GIRK2/3 channels. If our experiments above are inconclusive or unsuccessful, we will aim to remove the influence of GIRK3 on our measurements of GIRK2 channels in isolated DA neurons. We propose utilizing a GIRK3 knockout mouse with similar expression of TH-dependent GFP. In this way, if we conduct the series of experiments outlined above, confirming GIRK currents through a GPCR that are not GIRK1-subunit mediated, then we will be able to definitively study GIRK2 currents on DA neurons. Altogether, such a future study will be able to bring the field closer to definitively identifying whether homotetrameric GIRK2 channels may be present in DA neurons and whether the presence of GIRK3 affects the expression of these channels.

One unresolved question is whether GIRK1/X neurons only express heteromeric GIRK channels or whether there exists a mixture of GIRK1/X and non-GIRK1/X channels. VU0529331 may aid in answering this question. One experiment that we could conduct to answer this question involves combining SCEP and the transgenic mice in order to identify the populations of GIRK channels on the surface of isolated neurons. Since the DA neurons do not express the GIRK1 subunit, then we could aim to record the non-fluorescent neurons, which should express GIRK1, GIRK2, and GIRK3 subunits. Further, if we utilize the GIRK3 KO mice for this work, then the non-fluorescent neurons would only express GIRK1 and GIRK2 subunits. By using SCEP to record individual GIRK channels isolated from the surface of neurons, we could identify the population of GIRK1/2 heterotetrameric and GIRK2 homotetrameric channels. By bathing the isolated channel with VU0529331, we can confirm whether we record the activity of a GIRK channel. By bathing the channels with VU0466551, which could only activate GIRK1/2 channels, we would identify whether a channel is a GIRK1/2 or a GIRK2 channel. Ivermectin would serve

as a control for the activity of a GIRK channel, as may baclofen, although it could be possible that GABA<sub>B</sub>R may not be present near the patched GIRK channel. Currently, it is thought that the expression of a GIRK1 subunit limits the surface expression of homotetrameric GIRK2 channels, and using this experiment we will be able to discern whether there exist homotetrameric and heterotetramer populations of GIRK channels on a cell membrane and, if so, then what proportion of each there is.

### **Discovery of GIRK Channel Inhibitors from the GIRK2 High-Throughput Screen**

Future work may involve repurposing our results from the primary screen to focus on the discovery of efficacious, potent, and selective inhibitors of GIRK channels. In the process of designing the GIRK2 HTS, we made a conscious decision to screen a partially-activated GIRK2 channels. This was done in order to enable the later discovery and study of GIRK channel inhibitors. We even analyzed our data to enable quick identification of inhibitory molecules. We had identified thousands of molecules that decreased the fluorescence of our system to, or greater, than our negative control, SCH-23390. These compounds dramatically blocked either the influx of Tl<sup>+</sup> or the development of fluorescence. While there are many processes that can affect the development of fluorescence, such as by quenching Thallo or by binding up the Tl<sup>+</sup> ions, we propose to counter screen these inhibitors. We suspect that many, if not most, of the molecules we discovered will be non-selective K<sup>+</sup> channel inhibitors considering the plethora of such compounds already reported (see **Chapter 1**). However, by utilizing non-GIRK channels early in our counter screening efforts to eliminate these off-target compounds then we can quickly narrow down the hit list to GIRK-selective molecules, if they do indeed exist.

Identifying selective GIRK2 channel inhibitors would enable the study of GIRK2 homotetrameric channels without genetic knockout. In this way, a selective GIRK2 channel inhibitor would enable the study of GIRK2 in animal development along different parts of an animals' lifecycle. Additionally, selective inhibitors would enable the study of GIRK2-knockout-related effects on drug addiction and reward behaviors in rodents. A pharmacological means of inhibiting GIRK2-dependent pathways is both reversible and can provide temporal resolution of physiological events, enabling testing of GIRK2 inhibition at different times throughout an animal behavior protocol. Such results would be interesting to compare against a genetic knockout, since with a compound, the channels would have been present during development and only inhibited during testing. However, as with any probe, there could be off-target effects that could confound the results. Data gathered using a probe could be compared against inducible knockout models of GIRK channels, and together these two mechanisms could inform the validity of any observed phenotypic changes. All data inhibiting or mutating GIRK channels in animals would strengthen any case for targeting GIRK channels therapeutically.

Diseases where improper activity of GIRK channels may be implicated include , GIRK inhibitors have been implicated include Keppen-Lubinsky Syndrome<sup>60</sup> (KLS), familial hyperaldosteronism (FHA),<sup>156</sup> Down Syndrome, and Parkinson's Disease.<sup>157,158</sup> FHA is due to mutations in GIRK4 channels where the pore is no longer K<sup>+</sup> selective and enables Na<sup>+</sup> diffusion when open. KLS was only recently identified as a disease due to mutations in the pore-forming region of the GIRK2 subunit, although the effects of these mutation have not been determined *in vitro*. Similar loss of selectivity is thought to underlie KLS. Finally, Down Syndrome is due to the triplicate expression of the 21<sup>st</sup> chromosome, which encodes GIRK2, causing excess expression of GIRK2 and enhanced GABA<sub>B</sub>R-dependent signaling through GIRK channels.<sup>159</sup> In all of these

diseases, GIRK channel inhibitors may help patients lead more normal lives if GIRK function could be inhibited without causes another set of issues. To study this, first inhibitors, hopefully GIRK subunit-selective, need to be identified, which will in turn enable scientists explore which composition of GIRK channels is important to disease progress. Further, analogs of inhibitors could be explored in the search of compounds selective for mutant channels over normal ones. Since KLS and FHA are diseases with heterozygous mutations, inhibiting just channels expressed with the mutant GIRK2 may help improve functioning and development of patients. Although exciting, such a targeted therapy still requires much work to be done, first with identifying GIRK-selective channel inhibitors.

In addition to the utility of inhibitors in studies with animals and as potential human therapeutics, characterizing inhibitors and their analogs may be useful for returning to our discovery of potent and efficacious non-GIRK1/X channel activators. Our laboratory has previously discovered compounds with analogs that switched from being activators to inhibitors of GIRK channels (see **Chapter 1**). Therefore, it is possible, although it is likely a rarer occurrence, that analogs may demonstrate a switch from inhibitors to activators. Through such investigations, hope remains that one of the scaffolds of GIRK inhibitors may provide the framework for the future discovery of more potent and more efficacious GIRK2 activators.

## **Interpretation and Impact**

GIRK channel involvement in maintaining proper neuronal excitability has been identified in cellular and rodent models, and clinical studies have identified the importance of GIRK channels to human development and human health. By continuing to study the intricate mysteries of GIRK channels and by developing chemical probes with which to modulate the activity of these channels, we get closer each day to bringing our benchwork to a patient's bedside. The future outlook of GIRK channel modulators improving human health is astounding to consider given that 30 years prior, scientists were unsure of the combinations of GIRK channels important to human health, the structure of a GIRK channel, or the channel's mechanism of activation. Small molecules that can activate these channels have only been developed within the last decade, and here we reported our most recent efforts to continue improving our library of GIRK channel modulators. We hope that our discovery of VU0529331 as a GIRK channel probe is able to inform future studies regarding the roles of different GIRK channel combinations throughout the body. We also aim to continue identifying small molecules from our screen that may be developed into new GIRK channel probes.

Progress is being made towards GIRK subunit-selective channel modulators, yet the GIRK channel field is not close to having all the ideal tools identified. While targeting GIRK channels therapeutically may be a reality within the next half century, we currently aim to help enable the study of GIRK channels importance in various disease processes. For this reason, we were excited to report our efforts in identifying VU0529331, even if it does not engender subunit-selectivity. We were excited to share the structure of this molecule with those who may wish to continue expanding its analog library in the search of more efficacious, more potent, and subunit-selective GIRK channel activators. We are eager to observe how this probe is used to identify GIRK2



homotetrameric channels in DA neurons, and how VU0529331 pushes our understanding of GIRK channels' role in regulating addiction circuitry. Overall, it is our wish that VU0529331 helps scientists learn new information regarding the importance of targeting GIRK channels therapeutically for the betterment of human health.

## REFERENCES

- (1) Hille, B. *Ion Channels of Excitable Membranes*, 3rd ed.; Sinauer Associates, Inc.: Sunderland, Massachusetts, 2001.
- (2) Hille, B. Potassium Channels in Myelinated Nerve. Selective Permeability to Small Cations. *J. Gen. Physiol.* **1973**, *61* (6), 669–686.
- (3) Hibino, H.; Inanobe, A.; Furutani, K.; Murakami, S.; Findlay, I.; Kurachi, Y. Inwardly Rectifying Potassium Channels: Their Structure, Function, and Physiological Roles. *Physiol. Rev.* **2010**, *90*, 291–366.
- (4) Karschin, C.; Dißmann, E.; Stu, W.; Karschin, A. IRK (1–3) and GIRK (1–4) Inwardly Rectifying K<sup>+</sup> Channel MRNAs Are Differentially Expressed in the Adult Rat Brain. *J. Neurosci.* **1996**, *16* (11), 3559–3570.
- (5) Tipps, M. E.; Buck, K. J. *GIRK Channels: A Potential Link Between Learning and Addiction*, 1st ed.; Elsevier Inc., 2015; Vol. 123.
- (6) Lüscher, C.; Slesinger, P. A. Emerging Roles for G Protein-Gated Inwardly Rectifying Potassium (GIRK) Channels in Health and Disease. *Nat. Rev. Neurosci.* **2010**, *11* (5), 301–315.
- (7) Luján, R.; Marron Fernandez de Velasco, E.; Aguado, C.; Wickman, K. New Insights into the Therapeutic Potential of Girk Channels. *Trends Neurosci.* **2014**, *37* (1), 20–29.
- (8) Schuetze, S. M. The Discovery of the Action Potential. *Trends Neurosci.* **1983**, *6* (C), 164–168.
- (9) Petersen, C. C. H. Whole-Cell Recording of Neuronal Membrane Potential during Behavior. *Neuron* **2017**, *95* (6), 1266–1281.
- (10) Nimigean, C. M.; Allen, T. W. Origins of Ion Selectivity in Potassium Channels from the Perspective of Channel Block. *J. Gen. Physiol.* **2011**, *137* (5), 405–413.
- (11) Bichet, D.; Haass, F. A.; Jan, L. Y. Merging Functional Studies with Structures of Inward-Rectifier K<sup>+</sup> Channels. *Nat. Rev. Neurosci.* **2003**, *4* (12), 957–967.
- (12) Coetzee, W. A.; Amarillo, Y.; Chiu, J.; Chow, A.; Lau, D.; McCormack, T.; Morena, H.; Nadal, M. S.; Ozaita, A.; Pountney, D.; et al. Molecular Diversity of K<sup>+</sup> Channels. *Ann. N. Y. Acad. Sci.* **1999**, *868* (1), 233–255.
- (13) Kharade, S. V.; Nichols, C.; Denton, J. S. The Shifting Landscape of KATP Channelopathies and the Need for “sharper” Therapeutics. *Futur. Med Chem.* **2016**, *8* (7), 789–802.
- (14) Loewi, O. Über Humorale Übertragbarkeit Der Herznervenwirkung. *Pflüger's Arch. für die gesamte Physiol. des Menschen und der Tiere* **1921**, *189* (1), 239–242.
- (15) Logothetis, D. E.; Mahajan, R.; Adney, S. K.; Ha, J.; Kawano, T.; Meng, X. Y.; Cui, M. *Unifying Mechanism of Controlling Kir3 Channel Activity by G Proteins and Phosphoinositides*, 1st ed.; Elsevier Inc., 2015; Vol. 123.
- (16) Salazar-Fajardo, P. D.; Aréchiga-Figueroa, I. A.; López-Serrano, A. L.; Rodriguez-Elias, J. C.; Alamilla, J.; Sánchez-Chapula, J. A.; Tristani-Firouzi, M.; Navarro-Polanco, R. A.; Moreno-Galindo, E. G. The Voltage-Sensitive Cardiac M2 Muscarinic Receptor Modulates the Inward Rectification of the G Protein-Coupled, ACh-Gated K<sup>+</sup> Current. *Pflügers Arch. - Eur. J. Physiol.* **2018**.
- (17) Baronas, V. A.; Kurata, H. T. Inward Rectifiers and Their Regulation by Endogenous

- Polyamines. *Front. Physiol.* **2014**, *5* (August), 1–14.
- (18) Lüscher, C.; Jan, L. Y.; Stoffel, M.; Malenka, R. C.; Nicoll, R. A. G Protein-Coupled Inwardly Rectifying K<sup>+</sup> Channels (GIRKs) Mediate Postsynaptic but Not Presynaptic Transmitter Actions in Hippocampal Neurons. *Neuron* **1997**, *19* (3), 687–695.
  - (19) Lesage, F.; Duprat, F.; Fink, M.; Guillemare, E.; Coppola, T.; Lazdunski, M.; Hugnot, J. P. Cloning Provides Evidence for a Family of Inward Rectifier and G-Protein Coupled K<sup>+</sup> Channels in the Brain. *FEBS Lett.* **1994**, *353* (1), 37–42.
  - (20) Liao, Y. J.; Jan, Y. N.; Jan, L. Y. Heteromultimerization of G-Protein-Gated Inwardly Rectifying K<sup>+</sup> Channel Proteins GIRK1 and GIRK2 and Their Altered Expression in Weaver Brain. *J. Neurosci.* **1996**, *16* (22), 7137–7150.
  - (21) Krapivinsky, G.; Gordon, E. a; Wickman, K.; Velimirović, B.; Krapivinsky, L.; Clapham, D. E. The G-Protein-Gated Atrial K<sup>+</sup> Channel IKACH Is a Heteromultimer of Two Inwardly Rectifying K<sup>+</sup> Channel Proteins. *Nature*. 1995, pp 135–141.
  - (22) Anderson, A.; Kulkarni, K.; Marron Fernandez De Velasco, E.; Carlblom, N.; Xia, Z.; Nakano, A.; Martemyanov, K. A.; Tolkacheva, E. G.; Wickman, K. Expression and Relevance of the G Protein-Gated K<sup>+</sup>channel in the Mouse Ventricle. *Sci. Rep.* **2018**, *8* (1), 1–14.
  - (23) Iwanir, S.; Reuveny, E. Adrenaline-Induced Hyperpolarization of Mouse Pancreatic Islet Cells Is Mediated by G Protein-Gated Inwardly Rectifying Potassium (GIRK) Channels. *Pflugers Arch. Eur. J. Physiol.* **2008**, *456* (6), 1097–1108.
  - (24) Cruz, H. G.; Ivanova, T.; Lunn, M.-L.; Stoffel, M.; Slesinger, P. A.; Lüscher, C. Bi-Directional Effects of GABAB Receptor Agonists on the Mesolimbic Dopamine System. *Nat. Neurosci.* **2004**, *7* (2), 153–159.
  - (25) Ma, D.; Zerangue, N.; Raab-Graham, K.; Fried, S. R.; Jan, Y. N.; Jan, L. Y. Diverse Trafficking Patterns Due to Multiple Traffic Motifs in G Protein-Activated Inwardly Rectifying Potassium Channels from Brain and Heart. *Neuron* **2002**, *33* (5), 715–729.
  - (26) Munoz, M. B.; Padgett, C. L.; Rifkin, R.; Terunuma, M.; Wickman, K.; Contet, C.; Moss, S. J.; Slesinger, P. A. A Role for the GIRK3 Subunit in Methamphetamine-Induced Attenuation of GABAB Receptor-Activated GIRK Currents in VTA Dopamine Neurons. *J. Neurosci.* **2016**, *36* (11), 3106–3114.
  - (27) Herman, M. A.; Sidhu, H.; Stouffer, D. G.; Kreifeldt, M.; Le, D.; Cates-Gatto, C.; Munoz, M. B.; Roberts, A. J.; Parsons, L. H.; Roberto, M.; et al. GIRK3 Gates Activation of the Mesolimbic Dopaminergic Pathway by Ethanol. *Proc. Natl. Acad. Sci.* **2015**, *112* (22), 7091–7096.
  - (28) Lomazzi, M.; Slesinger, P. A.; Lüscher, C. Addictive Drugs Modulate GIRK-Channel Signaling by Regulating RGS Proteins. *Trends Pharmacol. Sci.* **2008**, *29* (11), 544–549.
  - (29) Munoz, M. B.; Slesinger, P. A. Sorting Nexin 27 Regulation of G Protein-Gated Inwardly Rectifying K<sup>+</sup>Channels Attenuates InVivo Cocaine Response. *Neuron* **2014**, *82* (3), 659–669.
  - (30) Kotecki, L.; Hearing, M.; McCall, N. M.; Marron Fernandez de Velasco, E.; Pravetoni, M.; Arora, D.; Victoria, N. C.; Munoz, M. B.; Xia, Z.; Slesinger, P. A.; et al. GIRK Channels Modulate Opioid-Induced Motor Activity in a Cell Type- and Subunit-Dependent Manner. *J. Neurosci.* **2015**, *35* (18), 7131–7142.
  - (31) Pravetoni, M.; Wickman, K. Behavioral Characterization of Mice Lacking GIRK/Kir3 Channel Subunits. *Genes, Brain Behav.* **2008**, *7* (5), 523–531.
  - (32) Jelacic, T. M.; Kennedy, M. E.; Wickman, K.; Clapham, D. E. Functional and

- Biochemical Evidence for G-Protein-Gated Inwardly Rectifying K<sup>+</sup> (GIRK) Channels Composed of GIRK2 and GIRK3. *J. Biol. Chem.* **2000**, 275 (46), 36211–36216.
- (33) Kofuji, P.; Davidson, N.; Lester, H. A. Evidence That Neuronal G-Protein-Gated Inwardly Rectifying K<sup>+</sup> Channels Are Activated by G<sub>I3</sub> Subunits and Function as Heteromultimers. *Neurobiology* **1995**, 92 (July), 6542–6546.
- (34) Huang, C. L.; Feng, S. Y.; Hilgemann, D. W. Direct Activation of Inward Rectifier Potassium Channels by PIP<sub>2</sub> and Its Stabilization by G $\beta\gamma$ . *Nature* **1998**, 391 (6669), 803–806.
- (35) Lei, Q.; Jones, M. B.; Talley, E. M.; Schrier, a D.; McIntire, W. E.; Garrison, J. C.; Bayliss, D. a. Activation and Inhibition of G Protein-Coupled Inwardly Rectifying Potassium (Kir3) Channels by G Protein Beta Gamma Subunits. *Proc. Natl. Acad. Sci. U. S. A.* **2000**, 97 (17), 9771–9776.
- (36) Logothetis, D. E.; Kurachi, Y.; Galper, J.; Neer, E. J.; Clapham, D. E. The  $\beta\gamma$  Subunits of GTP-Binding Proteins Activate the Muscarinic K<sup>+</sup> Channel in Heart. *Nature*. 1987, pp 321–326.
- (37) Riven, I.; Iwanir, S.; Reuveny, E. GIRK Channel Activation Involves a Local Rearrangement of a Preformed G Protein Channel Complex. *Neuron* **2006**, 51 (5), 561–573.
- (38) Clancy, S. M.; Fowler, C. E.; Finley, M.; Suen, K. F.; Arrabit, C.; Berton, F.; Kosaza, T.; Casey, P. J.; Slesinger, P. A. Pertussis-Toxin-Sensitive G $\alpha$ subunits Selectively Bind to C-Terminal Domain of Neuronal GIRK Channels: Evidence for a Heterotrimeric G-Protein-Channel Complex. *Mol. Cell. Neurosci.* **2005**, 28 (2), 375–389.
- (39) Lei, Q.; Talley, E. M.; Bayliss, D. A. Receptor-Mediated Inhibition of G Protein-Coupled Inwardly Rectifying Potassium Channels Involves G $\alpha$  Family Subunits, Phospholipase C, and a Readily Diffusible Messenger. *J. Biol. Chem.* **2001**, 276 (20), 16720–16730.
- (40) Smrcka, A.; Hepler, J.; Brown, K.; Sternweis, P. Regulation of Polyphosphoinositide-Specific Phospholipase C Activity by Purified G $\alpha_q$ . *Science* (80-. ). **1991**, 251 (4995), 804–807.
- (41) Ho, I. H. M. Molecular Determinants for Sodium-Dependent Activation of G Protein-Gated K<sup>+</sup> Channels. **1999**, 274 (13), 8639–8648.
- (42) Glaaser, I. W.; Slesinger, P. A. Dual Activation of Neuronal G Protein-Gated Inwardly Rectifying Potassium (GIRK) Channels by Cholesterol and Alcohol. *Sci. Rep.* **2017**, 7 (1), 1–11.
- (43) Rosenhouse-dantsker, A. Cholesterol-Binding Sites in GIRK Channels : The Devil Is in the Details. **2018**, 5–8.
- (44) Bukiya, A. N.; Durdagim, S.; Noskov, S.; Rosenhouse-Dantske, A. Cholesterol Up-Regulates Neuronal G Protein-Gated Inwardly Rectifying Potassium (GIRK) Channel Activity in the Hippocampus. *J. Biol. Chem.* **2017**, 292 (15), 6135–6147.
- (45) Müllner, C.; Vorobiov, D.; Bera, A. K.; Uezono, Y.; Yakubovich, D.; Frohnwieser-Steinecker, B.; Dascal, N.; Schreibmayer, W. Heterologous Facilitation of G Protein-Activated K(+) Channels by Beta-Adrenergic Stimulation via CAMP-Dependent Protein Kinase. *J. Gen. Physiol.* **2000**, 115 (5), 547–558.
- (46) Medina, I.; Krapivinsky, G.; Arnold, S.; Koo, P.; Krapivinsky, L.; Clapham, D. E. A Switch Mechanism for G $\beta\gamma$  Activation of IKACH. *J. Biol. Chem.* **2000**, 275 (38), 29709–29716.
- (47) Stevens, E. B.; Shah, B. S.; Pinnock, R. D.; Lee, K. Bombesin Receptors Inhibit G

- Protein-Coupled Inwardly Rectifying K<sup>+</sup> Channels Expressed in *Xenopus* Oocytes through a Protein Kinase C-Dependent Pathway. *Mol Pharmacol* **1999**, *55* (6), 1020–1027.
- (48) Lewohl, J. M.; Wilson, W. R.; Mayfield, R. D.; Brozowski, S. J.; Morrisett, R. A.; Harris, R. A. G-Protein-Coupled Inwardly Rectifying Potassium Channels Are Target of Alcohol Action. *Nat. Neurosci.* **1999**, *2* (12), 1084–1090.
- (49) Aryal, P.; Dvir, H.; Choe, S.; Slesinger, P. A. A Discrete Alcohol Pocket Involved in GIRK Channel Activation. *Nat. Neurosci.* **2009**, *12* (8), 988–995.
- (50) Bodhinathan, K.; Slesinger, P. A. Molecular Mechanism Underlying Ethanol Activation of G-Protein-Gated Inwardly Rectifying Potassium Channels. *Proc. Natl. Acad. Sci.* **2013**, *110* (45), 18309–18314.
- (51) Toyama, Y.; Kano, H.; Mase, Y.; Yokogawa, M.; Osawa, M.; Shimada, I. Structural Basis for the Ethanol Action on G-Protein-activated Inwardly Rectifying Potassium Channel 1 Revealed by NMR Spectroscopy. *Proc. Natl. Acad. Sci.* **2018**, *115* (15), 3858–3863.
- (52) Lunn, M. L.; Nassirpour, R.; Arrabit, C.; Tan, J.; Mcleod, I.; Arias, C. M.; Sawchenko, P. E.; Yates, J. R.; Slesinger, P. A. A Unique Sorting Nexin Regulates Trafficking of Potassium Channels via a PDZ Domain Interaction. *Nat. Neurosci.* **2007**, *10* (10), 1249–1259.
- (53) Balana, B.; Bahima, L.; Bodhinathan, K.; Taura, J. J.; Taylor, N. M.; Nettleton, M. Y.; Ciruela, F.; Slesinger, P. A. Ras-Association Domain of Sorting Nexin 27 Is Critical for Regulating Expression of GIRK Potassium Channels. *PLoS One* **2013**, *8* (3), 1–8.
- (54) Whorton, M. R.; MacKinnon, R. Crystal Structure of the Mammalian GIRK2 K<sup>+</sup> Channel and Gating Regulation by G Proteins, PIP 2, and Sodium. *Cell* **2011**, *147* (1), 199–208.
- (55) Tsantoulas, C.; McMahon, S. B. Opening Paths to Novel Analgesics: The Role of Potassium Channels in Chronic Pain. *Trends Neurosci.* **2014**, *37* (3), 146–158.
- (56) Wydeven, N.; Marron Fernandez de Velasco, E.; Du, Y.; Benneyworth, M. A.; Hearing, M. C.; Fischer, R. A.; Thomas, M. J.; Weaver, C. D.; Wickman, K. Mechanisms Underlying the Activation of G-Protein-Gated Inwardly Rectifying K<sup>+</sup> (GIRK) Channels by the Novel Anxiolytic Drug, ML297. *Proc. Natl. Acad. Sci.* **2014**, *111* (29), 10755–10760.
- (57) Ostrovskaya, O.; Xie, K.; Masuho, I.; Fajardo-Serrano, A.; Lujan, R.; Wickman, K.; Martemyanov, K. A. RGS7/Gbeta5/R7BP Complex Regulates Synaptic Plasticity and Memory by Modulating Hippocampal GABABR-GIRK Signaling. *Elife* **2014**, *3*, e02053.
- (58) Montandon, G.; Ren, J.; Victoria, N. C.; Liu, H.; Wickman, K.; Greer, J. J.; Horner, R. L. G Protein-Gated Inwardly-Rectifying Potassium Channels Modulate Respiratory Depression by Opioids. *Anesthesiology* **2015**, *124* (3), 1–10.
- (59) Kaufmann, K.; Romaine, I.; Days, E.; Pascual, C.; Malik, A.; Yang, L.; Zou, B.; Du, Y.; Sliwoski, G.; Morrison, R. D.; et al. ML297 (VU0456810), the First Potent and Selective Activator of the GIRK Potassium Channel, Displays Antiepileptic Properties in Mice. *ACS Chem. Neurosci.* **2013**, *4* (9), 1278–1286.
- (60) Masotti, A.; Uva, P.; Davis-Keppen, L.; Basel-Vanagaite, L.; Cohen, L.; Pisaneschi, E.; Celluzzi, A.; Bencivenga, P.; Fang, M.; Tian, M.; et al. Keppen-Lubinsky Syndrome Is Caused by Mutations in the Inwardly Rectifying K<sup>+</sup>channel Encoded by KCNJ6. *Am. J. Hum. Genet.* **2015**, *96* (2), 295–300.
- (61) Best, T. K.; Siarey, R. J.; Galdzicki, Z. Ts65Dn, a Mouse Model of Down Syndrome,

- Exhibits Increased GABAB-Induced Potassium Current. *J. Neurophysiol.* **2007**, *97* (1), 892–900.
- (62) Lee, J.; Blydt-hansen, I.; Dro, B. I. Gain-of-Function KCNJ6 Mutation in a Severe Hyperkinetic Movement. **2018**, No. June.
- (63) Mesirca, P.; Alig, J.; Torrente, A. G.; Müller, J. C.; Marger, L.; Rollin, A.; Marquilly, C.; Vincent, A.; Dubel, S.; Bidaud, I.; et al. Cardiac Arrhythmia Induced by Genetic Silencing of “funny” (f) Channels Is Rescued by GIRK4 Inactivation. *Nat. Commun.* **2014**, *5*.
- (64) Wickman, K.; Nemeč, J.; Gendler, S. J.; Clapham, D. E. Abnormal Heart Rate Regulation in GIRK4 Knockout Mice. *Neuron* **1998**, *20* (1), 103–114.
- (65) Hu, L.; Wada, K.; Mores, N.; Krsmanovic, L. Z.; Catt, K. J. Essential Role of G Protein-Gated Inwardly Rectifying Potassium Channels in Gonadotropin-Induced Regulation of GnRH Neuronal Firing and Pulsatile Neurosecretion. *J. Biol. Chem.* **2006**, *281* (35), 25231–25240.
- (66) Oki, K.; Plonczynski, M. W.; Lam, M. L.; Gomez-Sanchez, E. P.; Gomez-Sanchez, C. E. The Potassium Channel, Kir3.4 Participates in Angiotensin II-Stimulated Aldosterone Production by a Human Adrenocortical Cell Line. *Endocrinology* **2012**, *153* (9), 4328–4335.
- (67) Hashimoto, N. Acetylcholine-Activated Potassium Channel as a Novel Target for AF Treatment. *Atr. Fibrillation - Basic Res. Clin. Appl.* **2012**.
- (68) Ikeda, K.; Kobayashi, T.; Kumanishi, T.; Niki, H.; Yano, R. Involvement of G-Protein-Activated Inwardly Rectifying K<sup>+</sup> (GIRK) Channels in Opioid-Induced Analgesia. *Neurosci. Res.* **2000**, *38* (1), 113–116.
- (69) Herrup, K. The Weaver Mouse: A Most Cantankerous Rodent. *Proc. Natl. Acad. Sci. U. S. A.* **1996**, *93* (20), 10541–10542.
- (70) Kofuji, P.; Hofer, M.; Millen, K. J.; Millonig, J. H.; Davidson, N.; Lester, H. A.; Hatten, M. E. Functional Analysis of the Weaver Mutant GIRK2 K<sup>+</sup>channel and Rescue of Weaver Granule Cells. *Neuron* **1996**, *16* (5), 941–952.
- (71) Rifkin, R. A.; Moss, S. J.; Slesinger, P. A. G Protein-Gated Potassium Channels: A Link to Drug Addiction. *Trends Pharmacol. Sci.* **2017**, *38* (4), 378–392.
- (72) Ahrnsbrak, R.; Bose, J.; Hedden, S.; Lipari, R.; Park-Lee, E. Key Substance Use and Mental Health Indicators in the United States: Results from the 2016 National Survey on Drug Use and Health. *Subst. Abus. Ment. Heal. Serv. Adm.* **2017**, *7* (1), 877–726.
- (73) Sacks, J. J.; Gonzales, K. R.; Bouchery, E. E.; Tomedi, L. E.; Brewer, R. D. 2010 National and State Costs of Excessive Alcohol Consumption. *Am. J. Prev. Med.* **2015**, *49* (5), e73–e79.
- (74) Related Disease Impact (ARDI). Alcohol-Attributable Deaths Due to Excessive Alcohol Use: Average for United States 2006–2010 <https://goo.gl/zNS149> (accessed Sep 7, 2018).
- (75) Nations, U.; Narcotics, I.; Board, C.; Unies, N.; Junta, U.; Fiscalización, I. De. *Narcotic Drugs Stupéfiantes Estupefacientes*; 2014.
- (76) Artigiani, E. E.; Wish, E. D. Epidemiologic Trends in Drug Abuse, Volume II. **2013**, II (June).
- (77) National Institute on Drug Abuse. Overdose Death Rates <https://www.drugabuse.gov/related-topics/trends-statistics/overdose-death-rates> (accessed Sep 8, 2018).
- (78) Ahmad, F.; Rossen, L.; Spencer, M.; Warner, M.; Sutton, P. Provisional Drug Overdose Data <https://www.cdc.gov/nchs/nvss/vsrr/drug-overdose-data.htm> (accessed Sep 8, 2018).

- (79) Dahan, A.; Aarts, L.; Smith, T. W. Incidence, Reversal, and Prevention of Opioid-Induced Respiratory Depression. *Anesthesiology* **2010**, *112* (1), 226–238.
- (80) Marker, C. L.; Cintora, S. C.; Roman, M. I.; Stoffel, M.; Wickman, K. Hyperalgesia and Blunted Morphine Analgesia in G Protein-Gated Potassium Channel Subunit Knockout Mice. *Neuroreport* **2002**, *13* (18), 2509–2513.
- (81) Lobo, I. A.; Harris, R. A. GABAA Receptors and Alcohol. *Pharmacol. Biochem. Behav.* **2008**, *90* (1), 90–94.
- (82) Days, E.; Kaufmann, K.; Romaine, I.; Niswender, C.; Lewis, M.; Utley, T.; Du, Y.; Sliwoski, G.; Morrison, R.; Dawson, E. S.; et al. Discovery and Characterization of a Selective Activator of the G-Protein Activated Inward-Rectifying Potassium (GIRK) Channel. *Probe Reports from NIH Mol. Libr. Progr.* **2013**, No. Md.
- (83) Barber, D. M.; Schönberger, M.; Burgstaller, J.; Levitz, J.; Weaver, C. D.; Isacoff, E. Y.; Baier, H.; Trauner, D. Optical Control of Neuronal Activity Using a Light-Operated GIRK Channel Opener (LOGO). *Chem. Sci.* **2016**, *7* (3), 2347–2352.
- (84) Wen, W.; Wu, W.; Romaine, I. M.; Kaufmann, K.; Du, Y.; Sulikowski, G. A.; Weaver, C. D.; Lindsley, C. W. Discovery of “molecular Switches” within a GIRK Activator Scaffold That Afford Selective GIRK Inhibitors. *Bioorganic Med. Chem. Lett.* **2013**, *23* (16), 4562–4566.
- (85) Ramos-Hunter, S. J.; Engers, D. W.; Kaufmann, K.; Du, Y.; Lindsley, C. W.; Weaver, C. D.; Sulikowski, G. A. Discovery and SAR of a Novel Series of GIRK1/2 and GIRK1/4 Activators. *Bioorganic Med. Chem. Lett.* **2013**, *23* (18), 5195–5198.
- (86) Wen, W.; Wu, W.; Weaver, C. D.; Lindsley, C. W. Discovery of Potent and Selective GIRK1/2 Modulators via “molecular Switches” within a Series of 1-(3-Cyclopropyl-1-Phenyl-1H-Pyrazol-5-Yl)Ureas. *Bioorganic Med. Chem. Lett.* **2014**, *24* (21), 5102–5106.
- (87) Wieting, J. M.; Vadukoot, A. K.; Sharma, S.; Abney, K. K.; Bridges, T. M.; Daniels, J. S.; Morrison, R. D.; Wickman, K.; Weaver, C. D.; Hopkins, C. R. Discovery and Characterization of 1H-Pyrazol-5-Yl-2-Phenylacetamides as Novel, Non-Urea-Containing GIRK1/2 Potassium Channel Activators. *ACS Chem. Neurosci.* **2017**, *8* (9), 1873–1879.
- (88) Su, Z.; Brown, E. C.; Wang, W.; MacKinnon, R. Novel Cell-Free High-Throughput Screening Method for Pharmacological Tools Targeting K<sup>+</sup> Channels. *Proc. Natl. Acad. Sci.* **2016**, *113* (20), 5748–5753.
- (89) Chen, I. S.; Tateyama, M.; Fukata, Y.; Uesugi, M.; Kubo, Y. Ivermectin Activates GIRK Channels in a PIP2-Dependent, Gβγ-Independent Manner and an Amino Acid Residue at the Slide Helix Governs the Activation. *J. Physiol.* **2017**, *595* (17), 5895–5912.
- (90) Jackson, H. C. C. Ivermectin as a Systemic Insecticide. *Parasitol. Today* **1989**, *5* (1988), 146–156.
- (91) Barragry, T. B. A Review of the Pharmacology and Clinical Uses of Ivermectin. *Can. Vet. J.* **1987**, *28* (8), 512–517.
- (92) Yow, T. T.; Pera, E.; Absalom, N.; Heblinski, M.; Johnston, G. A.; Hanrahan, J. R.; Chebib, M. Naringin Directly Activates Inwardly Rectifying Potassium Channels at an Overlapping Binding Site to Tertiapin-Q. *Br. J. Pharmacol.* **2011**, *163* (5), 1017–1033.
- (93) Torrecilla, M.; Marker, C. L.; Cintora, S. C.; Stoffel, M.; Williams, J. T.; Wickman, K. G-Protein-Gated Potassium Channels Containing Kir3.2 and Kir3.3 Subunits Mediate the Acute Inhibitory Effects of Opioids on Locus Ceruleus Neurons. *J. Neurosci.* **2002**, *22* (11), 4328–4334.
- (94) Kuzhikandathil, E. V.; Oxford, G. S. Classic D1 Dopamine Receptor Antagonist R-(+)-7-

- Chloro-8-Hydroxy-3-Methyl-1-Phenyl-2,3,4,5-Tetrahydro-1H-3-Benzazepine Hydrochloride (SCH23390) Directly Inhibits G Protein-Coupled Inwardly Rectifying Potassium Channels. *Mol. Pharmacol.* **2002**, *62* (1), 119–126.
- (95) Kobayashi, T.; Washiyama, K.; Ikeda, K. Inhibition of G Protein-Activated Inwardly Rectifying K<sup>+</sup> by Fluoxetine (Prozac). *J. Pharmacol. Sci.* **2006**, *102* (3), 278–287.
- (96) Kobayashi, T.; Washiyama, K.; Ikeda, K. Inhibition of G Protein-Activated Inwardly Rectifying K<sup>+</sup> Channels by the Antidepressant Paroxetine. *J. Pharmacol. Sci.* **2006**, *102* (3), 278–287.
- (97) Kobayashi, T.; Washiyama, K.; Ikeda, K. Inhibition of G Protein-Activated Inwardly Rectifying K<sup>+</sup> Channels by Ifenprodil. *Neuropsychopharmacology* **2006**, *31* (3), 516–524.
- (98) Bhawe, G.; Lonergan, D.; Chauder, B. A.; Denton, J. S. Small-Molecule Modulators of Inward Rectifier K<sup>+</sup> Channels: Recent Advances and Future Possibilities. *Future Med. Chem.* **2010**, *2* (5), 757–774.
- (99) Tanaka, H.; Hashimoto, N. A Multiple Ion Channel Blocker, NIP-142, for the Treatment of Atrial Fibrillation. **2007**, *25* (4), 342–356.
- (100) Raphemot, R.; Lonergan, D. F.; Nguyen, T. T.; Utley, T.; Michelle Lewis, L.; Kadakia, R.; David Weaver, C.; Gogliotti, R.; Hopkins, C.; Lindsley, C. W.; et al. Discovery, Characterization, and Structure-Activity Relationships of an Inhibitor of Inward Rectifier Potassium (Kir) Channels with Preference for Kir2.3, Kir3.X, and Kir7.1. *Front. Pharmacol.* **2011**, *2* (November), 1–18.
- (101) Kobayashi, T.; Ikeda, K.; Kumanishi, T. Inhibition by Various Antipsychotic Drugs of the G-Protein-Activated Inwardly Rectifying K<sup>+</sup> (GIRK) Channels Expressed in *Xenopus* Oocytes. *Br. J. Pharmacol.* **2000**, *129* (8), 1716–1722.
- (102) Kobayashi, T.; Washiyama, K.; Ikeda, K. Inhibition of G Protein-Activated Inwardly Rectifying K<sup>+</sup> Channels by Various Antidepressant Drugs. *Neuropsychopharmacology* **2004**, *29* (10), 1841–1851.
- (103) Kanjhan, R.; Coulson, E. J.; Adams, D. J.; Bellingham, M. C. Tertiapin-Q Blocks Recombinant and Native Large Conductance K<sup>+</sup> Channels in a Use-Dependent Manner. *J. Pharmacol. Exp. Ther.* **2005**, *314* (3), 1353–1361.
- (104) Li, D.; Chen, R.; Chung, S. H. Molecular Dynamics of the Honey Bee Toxin Tertiapin Binding to Kir3.2. *Biophys. Chem.* **2016**, *219*, 43–48.
- (105) Matsuda, T.; Masumiya, H.; Tanaka, N.; Yamashita, T. Inhibition by a Novel Anti-Arrhythmic Agent, NIP-142, of Cloned Human Cardiac K<sup>+</sup> Channel Kv1.5 Current. **2017**, *68* (2001), 2017–2024.
- (106) Burg, R. W.; Miller, B. M.; Baker, E. E.; Birnbaum, J.; Currie, S. a; Hartman, R.; Monaghan, R. L.; Putter, I.; Tunac, J. B.; Wallick, H.; et al. Avermectins, New Family of Potent Anthelmintic Agents: Producing Organism and Fermentation. *Antimicrob. Agents Chemother.* **1979**, *15* (3), 361–367.
- (107) Egerton, J. R.; Ostlind, D. A.; Blair, L. S.; Eary, C. H.; Suhayda, D.; Cifelli, S.; Riek, R. F.; Campbell, W. C. Avermectins, New Family of Potent Anthelmintic Agents: Efficacy of the B1a Component. *Antimicrob. Agents Chemother.* **1979**, *15* (3), 372–378.
- (108) Scott, R. H.; Duce, I. R. Effects of 22,23-Dihydroavermectin B1a on Locust (*Schistocerca gregaria*) Muscles May Involve Several Sites of Action. *Pestic. Sci.* **1985**, *16* (April), 599–604.
- (109) Arena, P.; Cully, D. F. Expression of a Glutamate-Activated Chloride Current in *Xenopus* Oocytes Injected with *Caenorhabditis elegans* RNA : Evidence for Modulation by



- Avermectin. **2000**, *15* (1992), 339–348.
- (110) The Nobel Assembly at Karolinska Institutet. 2015 Nobel Prize in Physiology or Medicine. *Nobel Prize Press Release* **2015**, 1–5.
- (111) Edwards, G. Ivermectin: Does P-Glycoprotein Play a Role in Neurotoxicity? *Filaria J* **2003**, *2 Suppl 1*, S8.
- (112) Nau, R.; Sorgel, F.; Eiffert, H. Penetration of Drugs through the Blood-Cerebrospinal Fluid/Blood-Brain Barrier for Treatment of Central Nervous System Infections. *Clin. Microbiol. Rev.* **2010**, *23* (4), 858–883.
- (113) Khakh, B. S.; Proctor, W. R.; Dunwiddie, T. V.; Labarca, C.; Lester, H. A. Allosteric Control of Gating and Kinetics at P2X(4) Receptor Channels. *J. Neurosci.* **1999**, *19* (17), 7289–7299.
- (114) Priel, A.; Silberberg, S. D. Mechanism of Ivermectin Facilitation of Human P2X<sub>4</sub> Receptor Channels. *J. Gen. Physiol.* **2004**, *123* (3), 281–293.
- (115) Robertson, B. Actions of Anaesthetics and Avermectin on GABA(A) Chloride Channels in Mammalian Dorsal Root Ganglion Neurones. *Br. J. Pharmacol.* **1989**, *98* (1), 167–176.
- (116) Dawson, G. R.; Wafford, K. A.; Smith, A.; Marshall, G. R.; Bayley, P. J.; Schaeffer, J. M.; Meinke, P. T.; Mckernan, R. M. Anticonvulsant and Adverse Effects of Avermectin Analogs in Mice Are Mediated through the  $\alpha$ -Aminobutyric Acid A Receptor. **2000**, *295* (3), 1051–1060.
- (117) Shan, Q.; Haddrill, J. L.; Lynch, J. W. Ivermectin, an Unconventional Agonist of the Glycine Receptor Chloride Channel. *J. Biol. Chem.* **2001**, *276* (16), 12556–12564.
- (118) Krause, R. M.; Buisson, B.; Bertrand, S.; Corringer, P. J.; Galzi, J. L.; Changeux, J. P.; Bertrand, D. Ivermectin: A Positive Allosteric Effector of the Alpha7 Neuronal Nicotinic Acetylcholine Receptor. *Mol. Pharmacol.* **1998**, *53* (2), 283–294.
- (119) Miller, P. S.; Smart, T. G. Binding, Activation and Modulation of Cys-Loop Receptors. *Trends Pharmacol. Sci.* **2010**, *31* (4), 161–174.
- (120) Danishefsky, S. J.; Armistead, D. M.; Wincott, F. E.; Selnick, H. G.; Hungate, R. The Total Synthesis of Avermectin Ala. *J. Am. Chem. Soc.* **1989**, No. 111, 2967–2980.
- (121) Kozek, K. A.; Du, Y.; Sharma, S.; Prael, F. J.; Spitznagel, B. D.; Kharade, S. V.; Denton, J. S.; Hopkins, C. R.; Weaver, C. D. Discovery and Characterization of VU0529331, a Synthetic Small-Molecule Activator of Homomeric G Protein-Gated, Inwardly-Rectifying, Potassium (GIRK) Channels. *ACS Chem. Neurosci.* **2018**, aacschemneuro.8b00287.
- (122) Niswender, C. M.; Johnson, K. A.; Luo, Q.; Ayala, J. E.; Kim, C.; Conn, P. J.; Weaver, C. D. A Novel Assay of G<sub>i/o</sub>-Linked G Protein-Coupled Receptor Coupling to Potassium Channels Provides New Insights into the Pharmacology of the Group III Metabotropic Glutamate Receptors. *Prism* **2008**, *73* (4), 1213–1224.
- (123) Niswender, C. M.; Johnson, K. A.; Weaver, C. D.; Jones, C. K.; Xiang, Z.; Luo, Q.; Rodriguez, A. L.; Marlo, J. E.; de Paulis, T.; Thompson, A. D.; et al. Discovery, Characterization, and Antiparkinsonian Effect of Novel Positive Allosteric Modulators of Metabotropic Glutamate Receptor 4. *Mol. Pharmacol.* **2008**, *74* (5), 1345–1358.
- (124) Williams, R.; Johnson, K. A.; Gentry, P. R.; Niswender, C. M.; Weaver, C. D.; Conn, P. J.; Lindsley, C. W.; Hopkins, C. R. Synthesis and SAR of a Novel Positive Allosteric Modulator (PAM) of the Metabotropic Glutamate Receptor 4 (MGluR4). *Bioorganic Med. Chem. Lett.* **2009**, *19* (17), 4967–4970.
- (125) Utey, T.; Haddenham, D.; Salovich, J. M.; Zamorano, R.; Vinson, P. N.; Lindsley, C. W.;

- Hopkins, C. R.; Niswender, C. M. Synthesis and SAR of a Novel Metabotropic Glutamate Receptor 4 (mGlu4) Antagonist: Unexpected “molecular Switch” from a Closely Related mGlu4positive Allosteric Modulator. *Bioorganic Med. Chem. Lett.* **2011**, *21* (23), 6955–6959.
- (126) Ghamari-Langroudi, M.; Digby, G. J.; Sebag, J. A.; Millhauser, G. L.; Palomino, R.; Matthews, R.; Gillyard, T.; Panaro, B. L.; Tough, I. R.; Cox, H. M.; et al. G-Protein-Independent Coupling of MC4R to Kir7.1 in Hypothalamic Neurons. *Nature* **2015**, *520* (7545), 94–98.
- (127) Raphemot, R.; Rouhier, M. F.; Hopkins, C. R.; Gogliotti, R. D.; Lovell, K. M.; Hine, R. M.; Ghosalkar, D.; Longo, A.; Beyenbach, K. W.; Denton, J. S.; et al. Eliciting Renal Failure in Mosquitoes with a Small-Molecule Inhibitor of Inward-Rectifying Potassium Channels. *PLoS One* **2013**, *8* (5).
- (128) Raphemot, R.; Rouhier, M. F.; Swale, D. R.; Days, E.; Weaver, C. D.; Lovell, K. M.; Konkell, L. C.; Engers, D. W.; Bollinger, S. F.; Hopkins, C.; et al. Discovery and Characterization of a Potent and Selective Inhibitor of *Aedes Aegypti* Inward Rectifier Potassium Channels. *PLoS One* **2014**, *9* (11).
- (129) Du, Y.; Days, E.; Romaine, I.; Abney, K. K.; Kaufmann, K.; Sulikowski, G.; Stauffer, S.; Lindsley, C. W.; Weaver, C. D. Development and Validation of a Thallium Flux-Based Functional Assay for the Sodium Channel NaV1.7 and Its Utility for Lead Discovery and Compound Profiling. *ACS Chem. Neurosci.* **2015**, *6* (6), 871–878.
- (130) Delpire, E.; Days, E.; Lewis, L. M.; Mi, D.; Kim, K.; Lindsley, C. W.; Weaver, C. D. Small-Molecule Screen Identifies Inhibitors of the Neuronal K-Cl Cotransporter KCC2. *Proc. Natl. Acad. Sci.* **2009**, *106* (13), 5383–5388.
- (131) Shaw, G.; Morse, S.; Ararat, M.; Graham, F. L. Preferential Transformation of Human Neuronal Cells by Human Adenoviruses and the Origin of HEK 293 Cells. *Faseb J* **2002**, *16* (8), 869–871.
- (132) Mangmool, S.; Kurose, H. Gi/o Protein-Dependent and -Independent Actions of Pertussis Toxin (PTX). *Toxins (Basel)*. **2011**, *3* (7), 884–899.
- (133) Pedragosa-Badia, X.; Sliwoski, G. R.; Nguyen, E. D.; Lindner, D.; Stichel, J.; Kaufmann, K. W.; Meiler, J.; Beck-Sickinger, A. G. Pancreatic Polypeptide Is Recognized by Two Hydrophobic Domains of the Human Y4 Receptor Binding Pocket. *J. Biol. Chem.* **2014**, *289* (9), 5846–5859.
- (134) Mäde, V.; Bellmann-Sickert, K.; Kaiser, A.; Meiler, J.; Beck-Sickinger, A. G. Position and Length of Fatty Acids Strongly Affect Receptor Selectivity Pattern of Human Pancreatic Polypeptide Analogues. *ChemMedChem* **2014**, *9* (11), 2463–2474.
- (135) Weaver, C. D.; Harden, D.; Dworetzky, S. I.; Robertson, B.; Knox, R. J. A Thallium-Sensitive, Fluorescence-Based Assay for Detecting and Characterizing Potassium Channel Modulators in Mammalian Cells. *J. Biomol. Screen.* **2004**, *9* (8), 671–677.
- (136) Weaver, C. D. Thallium Flux Assay for Measuring the Activity of Monovalent Cation Channels and Transporters. In *Potassium Channels: Methods and Protocols*; Shyng, S.-L., Valiyaveetil, F. I., Whorton, M., Eds.; Springer New York: New York, NY, 2018; pp 105–114.
- (137) Kozek, K. A.; Weaver, C. D. Discovering small molecule activators of G protein-gated inwardly-rectifying potassium subunit 2 (GIRK2) containing channels utilizing a G protein-coupled receptor (GPCR) for partial channel activation during screening <https://pubchem.ncbi.nlm.nih.gov/bioassay/1259325> (accessed May 7, 2018).

- (138) Torkamani, A.; Bersell, K.; Jorge, B. S.; Bjork, R. L.; Friedman, J. R.; Bloss, C. S.; Cohen, J.; Gupta, S.; Naidu, S.; Vanoye, C. G.; et al. De Novo KCNB1 Mutations in Epileptic Encephalopathy. *Ann. Neurol.* **2014**, *76* (4), 529–540.
- (139) Lewis, L. M.; Bhawe, G.; Chauder, B. A.; Banerjee, S.; Lornsen, K. A.; Redha, R.; Fallen, K.; Lindsley, C. W.; Weaver, C. D.; Denton, J. S. High-Throughput Screening Reveals a Small-Molecule Inhibitor of the Renal Outer Medullary Potassium Channel and Kir7.1. *Mol. Pharmacol.* **2009**, *76* (5), 1094–1103.
- (140) Raphemot, R.; Kadakia, R. J.; Olsen, M. L.; Banerjee, S.; Days, E.; Smith, S. S.; Weaver, C. D.; Denton, J. S. Development and Validation of Fluorescence-Based and Automated Patch Clamp–Based Functional Assays for the Inward Rectifier Potassium Channel Kir4.1. *Assay Drug Dev. Technol.* **2013**, *11* (9–10), 532–543.
- (141) Raphemot, R.; Swale, D. R.; Dadi, P. K.; Jacobson, D. A.; Cooper, P.; Wojtovich, A. P.; Banerjee, S.; Nichols, C. G.; Denton, J. S. Direct Activation of Beta-Cell KATP Channels with a Novel Xanthine Derivative. *Mol. Pharmacol.* **2014**, *85* (6), 858–865.
- (142) Grimley, J. S.; Li, L.; Wang, W.; Wen, L.; Beese, L. S.; Hellinga, H. W.; Augustine, G. J. Visualization of Synaptic Inhibition with an Optogenetic Sensor Developed by Cell-Free Protein Engineering Automation. *J. Neurosci.* **2013**, *33* (41), 16297–16309.
- (143) Boffi, J. C.; Knabbe, J.; Kaiser, M.; Kuner, T. KCC2-Dependent Steady-State Intracellular Chloride Concentration and PH in Cortical Layer 2/3 Neurons of Anesthetized and Awake Mice. *Front. Cell. Neurosci.* **2018**, *12* (January), 1–14.
- (144) Seino, S. ATP-SENSITIVE POTASSIUM CHANNELS: A Model of Heteromultimeric Potassium Channel/Receptor Assemblies. *Annu. Rev. Physiol.* **1999**, *61* (1), 337–362.
- (145) Suzuki, M.; Fujikura, K.; Inagaki, N.; Seino, S.; Takata, K. Localization of the ATP-Sensitive K<sup>+</sup> Channel Subunit Kir6.2 in Mouse Pancreas. **1997**, *46* (September).
- (146) Hattersley, A. T.; Ashcroft, F. M. Activating Mutations in Kir6.2 and Neonatal Diabetes: New Clinical Syndromes, New Scientific Insights, and New Therapy. *Diabetes* **2005**, *54* (9), 2503–2513.
- (147) Thomzig, A.; Laube, G.; Prüss, H.; Veh, R. W. Pore-Forming Subunits of K-ATP Channels, Kir6.1 and Kir6.2, Display Prominent Differences in Regional and Cellular Distribution in the Rat Brain. *J. Comp. Neurol.* **2005**, *484* (3), 313–330.
- (148) Zhang, C.; Bosch, M. A.; Levine, J. E.; Ronnekleiv, O. K.; Kelly, M. J. Gonadotropin-Releasing Hormone Neurons Express KATP Channels That Are Regulated by Estrogen and Responsive to Glucose and Metabolic Inhibition. *J. Neurosci.* **2007**, *27* (38), 10153–10164.
- (149) Ortega, F. J.; Gimeno-Bayon, J.; Espinosa-Parrilla, J. F.; Carrasco, J. L.; Batlle, M.; Pugliese, M.; Mahy, N.; Rodríguez, M. J. ATP-Dependent Potassium Channel Blockade Strengthens Microglial Neuroprotection after Hypoxia-Ischemia in Rats. *Exp. Neurol.* **2012**, *235* (1), 282–296.
- (150) Nelson, P.; Jicha, G.; Wang, W.; Ihgodaro, E.; Artiushin, S.; Nichlos, C.; Fardo, D. ABCC9/SUR2 in the Brain: Implications for Hippocampal Sclerosis of Aging and a Potential Therapeutic Target. **2016**, *70* (12), 773–779.
- (151) Itsuki, K.; Imai, Y.; Okamura, Y.; Abe, K.; Inoue, R.; Mori, M. X. Voltage-Sensing Phosphatase Reveals Temporal Regulation of TRPC3/C6/C7 Channels by Membrane Phosphoinositides. *Channels* **2012**, *6* (3), 206–209.
- (152) Ford, C. P.; Stemkowski, P. L.; Light, P. E.; Smith, P. a. Experiments to Test the Role of Phosphatidylinositol 4,5-Bisphosphate in Neurotransmitter-Induced M-Channel Closure in

- Bullfrog Sympathetic Neurons. *J. Neurosci.* **2003**, 23 (12), 4931–4941.
- (153) Burke, M. A.; Mutharasan, R. K.; Ardehali, H. The Sulfonylurea Receptor, an Atypical ATP-Binding Cassette Protein, and Its Regulation of the KATP Channel. *Circ. Res.* **2008**, 102 (2), 164–176.
- (154) Dennis, M. S.; Zhang, M.; Gloria Meng, Y.; Kadkhodayan, M.; Kirchhofer, D.; Combs, D.; Damico, L. A. Albumin Binding as a General Strategy for Improving the Pharmacokinetics of Proteins. *J. Biol. Chem.* **2002**, 277 (38), 35035–35043.
- (155) Weinert, M.; Selvakumar, T.; Tierney, T. S.; Alavian, K. N. Isolation, Culture and Long-Term Maintenance of Primary Mesencephalic Dopaminergic Neurons From Embryonic Rodent Brains. *J. Vis. Exp.* **2015**, No. 96, 1–5.
- (156) Perez-rivas, L. G.; Williams, T. A.; Reincke, M.; Maximilian, L.; Clin, E.; Diabetes, E. Inherited Forms of Primary Hyperaldosteronism : New Genes , New Phenotypes and Proposition of A New Classification Authors. **2018**.
- (157) Lüscher, C.; Slesinger, P. a. Emerging Concepts for G Protein-Gated Inwardly Rectifying (GIRK) Channels in Health and Disease. *Nat. Rev. Neurosci.* **2010**, 11 (5), 301–315.
- (158) Mayfield, J.; Blednov, Y. A.; Harris, R. A. *Behavioral and Genetic Evidence for GIRK Channels in the CNS: Role in Physiology, Pathophysiology, and Drug Addiction*, 1st ed.; Elsevier Inc., 2015; Vol. 123.
- (159) Coussons-Read, M. E.; Crnic, L. S. Behavioral Assessment of the Ts65Dn Mouse, a Model for Down Syndrome: Altered Behavior in the Elevated plus Maze and Open Field. *Behav. Genet.* **1996**, 26 (1), 7–13.